CLIMAAX
climate ready regions

Deliverable Phase 1 – Climate risk assessment

climate aDApTaIon for vulnerABLe regions using the “CLIMAAX” framEwork (DATABLE)

Greece, Region of Central Macedonia

HORIZON-MISS-2021-CLIMA-02-01 - Development of climate change risk assessments in European regions and communities based on a transparent and harmonized Climate Risk Assessment approach

Funded by the European Union

This project has received funding from the European Union’s Horizon Europe research and innovation programme under grant agreement No 101093864. Views and opinions expressed are however those of the author(s) only and do not necessarily reflect those of the European Union or the European Climate, Infrastructure and Environment Executive Agency (CINEA). Neither the European Union nor the granting authority can be held responsible for them.

1. Document Information

Deliverable Title	Phase 1 – Climate risk assessment
Brief Description	This document describes, includes and reports the results of the application of the CLIMAAX framework for the Region of Central Macedonia (RCM) for the floods and fires workflows respectively. All necessary data, methodologies, and tools to implement the framework for the RCM were provided with small modification when needed, from the digital handbook of the CLIMAAX project.
Project name	climate aDApTaIon for vulnerABLe regions using the "CLIMAAX" framEwork (DATABLE)
Country	Greece
Region/Municipality	RCM
Leading Institution	RCM
Author(s)	• Ioannis Kompatsiaris (CDXi[1]) • Stefanos Vrochidis (CDXi) • Ilias Gialampoukidis (CDXi) • Anastasia Moumtzidou (CDXi) • Konstantinos Karystinakis (CDXi) • Konstantinos Vlachos (CDXi)
Deliverable submission date	30/05/2025
Final version delivery date	30/05/2025
Nature of the Deliverable	R – Report
Dissemination Level	PU - Public

Version	Date	Change editors	Changes
1.0	10/03/2025	Nikolaos Papadopoulos (RCM)	Initial structure of the document. Preliminary guidelines, and descriptions were included.
1.1	24/03/2025	Nikolaos Papadopoulos (RCM)	Corrections and updates. Preliminary format of the document.
1.2	28/05/2025	CDXi	Update Floods and Fire workflows.
1.3	29/05/2025	Nikolaos Papadopoulos (RCM)	Reviewing and final updates.

[1] **CDXi Solutions P.C.**: **https://cdxi.gr/.**

2. Table of contents

3. List of figures

4. List of tables

5. Abbreviations and acronyms

Abbreviation / acronym	Description
AOI	Area of interest
Aqueduct	Mission from the World Resources Institute
CDS	Copernicus Climate Data Store
CHELSA	Climatologies at high resolution for the earth's land surface areas
CLIMAAX	CLIMAte risk and vulnerability Assessment framework and toolbox
CMIP6	Coupled Model Intercomparison Project Phase 6
CRA	Climate Risk Assessment
CSV	Comma-separated-values file format
DEMs	Digital Elevation Models
EAD	Expected Annual Damage
EADP	Expected Annual Displaced Population
EAEP	Expected Annual Exposed Population
EAPD	Expected Annual Population Displacement
EAPE	Expected Annual Population Exposure
ECLIPSE	European CLimate Index ProjectionS
ECMWF	European Centre for Medium-Range Weather Forecasts
EFFIS	European Forest Fire Information System
EPSG	European Petroleum Survey Group
ERA5	ECMWF Reanalysis v5
EU	European Union
EU-DEM	European Digital Elevation Model
EURO-CORDEX	Coordinated Downscaling Experiment - European Domain
FWI	Fire Weather Index
GDP	Gross Domestic Product
GeoJSON	Geographic JavaScript Object Notation
GeoTIFF	Geographic Tagged Image File Format
GFDL-ESM2M	Geophysical Fluid Dynamics Laboratory Earth System Model version 2 - Medium resolution
GHS-POP	Global Human Settlement (GHS Population Grid European Commission GHS-POP-R2023A)
gpkg	Geopackage open format
GTSM	Global Tide and Surge Model for current sea level
HadGEM2-ES	Hadley Centre Global Environment Model version 2 - Earth System
IPCC	Intergovernmental Panel on Climate Change

IPSL-CM5A-LR	Institut Pierre-Simon Laplace Climate Model version 5A - Low Resolution
JRC	Joint Research Centre
KPI	Key Performance Indicator
LCL	LUISA Land Cover Codes
LUISA	Land Use-based Integrated Sustainability Assessment
MERIT-DEM	Multi-Error-Removed Improved-Terrain DEM
MIROC-ESM-CHEM	Model for Interdisciplinary Research on Climate - Earth System Model with Chemistry
ML	Machine Learning
NorESM1-M	Norwegian Earth System Model version 1 - Medium resolution
NUTS	Nomenclature of territorial units for statistics
OSM	OpenStreetMaps
RCM	Region of Central Macedonia
RCP	Representative Concentration Pathways
ROI	Region of Interest
RP/rp	Return period
shp	Shapefile format
SLR	Sea-level rise projections
SSPs	Shared Socioeconomic Pathways
WGS	World Geodesic System

6. Executive summary

This deliverable presents a preliminary framework for assessing flood and wildfire risks by integrating hazard, exposure, and vulnerability data to support informed decision-making applied in the RCM. The methodology outlines the use and application of datasets (including high-resolution and large-scale data) to enable future evaluation of current and projected climate-driven risks, thereby contributing to resilience planning within the CLIMAAX framework. The flood risk assessment was designed around river and coastal flood hazard maps, which include high-resolution datasets from the JRC and broader, sparse datasets from the Aqueduct Floods, covering return periods of different ranges. Coastal flood projections estimating sea level rise to the year 2150 were included in the proposed approach. Furthermore, land-use information from CORINE Land Cover and elevation data were identified as key inputs for a more refined exposure analysis. The vulnerability of infrastructure was assessed using global flood depth-damage functions. The proposed methodology for wildfire risk incorporates a fire danger indicator (FWI, derived from EURO-CORDEX models). Historical fire data from the EFFIS (European Forest Fire Information System), together with land cover classifications and population exposure datasets, informed the analysis. Metrics for building exposure and vulnerability were sourced from OSM and relevant wildfire damage functions. This deliverable includes the results from the initial implementation of the risk assessments, consolidating both the necessary datasets and the methodological components required for their execution. The organizational structure developed herein guided the application of the flood and wildfire workflows in the respective phases. The approach adopted remains flexible and allows for updates as new data and methods become available, especially at the regional level, following the guidelines given by the CLIMAAX framework. It also contributes to the alignment of climate risk assessment practices across regions participating in the CLIMAAX project, as RCM covers an extensive area of the country, serving almost one-fifth of the total population. Additionally, this work provides a foundation for future integration of compound risks and cross-sectoral impact analyses. The conclusions presented here aim to inform the following tasks and deliverables focused on implementing risk assessment at the regional level.

1 Introduction

1.1 Background

RCM functions as a second-level local self-government authority and consists of seven (7) regional units and civil protection departments, serving nearly two million residents. These units include Imathia (Ημαθία), Thessaloniki (Θεσσαλονίκη), Pella (Πέλλα), Kilkis (Κιλκίς), Pieria (Πιερία), Serres (Σέρρες), and Halkidiki (Χαλκιδική). RCM carries out governmental responsibilities and implements policies related to environmental protection, resilience building, climate change adaptation, and disaster and risk management strategies. Additionally, RCM collaborates with local authorities, stakeholders, and scientific institutions to develop local-based policies and action plans dedicated to the local demands of each area. In *Figure 1* below, the area that RCM covers and the borders for each region unit can be seen, located in the northern part of the country, and occupying a rather wide area.

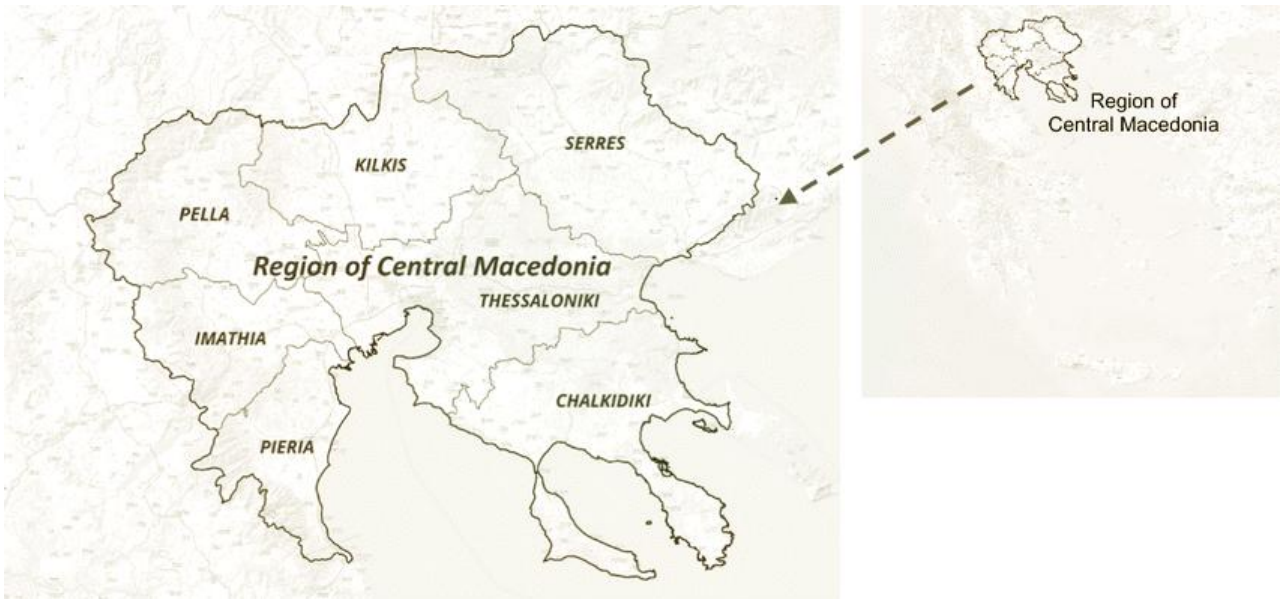

Figure 1: RCM and its seven (7) regional units.

In cooperation with the Fire Brigade Operations Centers, Civil Protection structures, and the Hellenic Police, RCM additionally manages data and materials generated from emergency events. The institutional and operational role of RCM positions it as a key actor in coordinating multi-agency strategies and responses, as well as aligning regional actions with national climate adaptation priorities. The proposed project was supervised by RCM, which ensured the provision of all necessary technical expertise and resources for the development of this framework. Primary beneficiaries include not only the Directorate of Civil Protection of the Metropolitan Unit of Thessaloniki but also the Civil Protection directorates of the remaining seven (7) regional units of RCM. In addition, potential beneficiaries comprise all competent regional departments responsible for urban, peri-urban, and rural oversight, including the Directorates of Health, Rural Development, Environment, and Technical Services. These services supervise agricultural development, safeguard public health, and ensure environmental protection. In the event of disasters such as floods and wildfires, the key actors require necessary information and assume an active role in response

operations. Given the increasing frequency and severity of climate-related hazards in the region (RCM scores 6.58 in the NUTS2 (Nomenclature of territorial units for statistics) index, with Chalkidiki County scoring 6.75 NUTS3 index[2], not far from the highest NUTS3 value in the EU), the need for an integrated, data-driven risk management framework is both urgent and significant. The development of a comprehensive action plan through the CLIMAAX project is expected to strengthen local preparedness, improve inter-agency coordination, and facilitate its eventual adoption by neighboring regions in Greece.

1.2 Main objectives of the project

The main objective of the project is to implement and utilize the CLIMAAX framework in the RCM through the application of the framework's methodologies in three (3) structured phases. The project aims to enhance climate risk governance at the regional level, improve decision-making capacity and potential applications, and support long-term resilience building and goals, particularly in relation to flood (both river and coastal) and wildfire hazards. The first phase focuses on the contextual exploration, analysis, and results required for the application of the CLIMAAX methodology, using the available tools and guidance provided by the project. The regional team and team of experts have reviewed the structure of the methodology, examined relevant data sources, identified key parameters for local implementation, and produced the final output maps for the two (2) selected hazards. Key activities during this phase included the identification of climate and environmental hazards relevant to the RCM, the analysis of socioeconomic factors influencing vulnerability and adaptive capacity, and the establishment of criteria and procedures for risk estimation aligned with national and European strategies. The CLIMAAX Handbook played a central role in guiding this process, offering structured and transferable procedures and quality standards that ensured consistency across all stages of implementation. Its practical orientation also might enable regional actors to apply complex risk methodologies in an accessible and context-sensitive manner. The second phase will focus on refining and localizing the risk assessment framework by integrating high-resolution, region-specific data. This includes the analysis of local datasets, the revision and adjustment of initial assumptions, and the management of data gaps (if any) through cooperation with competent authorities and data providers. An important objective is to ensure the compatibility of regional inputs with the existing analytical systems and to improve the reliability of outcomes once the workflows are implemented. The third phase will involve the evaluation of the results generated in the previous stages, with an emphasis on identifying and prioritizing adaptation strategies suited to the region's specific needs and if possible, to its specific regional units, taking into account its specific morphological uniqueness. It will include the development of at least one (1) adaptation strategy, the assessment of resilience measures under two (2) different climate hazard scenarios, and the organization of a stakeholder engagement meeting to present the proposed actions and gather valuable feedback. While these steps are foreseen in the overall implementation plan, this document focuses on preparatory work includes the results of the risk assessments. These include improved decision-making for climate risk prevention and management, enhanced resilience through the use of structured methodologies and quality-assured data, and the integration of local knowledge for more accurate and relevant assessments. Furthermore, the project supports alignment with European climate adaptation strategies, reinforces

[2] https://ec.europa.eu/eurostat/web/nuts

coherence with related initiatives, and promotes the long-term sustainability of regional adaptation planning through the use of innovative tools and frameworks. By adopting the CLIMAAX Handbook and its associated toolkit, RCM will be better equipped to embed risk assessment methodologies into local and regional policy-making. This will ultimately contribute to the potential protection of citizens, infrastructure, and natural ecosystems in the face of increasing climate-related hazards.

1.3 Project team

The management of the project is overseen by the legal representative of the contractor, who acts as the formal point of contact for contractual matters with the contracting authority. The legal representative represents the consortium, monitors the proper execution of the contract, manages any required amendments, and supervises internal coordination and financial administration. At the implementation level, the team is organized around a defined structure composed of the Project Manager and the Deputy Project Manager, who jointly coordinate the tasks of the Expert Team. The Project Manager holds the overall responsibility for the technical execution of the project. This role includes leading the design and implementation of activities, supervising the overall work plan, maintaining regular communication with both the legal representative and the contracting authority, guiding the project team, ensuring the availability of resources, approving deliverables, and ensuring compliance with quality standards and timelines. The Deputy Project Manager supports the Project Manager and is responsible for the day-to-day coordination and administrative functioning of the team. This includes the allocation of roles and responsibilities, scheduling, ensuring adherence to methodology, facilitating internal coordination, and reporting on progress. The Deputy Project Manager also handles operational issues and contributes to selected project tasks where required. The Project Team Members carry out the technical tasks assigned to them, maintain regular communication with the Deputy Project Manager, liaise with the contracting authority's relevant staff, and ensure timely delivery of outputs. Participation in meetings and cross-functional collaboration is also part of their responsibilities. The consolidation of outputs from the Deputy Project Manager and the Project Team is ensured through close collaboration and is under the overall responsibility of the Project Manager.

1.4 Outline of the document's structure

This document presents the work carried out as part of Phase 1 of the climate risk assessment in the RCM, following the structure and methodology outlined in the CLIMAAX Handbook. The initial phase focused on preparation and orientation, during which the RCM team reviewed the methodology, familiarized itself with the available materials, and laid the foundations for the technical implementation. With the appointment of the expert team, the complete suite of technical workflows has now been executed. As a result, this document includes both preparatory activities and the first set of spatially explicit outputs. The structure of the document reflects this progression:

- Section 2.1 presents the initial scoping activities, including the definition of assessment objectives, description of the regional context, and identification of relevant stakeholders.
- Section 2.2 describes the selection and implementation of technical workflows, covering hazard prioritization, scenario framing, and the processing of regional datasets.
- Section 2.3 provides an overview of key climate risks identified through the analyses, together with the first results of the exposure, vulnerability, and impact assessments. This

includes risk maps, damage estimates, and preliminary interpretation of critical areas of concern.
- Section 2.4 offers the summary of the preliminary key risk assessment for the RCM.

This deliverable includes the full set of results from the CLIMAAX technical workflows, such as river flood and wildfire susceptibility maps, coastal exposure assessments, and damage estimations by land use category. These outputs will support future adaptation planning and provide a structured basis for stakeholder engagement and policy development in subsequent phases.

2 Climate risk assessment – phase 1

This chapter presents the preliminary outcomes of the first phase of the Climate Risk Assessment (CRA) carried out by the RCM in the context of the CLIMAAX project. This initial phase was focused on clarifying objectives, understanding the regional context, and selecting the most relevant climate-related hazards. The process also involved exploring the available data, identifying suitable risk workflows, and preparing the ground for future technical work. At this stage, the region has chosen to concentrate on two (2) key climate risks, floods, and wildfires, both of which are assumed to increase their frequency and intensity in the years ahead. The risk modeling workflows have been launched, and the output results will contribute indirectly to the next phases of the project.

2.1 Scoping

2.1.1 Objectives

The main aim of the CLIMAAX project concentrates on helping the RCM to enhance the understanding and management of the risks posed by climate-related hazards, with a clear focus on wildfires and floods. By assessing the extent of exposure and vulnerability across different sectors, the region intends to support more informed decision-making in areas such as emergency response, land-use planning, and climate adaptation. The results of the CRA are expected to feed directly into policy planning at regional level, strengthening RCM's capacity to respond to changing climate conditions, and additionally will help to extend and update existing strategies and plans, including civil protection measures, the regional adaptation plans, and ensure alignment with national and EU frameworks. Access to high-resolution local data may also need to be addressed later in the process, especially for vulnerability and exposure mapping.

2.1.2 Context

RCM has experienced increasing climate-related challenges over the past decade. Wildfires during long dry summers, and floods caused by intense rainfall events and river overflow, have affected both urban and rural areas. These hazards have impacted public safety, damaged infrastructure and farmland, and put pressure on regional services. Until now, risk management in the region has relied primarily on emergency response protocols and civil protection structures, which dedicate resources to create particular resilience schemes applicable as much as possible to the whole region. While effective in a number of situations, these approaches cannot maintain the capacity to address the long-term nature of climate risks. There is growing recognition that proactive planning and forward-looking assessments are key factors, and the applicability of the CLIMAAX CRA provides a clear opportunity to move in this direction. The CRA is being developed within a broader governance and policy environment. It is aligned with the national adaptation guidelines provided by the ministry of Civil Protection[3], and it supports sectoral and territorial planning in areas like agriculture, health, environment, and infrastructure. At the same time, it reflects the principles of the

[3] https://civilprotection.gov.gr/sxedia-politikis-prostasias

EU's Green Deal and the European Climate Adaptation Mission[4]. Finally, the CRA also benefits from alignment with broader national and European initiatives, which will be important for scaling up future actions.

2.1.3 Participation and risk ownership

During this first phase, internal coordination was initiated across several departments within the regional authority. This included staff from civil protection, spatial planning, environment, and technical services. These departments contributed to defining the scope of the assessment and validating the focus on the indetermination of the occurrence of floods and wildfires. Broader stakeholder engagement (with the potential to involve municipalities, emergency responders, scientific experts, and representatives of vulnerable communities) was organized during this phase and planned to be in action for the next phase. The goal was to create an open and inclusive process that brings together practical experience, local knowledge, and scientific input. At present, the responsibility for managing risk lies mainly with public authorities under the regional civil protection framework. However, as the CLIMAAX project progresses, the opportunity for clarification and sharing the responsibility across more actors, including infrastructure providers, landowners, and local communities remains open. The results of the assessment will be communicated clearly and openly through summary reports, maps, and tables helping stakeholders to understand not only where the risks lay, but also what actions might be taken in response.

2.2 Risk Exploration

2.2.1 Screen risks (selection of main hazards)

The RCM is increasingly exposed to climate-related hazards that present significant risks to natural systems, infrastructure, the economy, and public safety. Based on initial screening aligned with the CLIMAAX methodology, the primary hazards relevant to the regional context are river and coastal flooding, and fires. Climate change is expected to intensify these hazards, with higher seasonal variability, extreme weather events, and interactions with land use dynamics, particularly in peri-urban and rural areas. Currently, river flooding also poses a severe hazard, particularly along river basins. These low-lying floodplains are highly sensitive to seasonal rainfall extremes and peak river discharges, which are projected to increase under both SSP2-4.5 and SSP5-8.5 climate scenarios. Recurrent floods affect agricultural land, road networks, residential developments, and critical infrastructure, resulting in economic losses and long-term disruption. Communities in flood-prone rural zones, especially those with inadequate protective infrastructure, are especially vulnerable. In Table ***1***, a brief list of the main rivers in the RCM can be seen. Additionally, coastal flooding represents a growing threat due to rising sea levels and extreme sea level events, particularly in the low-lying coastal municipalities along the Thermaic Gulf. Developments near Thessaloniki and coastal areas in Chalkidiki are at risk of inundation during storm surge events and sea level rise scenarios projected for 2050–2100. In Figure *2*, an approximate line drawn along the coastline of

[4] https://research-and-innovation.ec.europa.eu/funding/funding-opportunities/funding-programmes-and-open-calls/horizon-europe/eu-missions-horizon-europe/adaptation-climate-change_en

the RCM can be seen. This visualization provides a first spatial reference for the coastal boundary of the region, which is later used for hazard assessment and geospatial filtering. Further, wildfire risk is a recurrent and escalating issue in RCM, especially during the dry summer season. Contributing factors include elevated temperatures, increased frequency of heatwaves, accumulation of flammable biomass due to land abandonment, and expanding urban pressure into vegetated zones. Communities living near forested areas, agricultural workers, tourism-dependent businesses, and biodiversity hotspots are particularly affected.

Table 1: Main Rivers of the RCM[5].

River	Regional Unit
Aliakmonas	RCM
Angitis	Serres
Axios	Kilkis, Thessaloniki
Gallikos	Kilkis, Thessaloniki
Edesseos	Pella
Helikon	Pieria
Elpeus	Pieria
Ziliana	Pieria
Loudias	Pella, Thessaloniki
Moglitsas	Pella, Imathia
Strymonas	Serres

[5] Note: Tributaries, streams, and smaller watercourses are considered to fall under the corresponding main rivers and are not listed separately for the sake of simplicity.

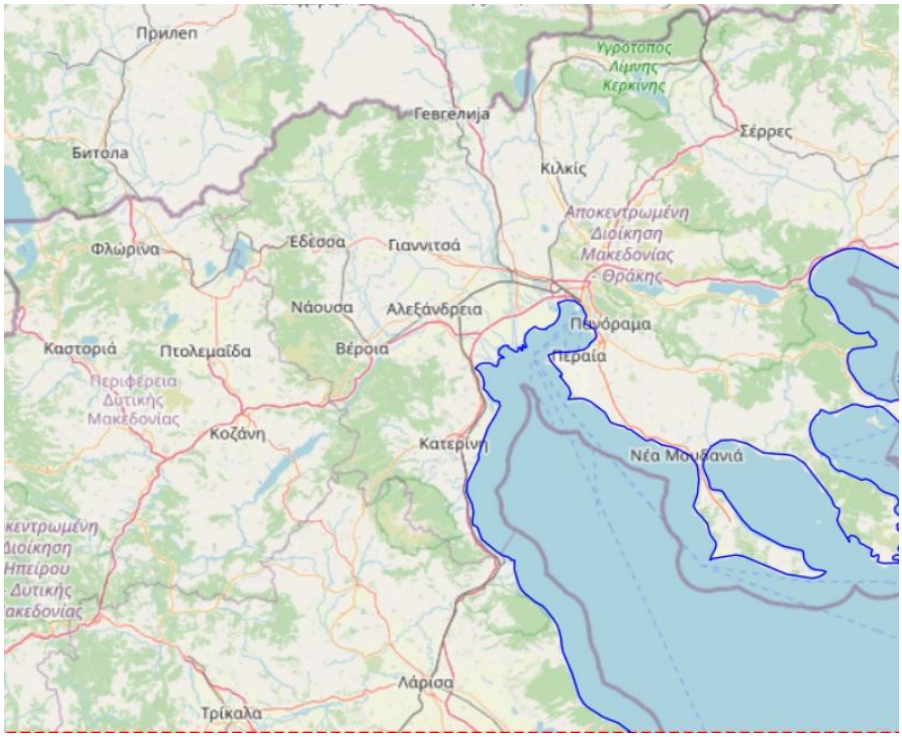

Figure 2: Coastline of the RCM (approximate), clipped to a bounding box. The coastline (blue) is overlaid on an OpenStreetMap (OSM) Map basemap, with the bounding box shown in red dashed lines.

The risk assessment for each of the mentioned hazards was examined through both baseline and future climate scenarios, using hazard-specific methodologies provided in the CLIMAAX toolbox. River flood risk was assessed using high-resolution JRC flood depth maps and land use overlays, while coastal flood risk was modeled using extreme sea level statistics combined with digital elevation data and passive flood mapping techniques. Wildfire risk was assessed using an FWI-based (Fire Weather Index) method (a meteorologically derived index used globally to quantify fire danger) that uses meteorological thresholds. At this stage, available data include European datasets (e.g., ERA5 (ECMWF Reanalysis v5), LUISA (Luisa Land Cover Code), CORINE, EU-DEM (European Digital Elevation Model), GTSMv3.0 (Global Tide and Surge Model for current sea level), NASA Sea Level Projection Tool, JRC flood maps), historic wildfire ignition data, and pre-calculated FWI time series. Open-source tools (e.g., damagescanner, geo-related Python libraries. etc.) were support processing and analysis. However, additional data and resources might be still required for optimal implementation. These might include local or national fire records, historic flood event data, land use vulnerability estimates, and region-specific damage valuation curves. Finally, deeper stakeholder engagement will be necessary to validate the relevance of selected hazards, define risk thresholds, and co-develop adaptation priorities.

2.2.2 Workflow selection

2.2.2.1 Workflow #1: Floods

2.2.2.1.1 River floods

The river floods risk assessment for the RCM enables the potential estimation of the economic damages from fluvial flooding through the transferable workflow implemented in the CLIMAAX handbook. The process aims to integrate European datasets from openly available databases, open-source tools, and local contextual information. As it appears in each workflow, hazard, and risk assessment parts are expected to be treated separately. This approach allows for a transparent, reproducible, and regionally relevant assessment of river flood risks and their impacts on assets, population, and infrastructure.

Hazard assessment: hazard data is expected to be pre-processed based on river flood depth maps provided by the JRC. The raster datasets will represent the expected flood depths under different return periods (e.g., 10-, 50-, and 100-year events) taking into consideration both baseline and climate-adjusted conditions. The expected file format (GeoTIFF (Geographic Tagged Image File Format) raster files) and the resolution (100m) are expected to be processed via the code blocks provided and implemented in the CLIMAAX flood workflow using geo-specific libraries such as *rasterio*, *rioxarray*, and *xarray*. The hazard layers will provide explicit data on flood depth and extent, forming the basis for downstream exposure and risk analysis.

Exposure assessment: the LUISA Land Use dataset at 100m resolution is expected to be used (in a raster format), providing a land use classification for each grid cell (by assigning flood depth values to land use pixels within hazard zones), and identifying which land use classes (e.g., agriculture, residential, industrial, natural areas, etc.) fail within flood-affected areas and are thus in risk of damage. This step quantifies the extent of human and economic activity located within potential flood zones in the RCM.

Vulnerability assessment: a dedicated section in the CLIMAAX handbook is expected to be utilized for working with damage curves. Vulnerability is modeled using initially the JRC damage curves (provided as "*LUISA_damage_info_curves.xlsx*"), which estimate economic losses as a function of flood depth per land use category. For regional conditions, adaptations area expect through a given xls file containing the GDP-based (Gross Domestic Product) adjustment factors. Depth-damage functions are expressed as damage ratios for each land use type, and the appointed expert team will adjust the values based on the regional GDP or any asset replacement costs. Integration is expected to happen via rasterizing the vulnerability values assigned per pixel via matching land use class. This step enables the translation of flood exposure into economic consequences, supporting the production of damage estimates in euros.

Risk calculation: risk will be computed by integrating hazard (flood depth, raster), exposure (land use, e.g., LUISA), and vulnerability (damage curves, in *JSON* or *CSV* formats) to calculate direct economic damages at a pixel level. It is expected that the raster will be merged into a common grid and for each cell the estimated damage will be calculated and results will be aggregated spatially to obtain losses (total, sector-related, location-specific, etc.). The result is a comprehensive damage map for each flood scenario, expressed in absolute monetary terms.

In RCM river basins are located in the principal flood-prone zones and are repeatedly affected by fluvial flooding, especially during high-intensity rainfall periods or events. Exposed assets include

but are not limited to agricultural lands in rural municipalities in each affected region, linear infostructure including roads, rail, and other utilities, and residential communities near unregulated riverbanks. Settlements in peri-urban areas are expected to be affected as well as farmers and seasonal workers in the area, and populations without adequate flood insurance or housing protections. The workflow is expected to accommodate both baseline and future climate scenarios, using climate-adjusted flood hazard maps reflecting increased peak discharge due to warming trends, including return periods of 10-, 50-, and 100-year events. Additionally, future socio-economic pathways (e.g., land use change, urban expansion) are expected to be addressed by using CMIP6 (Coupled Model Intercomparison Project Phase 6)-compatible discharge projections in future hazard models, enabling planning for short-term adaptation (5–10 years), medium-term risk reduction (2030–2050), and long-term resilience (up to 2100).

The workflow will focus solely on the fluvial flooding hazard in the RCM based on Europe-wide and open-source data and aiming to reproduce representative results for larger river basins for local situations. Streamline and processes with higher resolution are considered as the aim of the consecutive deliverable which will be based on local and regional data. All datasets used in the risk assessment framework are sourced via the CLIMAAX handbook resources and include: (i) river flood depth maps for different return period (source. JRC), (ii) land use maps (source: Copernicus Land Monitoring Service), (iii) flood damage curves for infrastructure (JRC), and (iv) economic value for different types of land use. As described in the CLIMAAX Handbook specific limitations apply including the following:

- Only large river basins (larger than 150km^2).
- Flood (man-made) protection measures (such as dams, levees, etc.) are not included.
- River water management is not included.
- Urban flash floods datasets lack detailed representations.

Hazard assessment methodology will cover both high- and coarse-resolution datasets both for modeled (source: JRC) and future (source: Aqueduct Floods) river flood hazard maps. The high-resolution datasets include a set of return periods ranging from 10 and up to 500 years. The coarse-resolution dataset includes "*extreme flood events in the baseline climate (ca. 1980) and in the future climates (2030, 2050, 2080 for RCP4.5 and RCP8.5 climate scenarios)*".

Hazard assessment

The region of interest (ROI) is given via coordinates in a CSV format following the WGS84 (World Geodesic System) coordinates (EPSG[6]:4326). In the table below a distinction between the main region and the sub-regions of the RCM can be seen. The purpose of this differentiation focuses on capturing any details of the topology of the areas and for extracting valuable information from the output. The tool provided in the CLIMAAX Handbook, the Bounding Box Tool was selected for collecting the coordinates[7].

[6] Refers to: European Petroleum Survey Group.
7 Due to the limitations of the Bounding Box tool (drawing a rectangle) any potential overlap between the regions' borders is considered unavoidable.

Table 2: Coordinates defining the bounding box for RCM and each subregion.

Coordinates	Description
21.6495,39.904,24.4137,41.5807	RCM
22.904656,39.876217,24.516351,40.643331	Chalkidiki
21.9238,40.2785,22.7409,40.74	Imathia
22.2462,40.7829,23.2537,41.346	Kilkis
21.704976,40.675608,22.604757,41.1687	Pella
22.099907,39.936457,22.698662,40.551135	Pieria
22.868576,40.771085,24.124897,41.412139	Serres
22.492776,40.342745,23.796385,41.012383	Thessaloniki

For each subregion the CLIMAAX framework was run to provide a more detailed depiction of the flooding events and of the potential flooding maps that were produced.

Flood hazard mapping based on the JRC's high-resolution river flood map dataset for present-day scenario

JRC flood map dataset was downloaded for a set of return periods[8]. Example of flood maps for several return can be found below for the region as an entity and for each subregion.

Table 3: Summation of example figures for flood hazard maps for each sub-region.

Example Figures	Description
Figure *3*	RCM
Figure *4*	Chalkidiki
Figure *5*	Imathia
Figure *6*	Kilkis
Figure *7*	Pella
Figure *8*	Pieria
Figure *9*	Serres
Figure *10*	Thessaloniki

8 JRC flood map dataset can be found in the following link: https://jeodpp.jrc.ec.europa.eu/ftp/jrc-opendata/CEMS-EFAS/flood_hazard/.

RCM

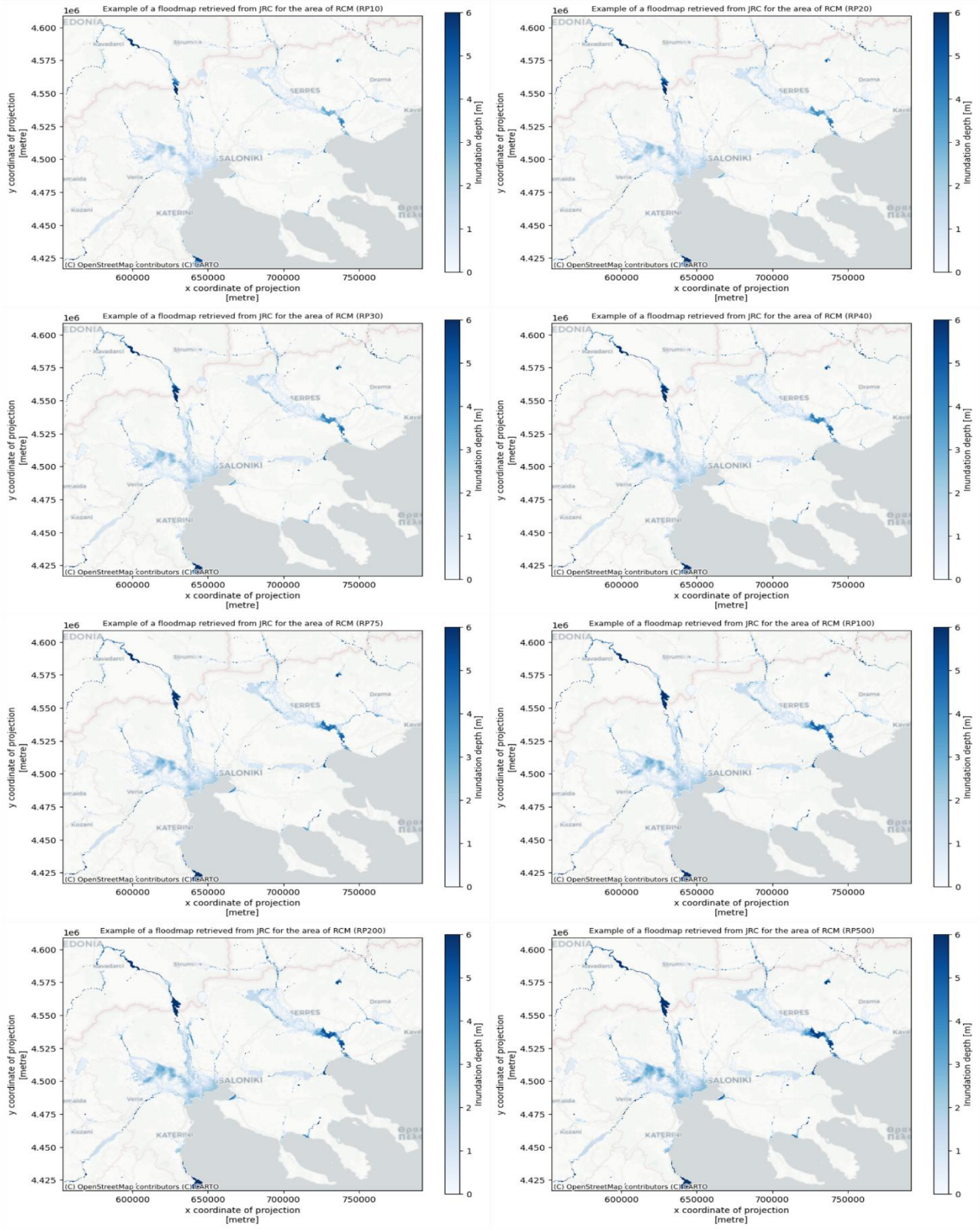

Figure 3: Example of flooding maps retrieved for the RCM for a range of return periods.

Chalkidiki

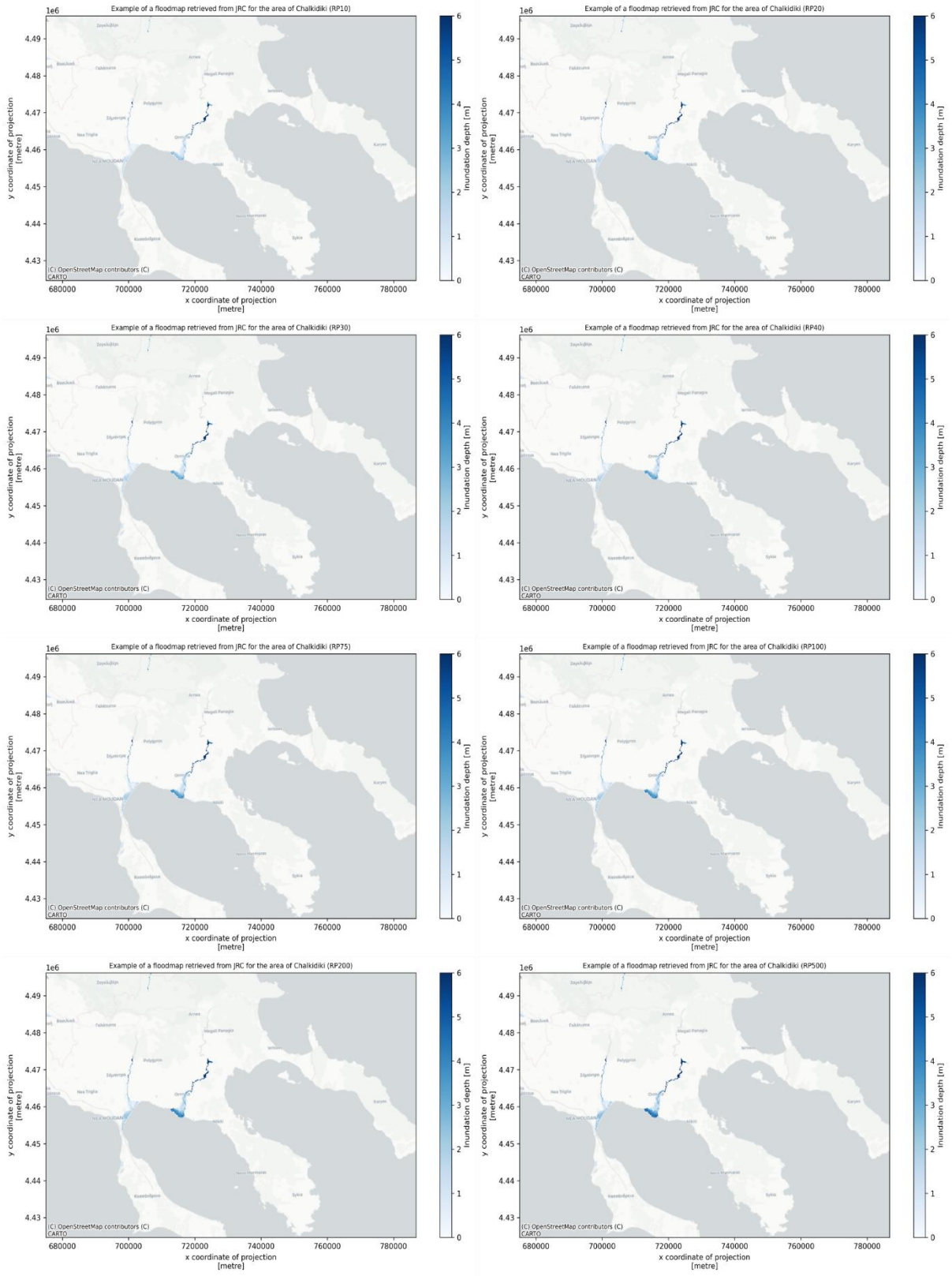

Figure 4: Example of flooding maps retrieved for the subregion of Chalkidiki for a range of return periods.

Imathia

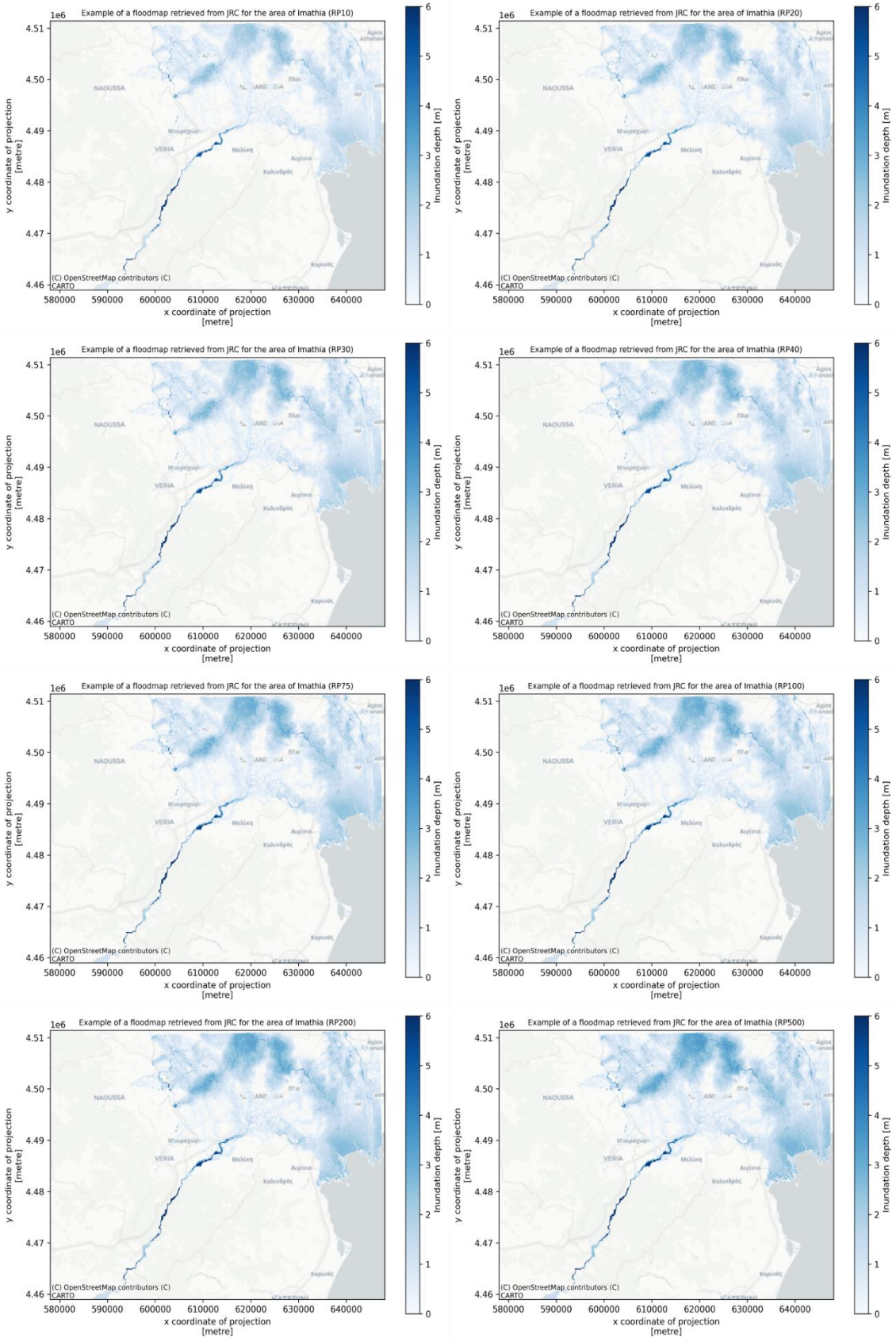

Figure 5: Example of flooding maps retrieved for the subregion of Imathia for a range of return periods.

Kilkis

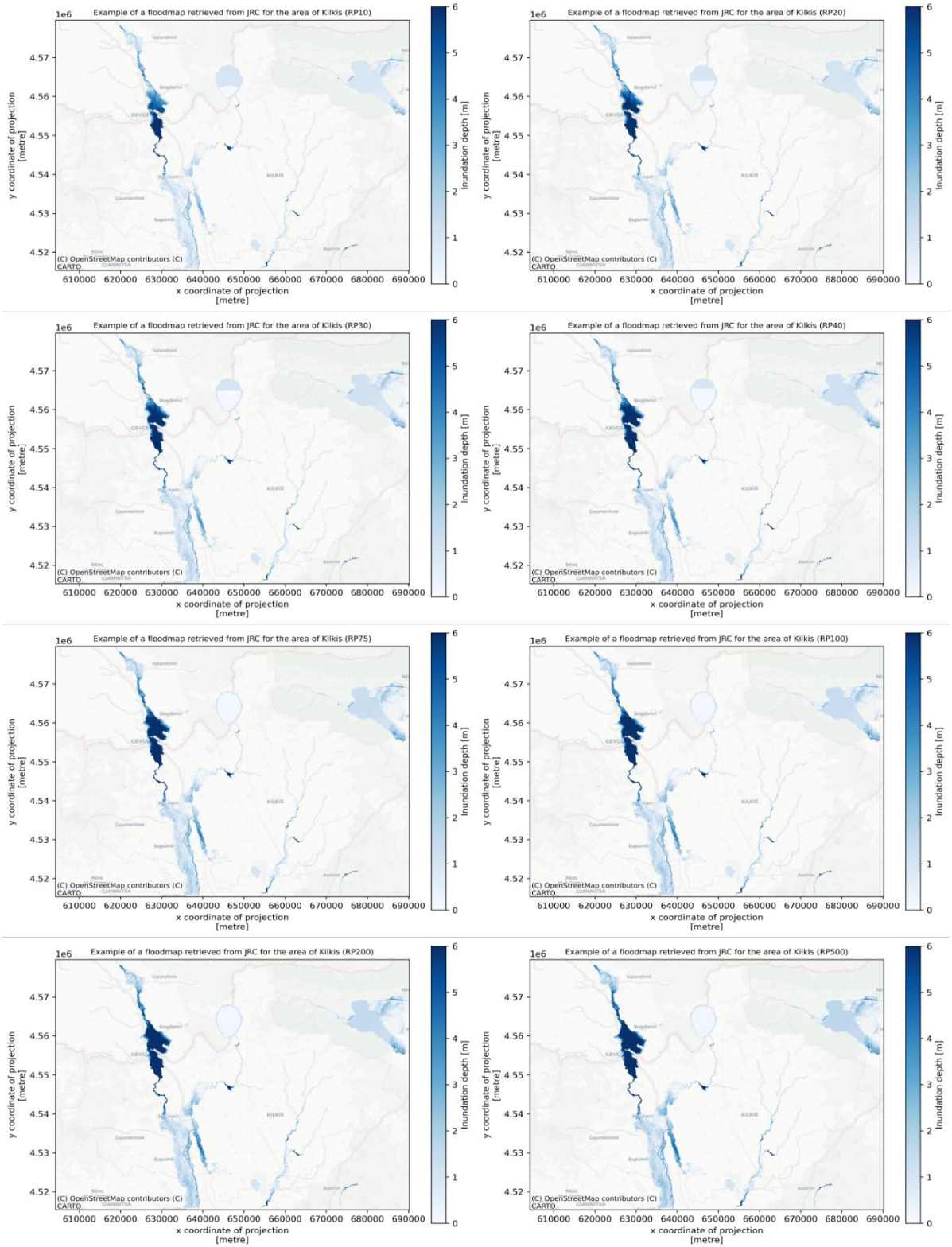

Figure 6: Example of flooding maps retrieved for the subregion of Kilkis for a range of return periods.

Pella

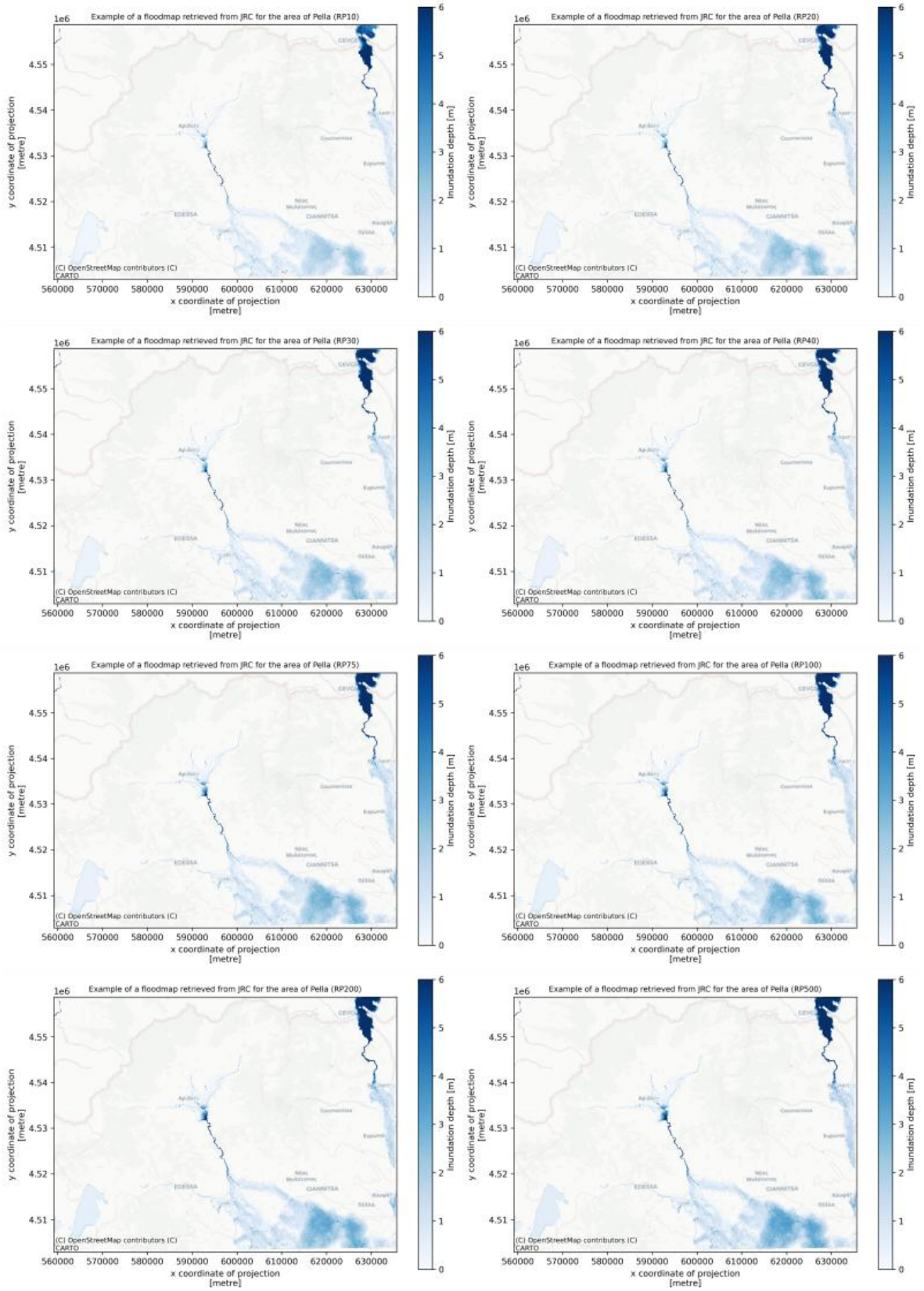

Figure 7: Example of flooding maps retrieved for the subregion of Pella for a range of return periods.

Pieria

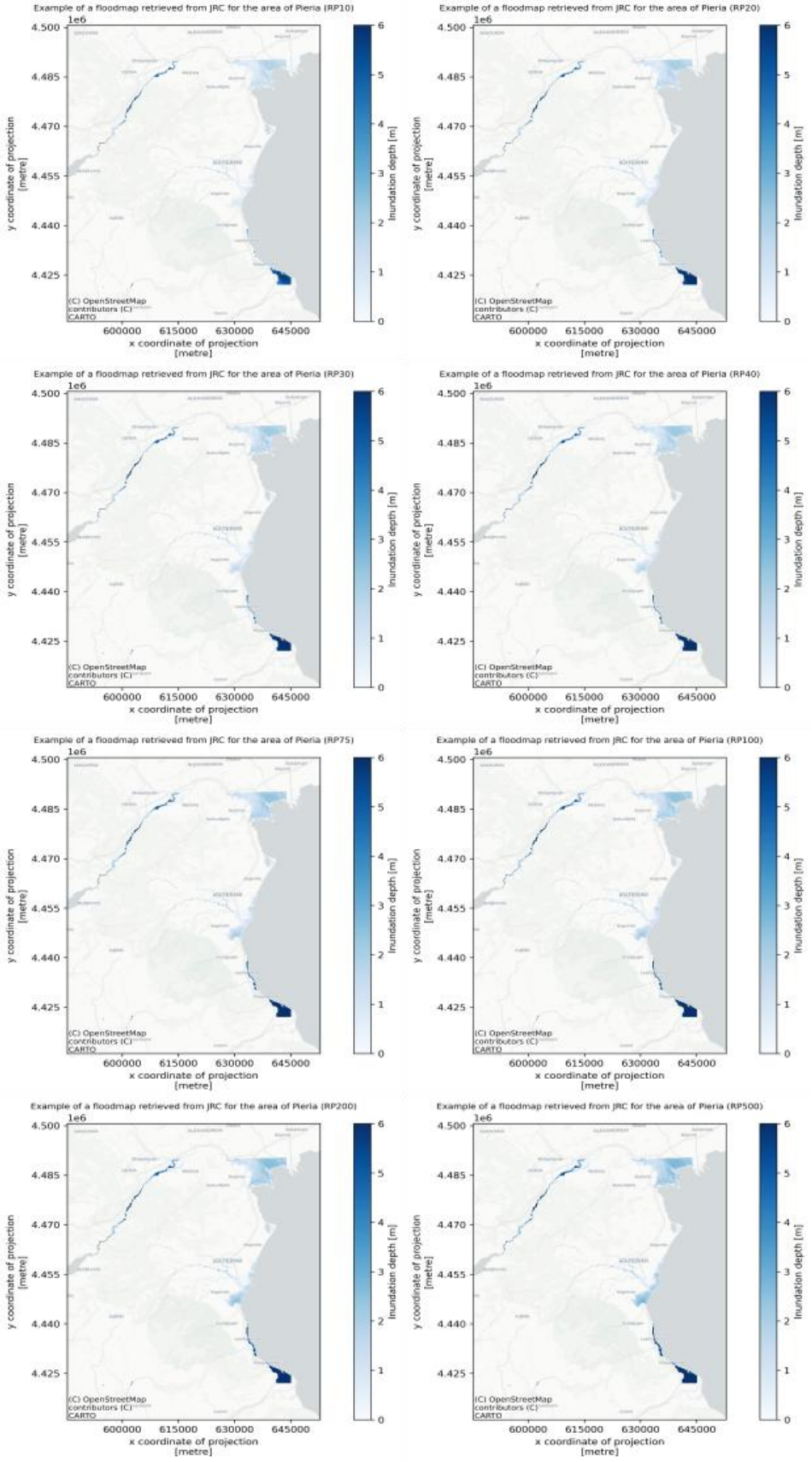

Figure 8: Example of flooding maps retrieved for the subregion of Pieria for a range of return periods.

Serres

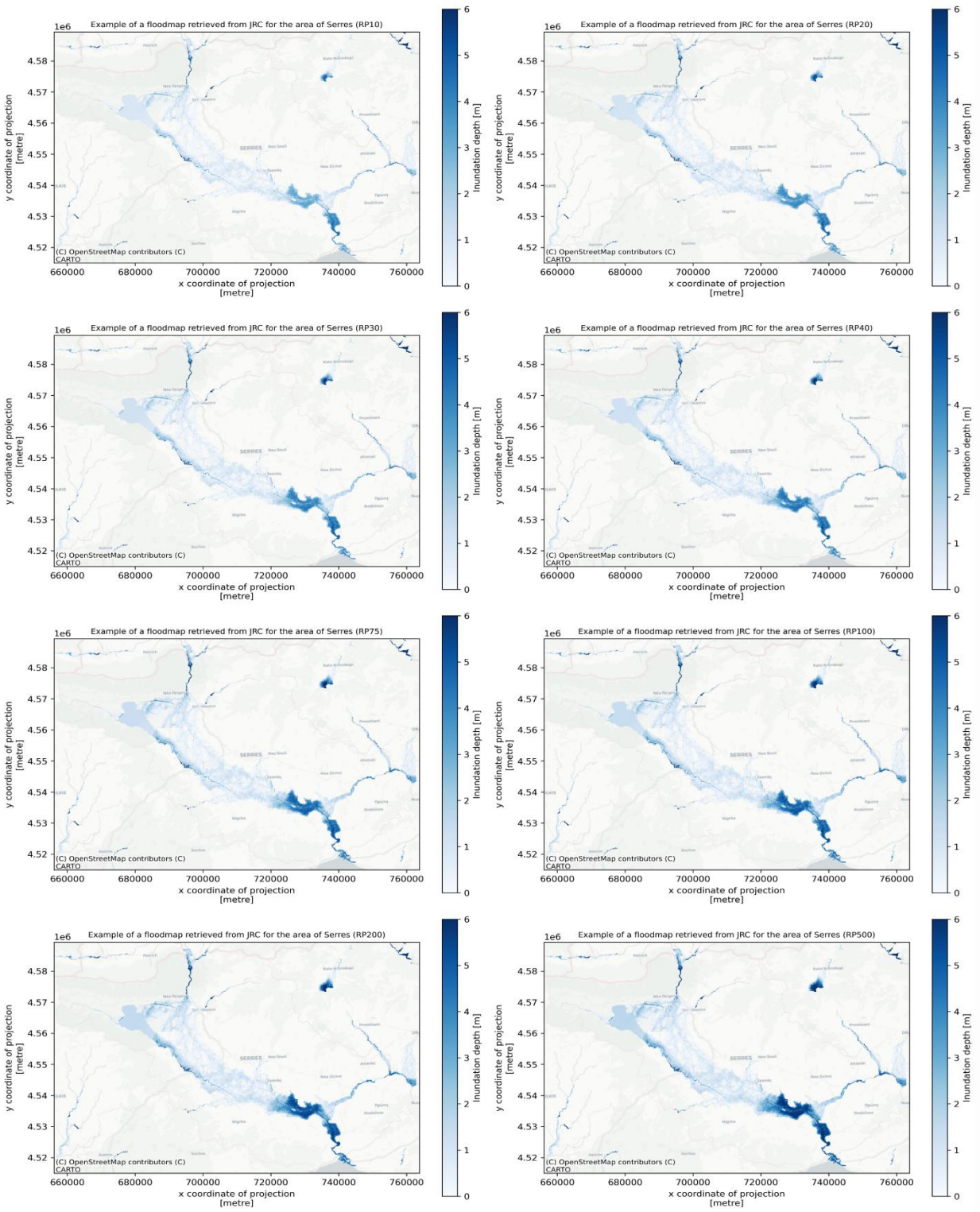

Figure 9: Example of flooding maps retrieved for the subregion of Serres for a range of return periods.

Thessaloniki

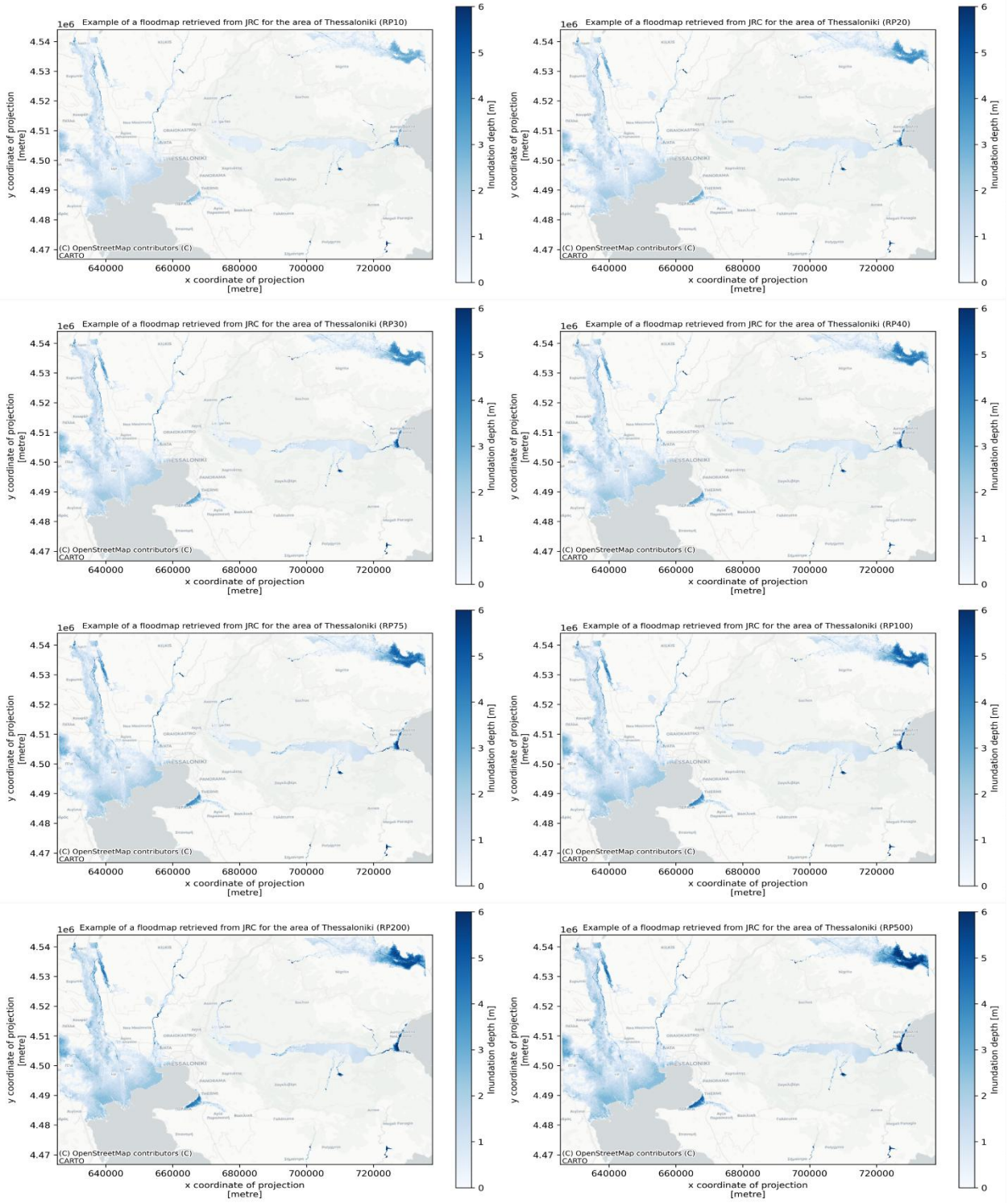

Figure 10: Example of flooding maps retrieved for the subregion of Thessaloniki for a range of return periods.

Rivers' "sieve"

A thorough analysis of all rivers within the RCM would deliver the optimal scenario, as it would enable the display of a broad range of data transferable, and applicable across multiple phases of the risk

assessment process. Such an approach would also strengthen the accuracy of exposure and vulnerability estimations by providing inputs at a finer spatial scale. However, given the structural complexity of the river network, and taking into account that rivers often flow through multiple administrative sub-regions and multiple smaller tributaries converge into larger basins, the RCM adopted a more targeted approach focusing on the four (4) major river systems within the region. This strategy permits for a more manageable yet sufficiently representative estimation of flood events and their spatial extent across the RCM, ensuring that the outputs retain relevance for regional-scale planning and adaptation measures.

Table 4: Coordinates defining the bounding box for the three (3) major rivers of interest.

Coordinates	River
21.745205,39.983264,22.693325,40.597937	Aliakmonas
22.490455,40.490162,22.762367,41.144498	Axios
22.449188,40.51491,22.710354,40.686536	Loudias
23.070766,40.76667,23.885136,41.42891	Strymonas

The first step in the CLIMAAX workflow involved the calculation of the river flood potential for a selected range of return periods (that of 10, 50, and 100 years) representing the frequency of extreme events. In Figure *6*, a series of maps corresponding to each return period and for all selected rivers under study is presented.

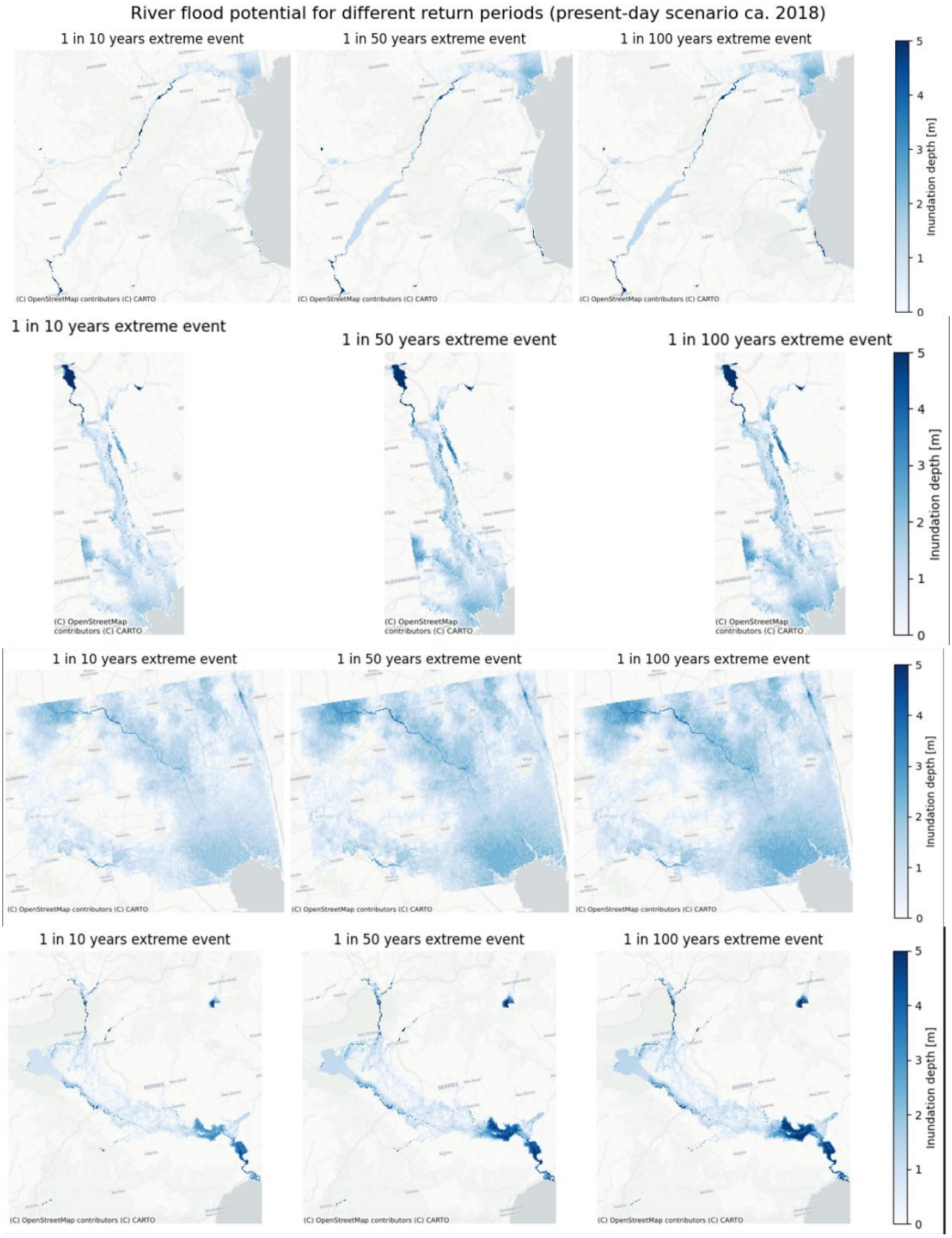

Figure 11: River flood potential for different return periods for four (4) selected main rivers in the RCM. From top to down: Aliakmonas, Axios, Loudias, and Strymonas.

For the Aliakmonas River (top row of figures), it is difficult to qualitatively assess the magnitude of the extreme flood event directly from the visualizations. However, it is evident that at the river's estuary, the transition from the “1-in-10-year” to the “1-in-50-year” return period reflects a modest increase in both intensity and spatial extent of the affected area. In contrast, the difference between the “1-in-50-year” and “1-in-100-year” scenarios appears minimal or not clearly discernible based on the available output maps. A similar pattern is observed for the Axios River. In this case, however, the river’s topography enables a more focused and detailed visualization, allowing distinctions between return periods to be more easily detected. The severity of the flood events increases noticeably as we move from the “1-in-10-year” to the “1-in-50-year” and subsequently to the “1-in-100-year” scenario. For the Loudias River, the trend continues but reveals a unique characteristic: the extent of the flooded area is exceptionally large, so extensive that the provided maps are insufficient to fully capture it. As with the other rivers, both the intensity and geographic spread of flooding increase significantly across higher return periods. This scenario highlights a potentially critical flood risk for the RCM, warranting dedicated preparedness, mitigation, and resilience measures. Finally, for the Strymonas River, the increased flood intensity is particularly concentrated at the lower reaches near the river’s estuary, as well as in the area downstream of Lake Kerkini and along the midstream course. This zone, characterized by agricultural activity and a dense network of tributaries, is especially vulnerable, given its role in regional food production. The flood risk in this area calls for strategic water management and robust adaptation planning to ensure long-term sustainability. In response to the projected hazards, the RCM will actively coordinating with local stakeholders, municipalities, and civil protection authorities to integrate these spatial flood risk assessments into participatory planning and regional adaptation strategies.

Estimating the effect of climate scenarios on the river flood hazard using the Aqueduct floods river flood maps

The objective of this step was to compare flood hazard maps for the four (4) selected rivers under a 250-year return period scenario, using the Aqueduct dataset (which is coarser in resolution compared to the JRC dataset), alongside a baseline historical scenario corresponding to the 1980

return period. The comparative results for all rivers are presented in Figure 12.

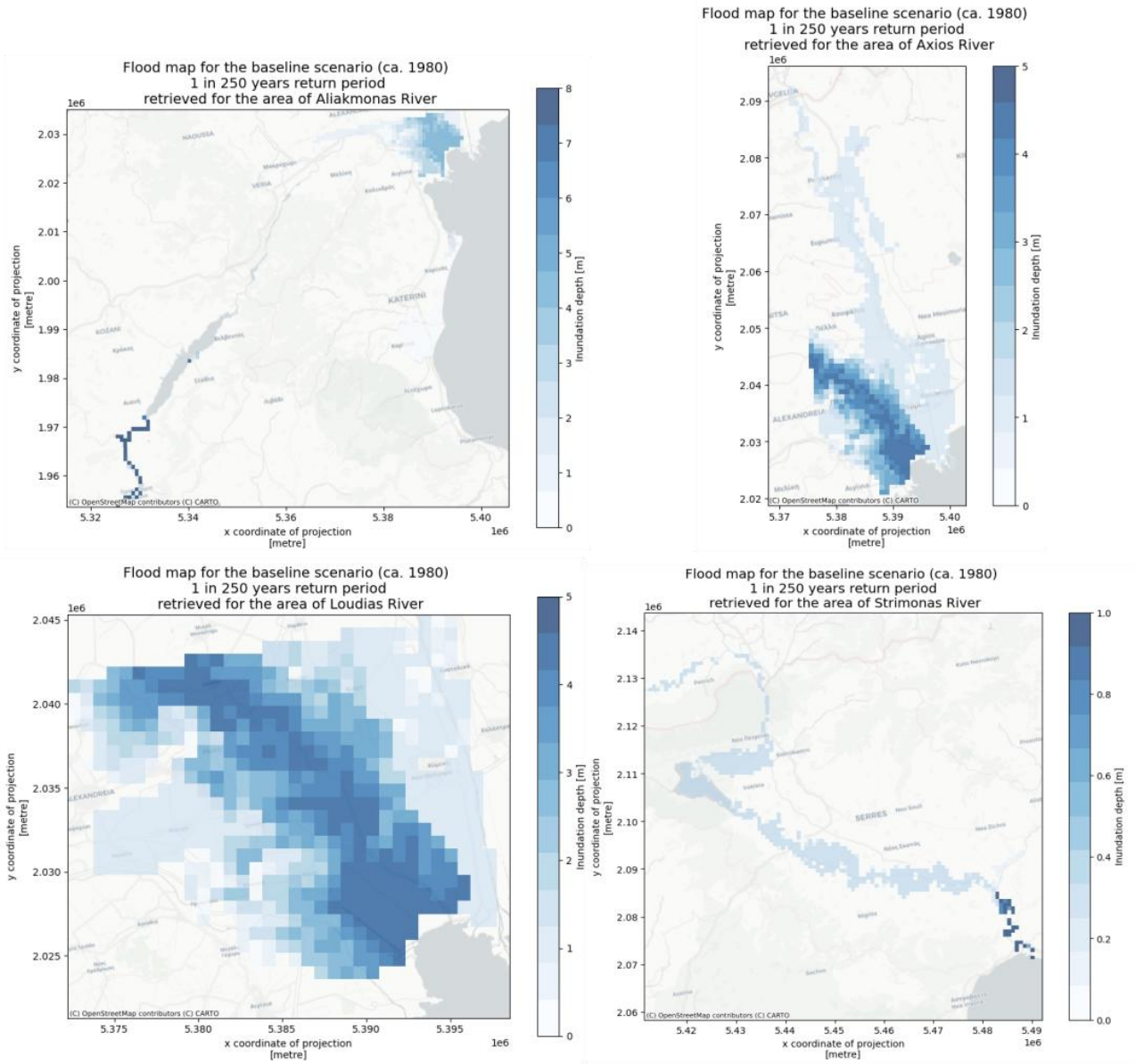

Figure 12: Flood map to baseline scenarios for all selected rivers. Top left represents Aliakmonas river, top right represents Axios river, down left represents Loudias river and finally, down right represents Strymonas river.

For the Aliakmonas river, the flood maps highlight areas at the river's upstream sections, where noticeable differences between the coarse and high-resolution datasets can be observed, particularly where pixelated dark blue zones indicate greater flood extent in the coarser dataset. In the case of the Axios river, the differences are even more pronounced. The downstream area, near the river's estuary, and adjacent regions across the administrative borders of Thessaloniki, Pella, and Kilkis show substantial discrepancies. In particular, the estuarine zone displays a nearly continuous swath of dark blue pixels, suggesting significant overestimation or generalization of flood extent in the coarse-resolution dataset. Similar findings are observed for the Loudias River, where a wide area of flood hazard appears more extensive in the coarse dataset, again highlighted in dark blue, emphasizing the limitations of lower-resolution spatial inputs. Finally, in the case of the Strymonas River, the flood hazard maps near the estuary exhibit some localized differences. In

certain areas, the coarse dataset suggests a larger flood extent, although the regional topography does not fully support this depiction, indicating potential inaccuracies due to resolution limitations. These observations underscore the need for high-resolution, locally validated data in flood risk analysis, and support the RCM's efforts to engage regional stakeholders, technical experts, and civil protection bodies in planning and implementing evidence-based flood resilience strategies.

In next step, the retrieval of a complete set of flood depth maps corresponding to a selected extreme return period ("1 in 250" years) was initiated. The objective was to estimate the projected changes in river flood potential due to climate change by comparing future projections against a historical baseline. This was achieved by systematically downloading and processing flood maps across a comprehensive set of combinations involving different climate models, emission scenarios, and time horizons. The models used in this analysis include: NorESM1-M (Norwegian Earth System Model version 1 - Medium resolution), GFDL-ESM2M (Geophysical Fluid Dynamics Laboratory Earth System Model version 2 - Medium resolution), HadGEM2-ES (Hadley Centre Global Environment Model version 2 - Earth System), IPSL-CM5A-LR (Institut Pierre-Simon Laplace Climate Model version 5A - Low Resolution), and MIROC-ESM-CHEM (Model for Interdisciplinary Research on Climate - Earth System Model with Chemistry). These were run under two (2) RCPs (Representative Concentration Pathways): RCP4.5 and RCP8.5, and across three (3) future periods: 2030, 2050, and 2080. Once the maps were downloaded, reprojected, organized, and preprocessed, the average flood depth across the ensemble of models for each scenario and time horizon was computed. This results in a single, representative flood map per combination of RCP and year, which can be used to visualize and quantify spatial flood hazard patterns under projected climate conditions. To evaluate the potential impact of climate change, the averaged future flood maps were directly compared against the baseline flood map associated with the same return period (i.e., "1 in 250" years around 1980). These comparisons were visualized in a series of plots, presenting inundation depths across 2030, 2050, and 2080 for the RCP4.5 and RCP8.5 scenarios. Additionally, difference maps were generated to highlight the spatial increase or reduction in flood risk relative to the historical benchmark, providing a clear indication of how flood hazards are expected to evolve in the coming decades under various emissions trajectories. Results for the RCP4.5 in the figures below, one for each river.

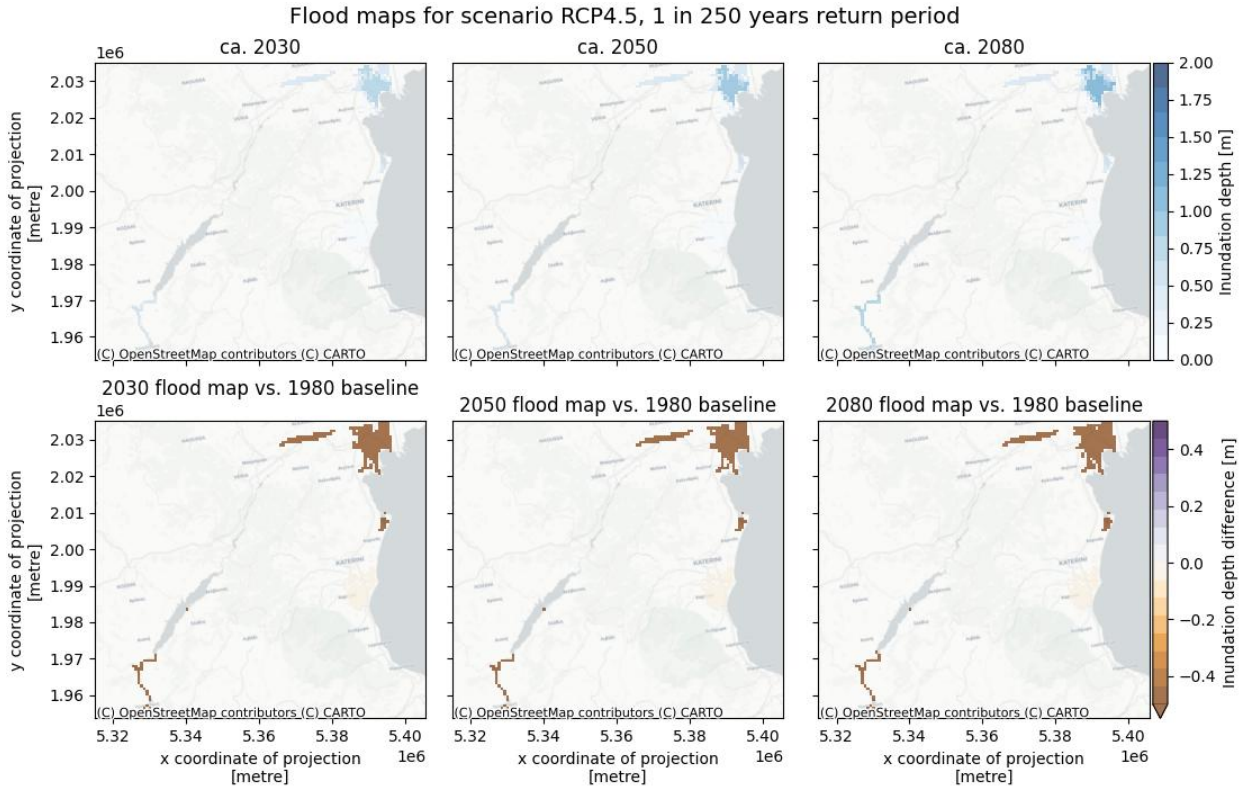

Figure 13: Comparison of projected flood maps for the Aliakmonas river under the RCP4.5 scenario, across three (3) future time horizons: 2030, 2050, and 2080.

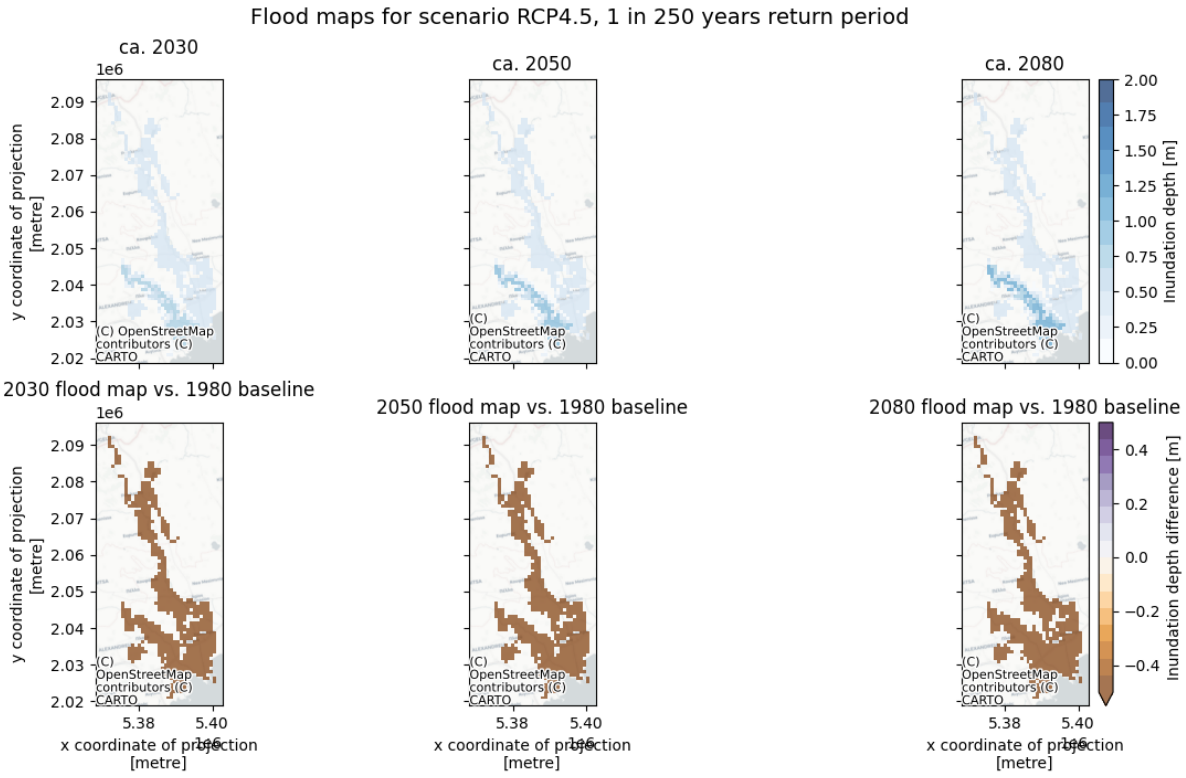

Figure 14: Comparison of projected flood maps for the Axios river under the RCP4.5 scenario, across three (3) future time horizons: 2030, 2050, and 2080.

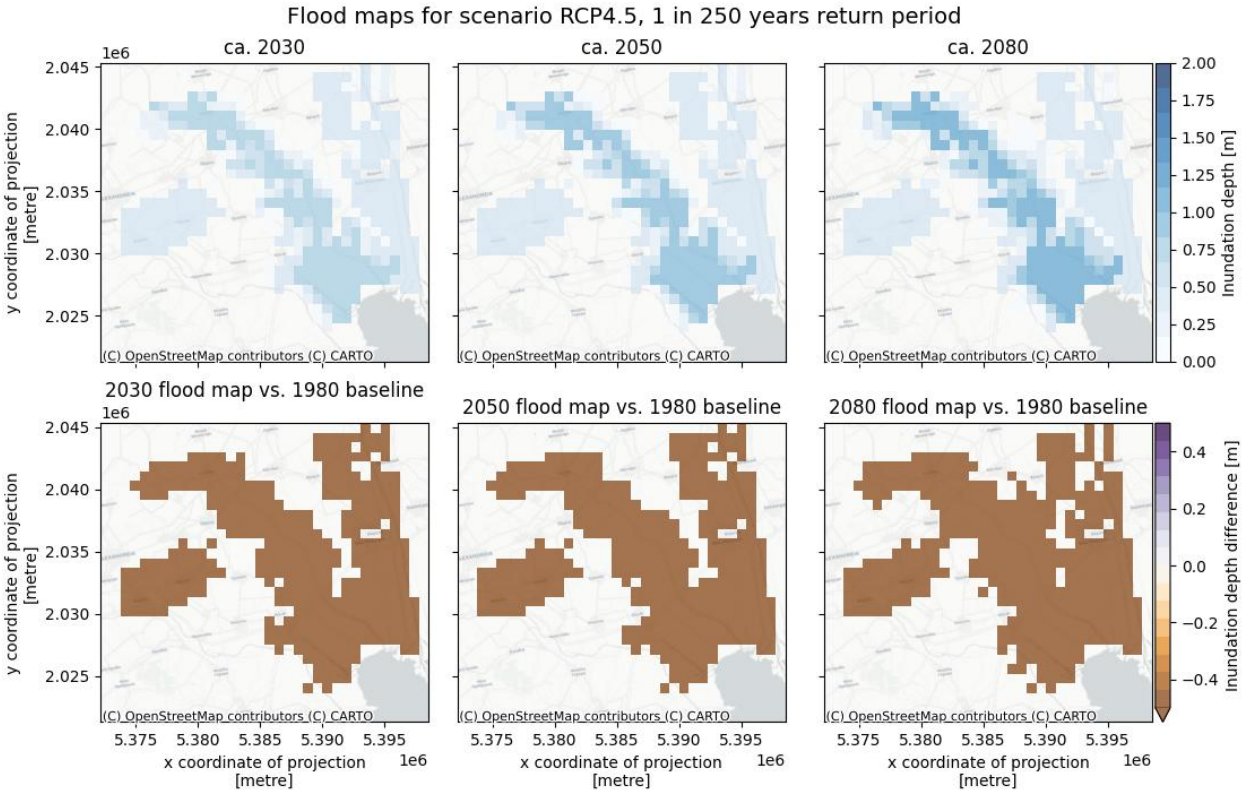

Figure 15: Comparison of projected flood maps for the Loudias river under the RCP4.5 scenario, across three (3) future time horizons: 2030, 2050, and 2080.

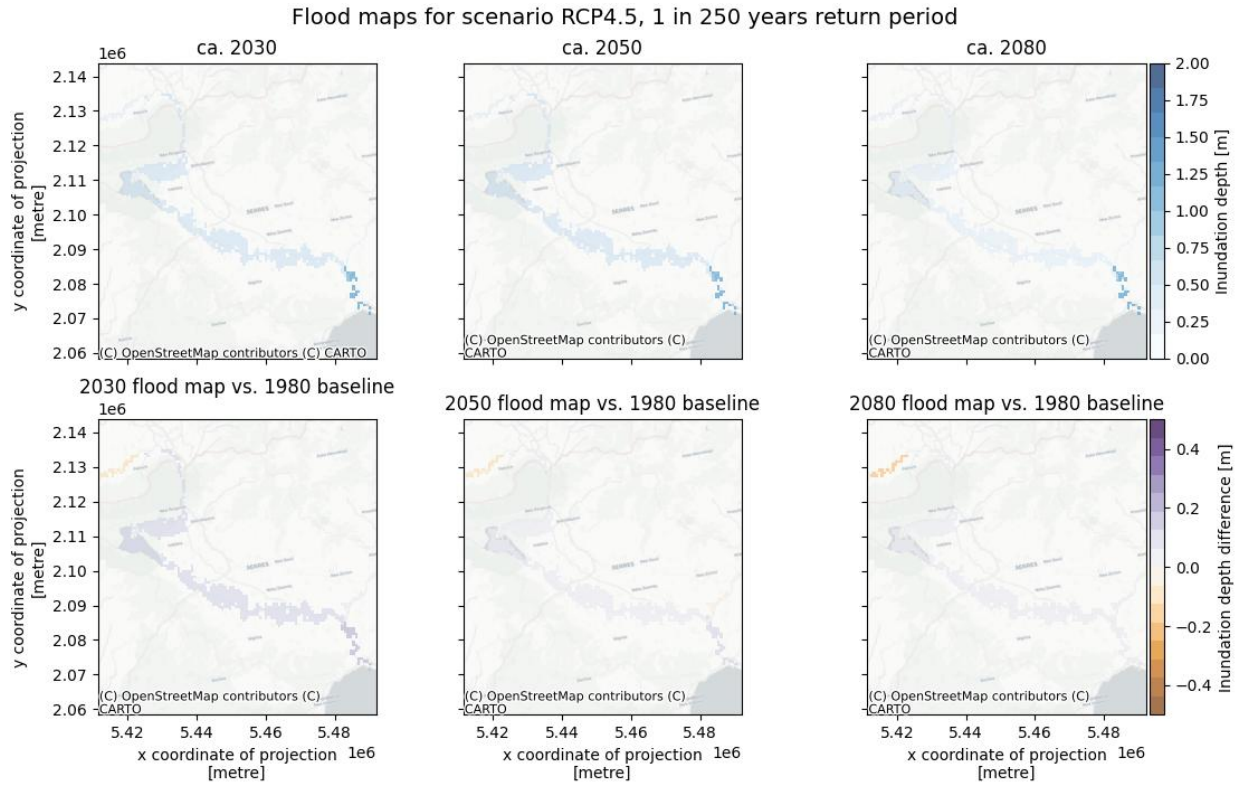

Figure 16: Comparison of projected flood maps for the Strymonas river under the RCP4.5 scenario, across three (3) future time horizons: 2030, 2050, and 2080.

A similar analysis has been conducted for the RCP8.5 scenario, following the same methodology applied under RCP4.5, across all four (4) selected rivers. The resulting flood maps are presented below.

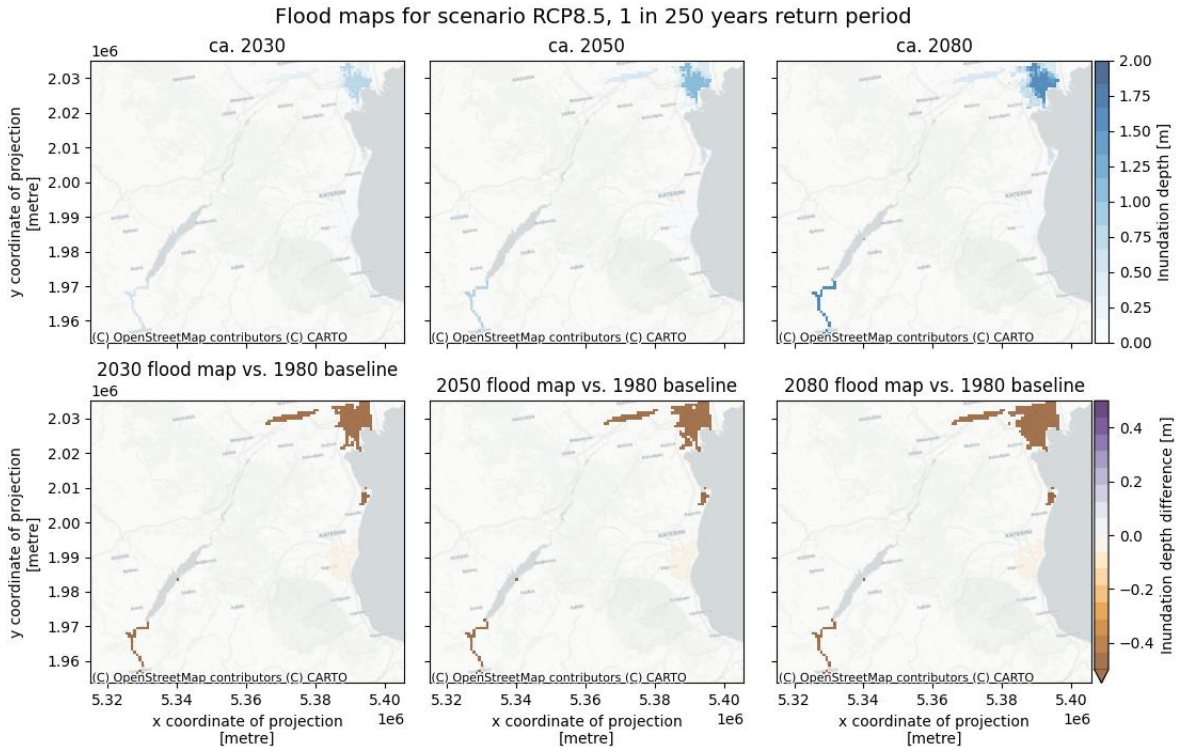

Figure 17: Comparison of projected flood maps for the Aliakmonas river under the RCP8.5 scenario, across three (3) future time horizons: 2030, 2050, and 2080.

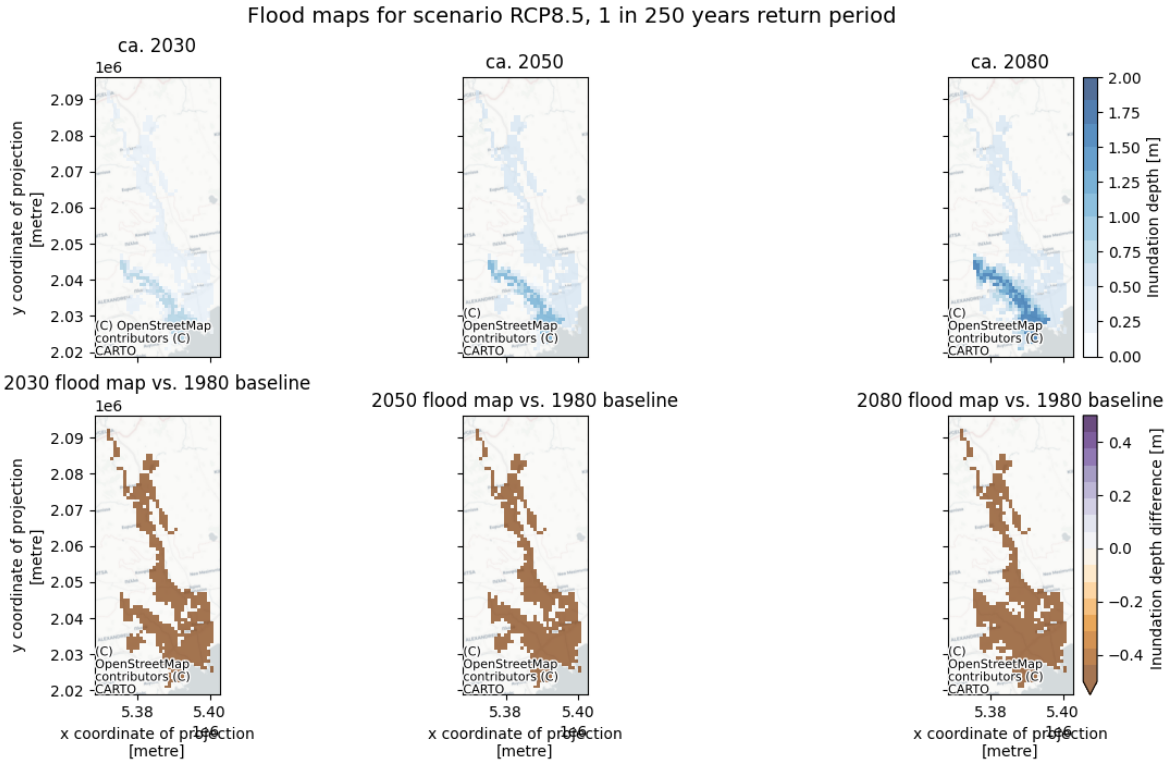

Figure 18: Comparison of projected flood maps for the Axios river under the RCP8.5 scenario, across three (3) future time horizons: 2030, 2050, and 2080.

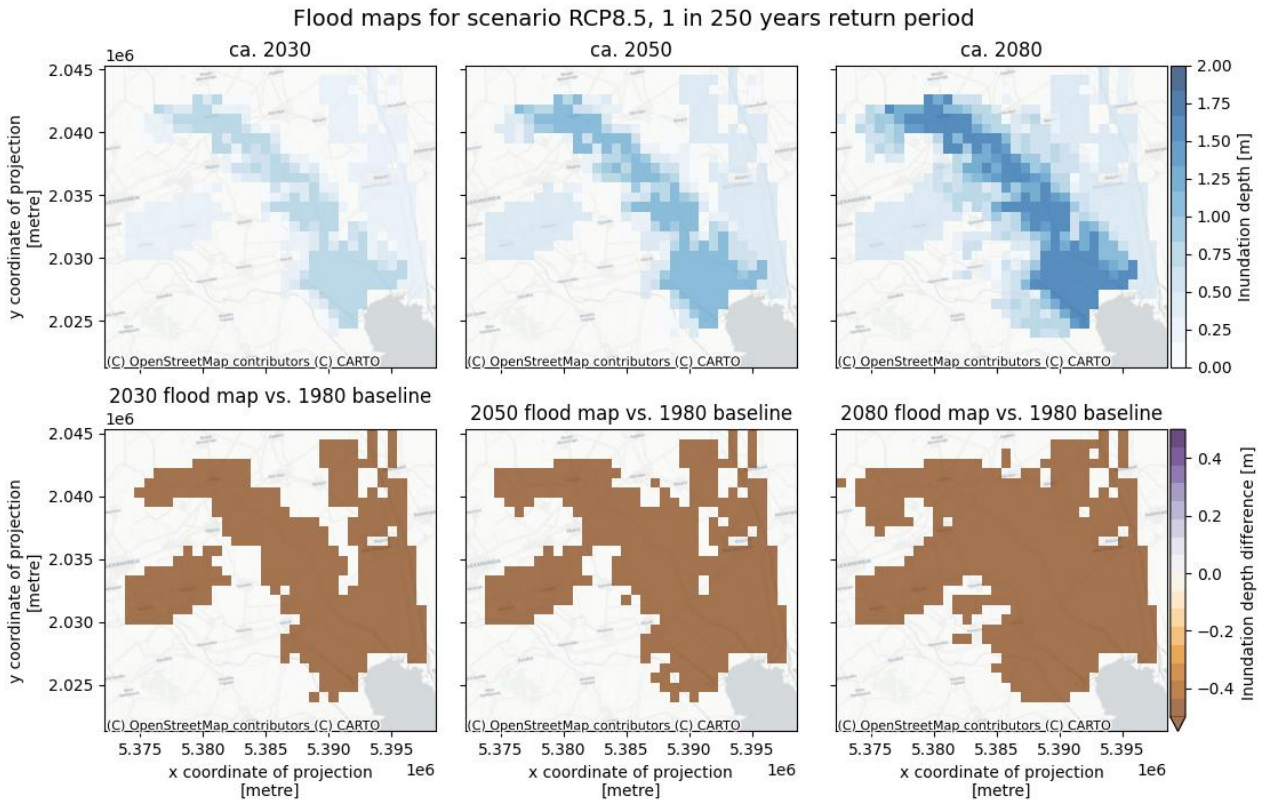

Figure 19: Comparison of projected flood maps for the Loudias river under the RCP8.5 scenario, across three (3) future time horizons: 2030, 2050, and 2080.

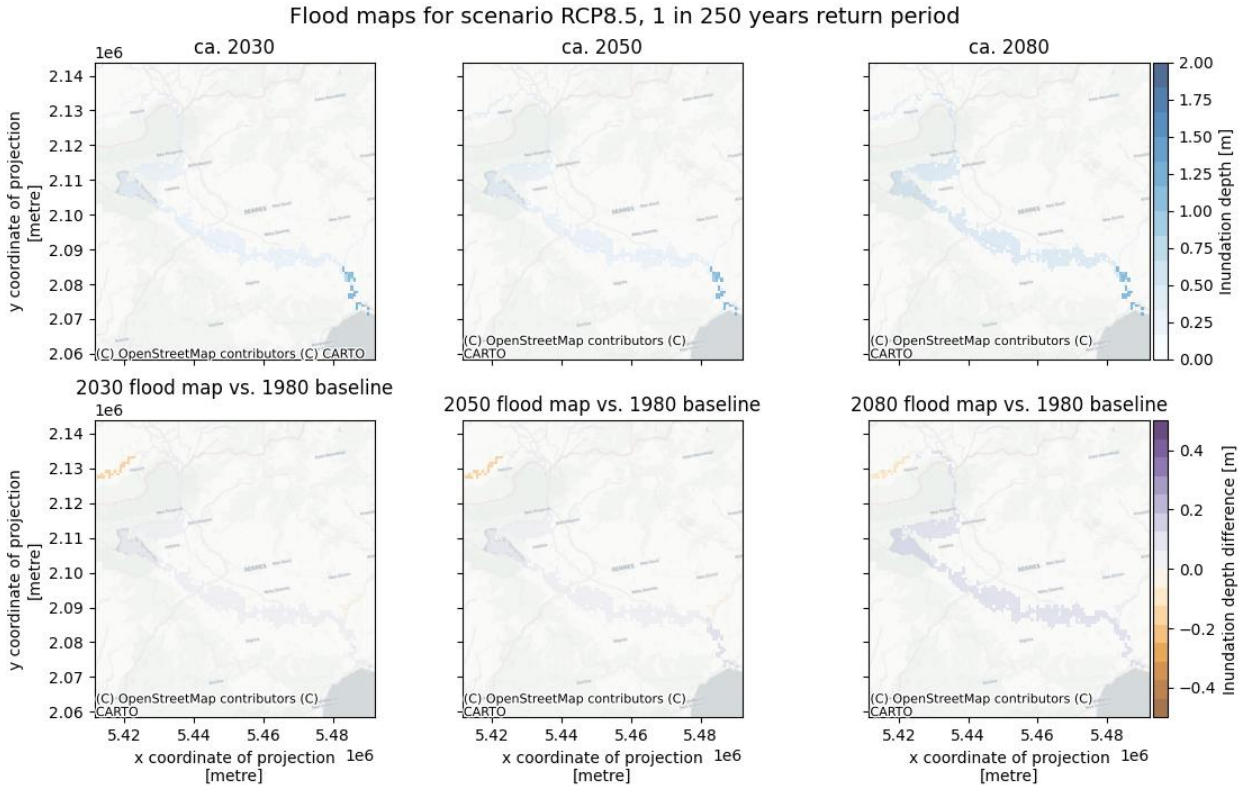

Figure 20: Comparison of projected flood maps for the Strymonas river under the RCP8.5 scenario, across three (3) future time horizons: 2030, 2050, and 2080.

To evaluate the evolution of river flood risk over time in the RCM, we examine two (2) climate change scenarios: RCP4.5 and RCP8.5, using projected flood maps for the years 2030, 2050, and 2080. We begin with the RCP4.5 scenario and assess the changes in flood intensity and spatial extent for each of the four (4) selected rivers in comparison to the 1980 baseline. For the Aliakmonas River, the flood maps from circa 2030 to 2080 indicate a moderate increase in flood intensity over time, although the spatial extent of the dark brown flood-prone areas shows only a slight expansion when compared to the baseline. A similar pattern is observed for the Axios and Loudias Rivers, where both the intensity and extent of flood hazards gradually increase with time, but the overall differences remain relatively small and consistent across the time horizon. In the case of the Strymonas River, the temporal comparison across 2030, 2050, and 2080 follows the same general trend. However, when comparing each time slice to the 1980 baseline, an unexpected reduction in the spatial extent of flood-prone areas is observed toward the river's lower reaches. This abnormal result may be attributed to limitations in map resolution or methodological artifacts and should be further examined when the RCM engages in decision-making for climate resilience planning and adaptation strategies. Comparable trends are observed under the RCP8.5 scenario for all four (4) rivers, without immediately noticeable differences based on the current visualization outputs. A detailed comparison between the RCP4.5 and RCP8.5 scenarios would require further in-depth analysis beyond the scope of the current mapping exercise to draw more conclusive insights.

Risk assessment

To assess exposure in the selected regions, the LUISA land use dataset as provided by the JRC was utilized. The dataset, available at a spatial resolution of 100 meters, provided detailed information on land use across Europe for the year 2018, including urban areas, agricultural land, infrastructure, natural vegetation, and water bodies. The data are retrieved programmatically and stored locally to facilitate processing and integration with the risk assessment workflow. For each river basin, the land use raster is clipped to the corresponding area of interest and reprojected to the dedicated system. A specific color scheme was assigned to the different land use categories (CLC codes) to support visual interpretation. The resulting land use maps representing the LUISA cover for each river, enabled a clear understanding of the spatial distribution of human and natural land use types, which was essential for identifying vulnerable assets and planning risk mitigation strategies. In Figure *21* below the land use cover for each river region can be seen.

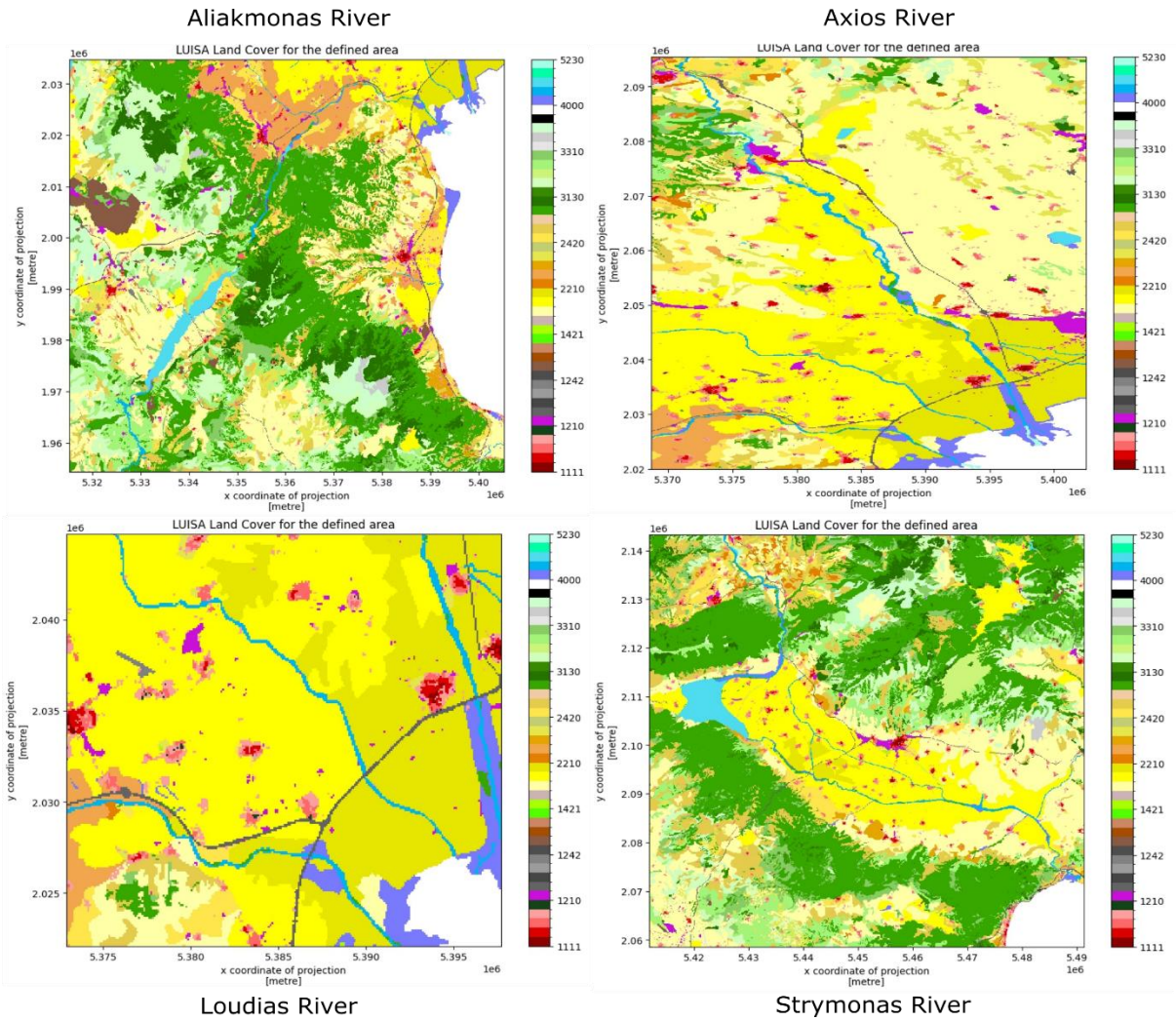

Figure 21: Land cover maps for the selected rivers in the RCM.

Vulnerability – *Flood Damage Curves for Land Use Types*

In the context of flood risk assessment, vulnerability was quantified through damage curves and empirical or model-derived functions that relate flood intensity (typically water depth) to the expected percentage of damage for different land use types. The pre-defined damage curve was utilized based on JRC data, which are available in the official CLIMAAX repository and directly integrated into the analytical pipeline. The JRC vulnerability curves were imported into a Python data frame and represent damage relationships for different building types, namely residential, commercial, and industrial. To make these applicable to the land use typologies defined in the LUISA 2018 dataset, the vulnerability curves were adjusted accordingly. This adjustment involved the following steps: (i) each LUISA land use class was matched to a corresponding composition of building types; (ii) based on this composition, a weighted damage curve was generated for each LUISA category by combining the individual JRC curves according to the building type shares; (iii) the output was a harmonized set of vulnerability curves tailored to the LUISA land cover categories, enabling a direct estimation of potential damage from flood depth. A scheme of the JRC curves can be seen in Figure 22.

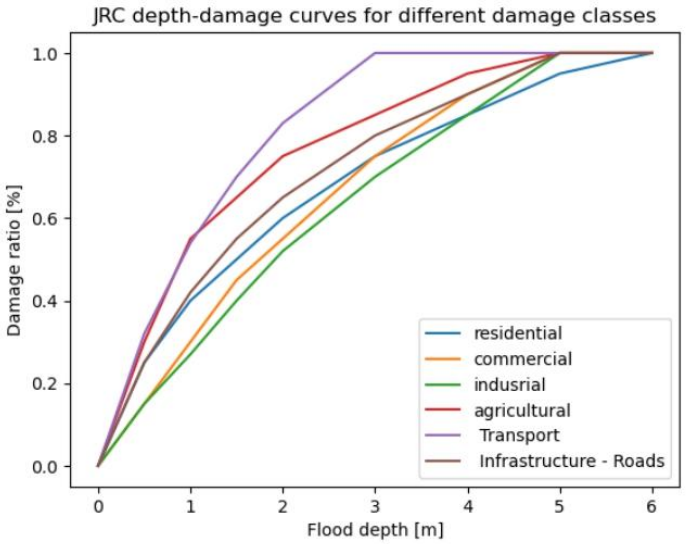

Figure 22: Depth-damage curves as given by the JRC.

These adjusted vulnerability curves were then used to compute economic damage maps. This requires aligning the spatial resolution and extent of the flood hazard and land use datasets. The flood depth maps, originally at a 30, 75 m resolution depending on latitude, are resampled and reprojected to match the regular 100 m grid of the LUISA maps, ensuring compatibility of pixel-wise calculations. As a result, a set of damage maps is generated for different return periods, namely RP10, RP50, RP100, RP200, and RP500. These maps express the expected flood-induced economic loss in euros per pixel, based on both the flood depth and the land use classification. In the table below the first 10 rows of the resulting DataFrame to view are presented and in Figure 23 the vulnerability curves for the first 10 land cover types for flood damages for the LUISA land cover types can be seen.

Table 5: Maximum damage for reconstruction in €/m² for the first land use codes.

Land use code	total €/m²
1111	435.471384
1121	301.449853
1122	177.769315
1123	50.409522
1130	0.000000
1210	288.913514
1221	28.666369
1222	401.329170
1230	171.998216
1241	401.329170

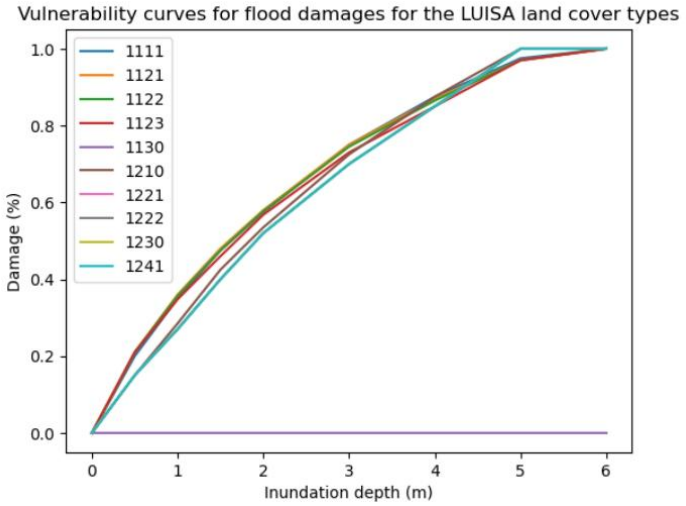

Figure 23: Vulnerability curves for the first ten (10) LUISA land cover types given following the methodology based on the "*LUISA_damage_info_curves.xlsx*".

Calculate potential economic damage to infrastructure

To estimate the potential economic damage to infrastructure caused by river flooding, the DamageScanner Python library was employed. This tool facilitates spatially explicit damage calculations by integrating hazard, exposure, and vulnerability data into a unified framework. The following inputs were required by DamageScanner:

- The clipped and resampled flood depth maps, aligned to the LUISA 100m land use grid.
- A set of vulnerability curves calibrated for each LUISA land use category.
- A table specifying the maximum damage value (in euros) per land use class.

Once the damage calculation was performed across all scenarios and return periods (i.e., RP10, RP50, RP100, RP200, and RP500), the resulting loss data frame contains the estimated economic losses for each land use category, expressed in euros. To facilitate interpretation, the following processing steps were applied:

- The LUISA legend was merged into the damage results to provide human-readable land use descriptions.
- All values were converted into million euros for reporting consistency.
- The table was sorted by damage magnitude, based on the scenario with the highest estimated losses.
- Only the top 10 land use classes with the highest economic exposure were displayed in the table.

The final results of the economic loss calculations for all return periods and all rivers are presented in the tables below, allowing direct comparison of the relative impact across different flood intensities.

Table 6: Codes with the largest economic damages for Aliakmonas river.

	Description	RP10	RP20	RP30	RP50	RP100	RP200	RP500
130	Rice fields	1035.916025	1152.990911	1207.099612	1265.804138	1332.560737	1392.885978	1464.968875
2120	Permanently irrigated land	569.623420	719.979039	800.018095	891.164119	1003.875059	1116.845243	1264.079935
2220	Fruit trees and berry plantations	253.475938	309.063998	338.546815	375.301292	423.983863	465.014170	516.938575
4000	Wetlands	335.201692	362.381197	376.433554	390.248010	406.936094	423.209001	447.266543
1210	Industrial or commercial units	146.616650	177.682627	193.348213	210.158733	234.347462	257.305424	280.814231
2420	Complex cultivation patterns	105.069614	139.675426	158.782657	181.478352	210.770715	238.123277	275.118533
2110	Non irrigated arable land	115.014472	131.365759	138.807616	147.700027	157.960832	167.284077	178.301408
1123	Isolated or very low density urban fabric	46.821502	59.554770	66.715528	76.174546	89.824805	104.597734	121.459199
1122	Low density urban fabric	37.886435	48.538653	57.280305	66.764471	79.365053	90.180566	110.192934
1330	Construction sites	17.416434	24.551749	33.094807	41.732887	57.504144	72.282329	88.946381

Table 7: Codes with the highest economic damages for Axios river.

	Description	RP10	RP20	RP30	RP50	RP100	RP200	RP500
2120	Permanently irrigated land	3365.961944	3780.606959	3997.789948	4254.210896	4565.485581	4847.910708	5176.619576
2130	Rice fields	2270.792076	2535.580368	2670.282430	2815.848073	2984.362282	3136.884825	3324.300677
2110	Non irrigated arable land	595.492873	653.386523	679.182604	712.219153	751.912629	786.281259	820.668852
1210	Industrial or commercial units	311.330200	366.252554	399.147752	430.373141	475.226551	515.520797	567.972924
4000	Wetlands	368.109364	415.846833	438.166116	462.509416	489.512992	515.001309	546.853001
2420	Complex cultivation patterns	132.795314	147.988382	155.445472	162.901094	172.075311	179.055293	187.855727

1122	Low density urban fabric	54.927120	73.220486	85.415587	102.550167	125.436397	145.292011	171.672099
2310	Pastures	102.278446	114.826298	119.982379	125.973543	133.250778	140.060455	148.314031
1123	Isolated or very low density urban fabric	71.101844	83.773420	92.022613	101.652389	113.370479	125.136979	139.459236
1121	Medium density urban fabric	14.640759	21.439737	23.685236	28.542986	40.100237	56.230545	78.176438

Table 8: Codes with the highest economic damages for Loudias river.

	Description	RP10	RP20	RP30	RP50	RP100	RP200	RP500
2120	Permanently irrigated land	1633.623458	1861.033858	1977.540641	2112.791723	2275.659511	2423.423485	2593.894704
2130	Rice fields	1565.704674	1732.475641	1812.905583	1901.007782	2003.109756	2094.129240	2200.929281
1210	Industrial or commercial units	97.680311	117.884245	129.554846	143.391821	164.174154	182.918718	206.650108
4000	Wetlands	114.173252	128.095777	134.880947	142.475421	151.309915	159.220997	169.006629
1241	Airport areas	35.415697	50.333064	58.448993	67.423954	77.513310	86.996384	97.647470
1122	Low density urban fabric	29.163473	37.084114	41.691892	47.007496	55.623423	63.901877	74.249864
1123	Isolated or very low density urban fabric	30.191168	36.835885	40.522080	45.467318	51.586949	57.394190	64.991580
2110	Non irrigated arable land	30.133782	32.961792	34.429602	36.007675	37.884108	39.676194	41.563641
1221	Road and rail networks and associated land	20.120083	24.007627	25.953490	28.361344	31.494125	34.497874	38.356340
1121	Medium density urban fabric	6.490846	11.863652	15.328563	19.977272	25.611602	30.758914	36.215648

Table 9: Codes with the highest economic damages for Strymonas river.

	Description	RP10	RP20	RP30	RP50	RP100	RP200	RP500
2120	Permanently irrigated land	4634.393463	5328.477557	5703.988124	6131.963798	6655.884719	7145.513116	7727.394193
2130	Rice fields	307.025992	351.371373	373.060711	398.868873	429.908530	458.897979	494.748727

2110	Non irrigated arable land	264.770615	308.989031	333.343926	361.145511	399.730806	435.936679	485.639401
4000	Wetlands	220.898011	242.190387	252.652320	264.378195	280.964197	295.966442	312.112455
1122	Low density urban fabric	107.896207	128.246149	140.077342	153.599221	172.213196	190.714919	216.445840
2430	Land principally occupied by agriculture	93.929593	102.855487	108.093917	114.805285	123.349852	131.540873	140.546849
2420	Complex cultivation patterns	83.934660	94.607833	99.376529	104.662880	111.074290	117.076889	124.289193
1123	Isolated or very low density urban fabric	61.148019	73.372304	80.516490	88.562055	99.227215	109.134601	121.152902
1121	Medium density urban fabric	41.557999	46.072406	51.339265	54.959906	60.043441	65.318970	71.687808
3230	Sclerophyllous vegetation	38.710969	41.417181	42.213248	43.476445	44.715388	45.685847	47.294605

Estimated economic damages (in million euros) by LUISA land use class for all selected rivers, calculated using the DamageScanner tool for five return periods (RP10 to RP500). Values reflect the maximum potential losses based on calibrated vulnerability curves and JRC land use data. Tables 5 through 8 present the estimated economic damages from river flooding for the four (4) major river basins in the RCM based on the LUISA land use codes and a range of return periods (RP10 up to RP500). The results revealed consistent patterns of exposure and vulnerability that have direct implications for spatial planning and regional adaptation strategies. Among all land use categories, permanently irrigated land (Code 2120) and rice fields (Code 2130) account for the highest damage values across all basins. In particular, the Strymonas basin records the highest overall damages for Code 2120, exceeding €7.7 billion by RP500. This figure notably surpasses the corresponding values for Axios (€5.1 billion) and Loudias (€2.6 billion). Similarly, rice cultivation areas in Axios and Loudias contribute substantially to flood-related losses, while Aliakmonas records its highest damages in this category reaching €1.46 billion by RP500. Industrial and commercial units (Code 1210) represent another highly exposed category, particularly in the Axios and Aliakmonas basins, where built-up zones intersect flood-prone areas. Additionally, urban fabric classes (Codes 1121, 1122, and 1123) show consistent, though moderate, levels of damage across all rivers, indicating widespread exposure in peri-urban settlements. Wetlands (Code 4000), although not typically associated with direct economic output, also appear among the top affected classes. Their inclusion reflects the spatial coincidence between flood extents and ecologically sensitive zones, reinforcing their relevance in both flood modeling and ecosystem-based adaptation approaches. These findings support the prioritization of targeted resilience measures in high-risk areas, especially in agricultural zones under Codes 2120 and 2130, and critical infrastructure categories such as Code 1210. Such prioritization will be essential in the development of integrated risk management strategies for RCM under current and projected climate conditions. The flood maps and the associated damages for extreme river water level scenarios for “1 in 100” year extreme event combined with the land cover maps can be seen in Figure 24.

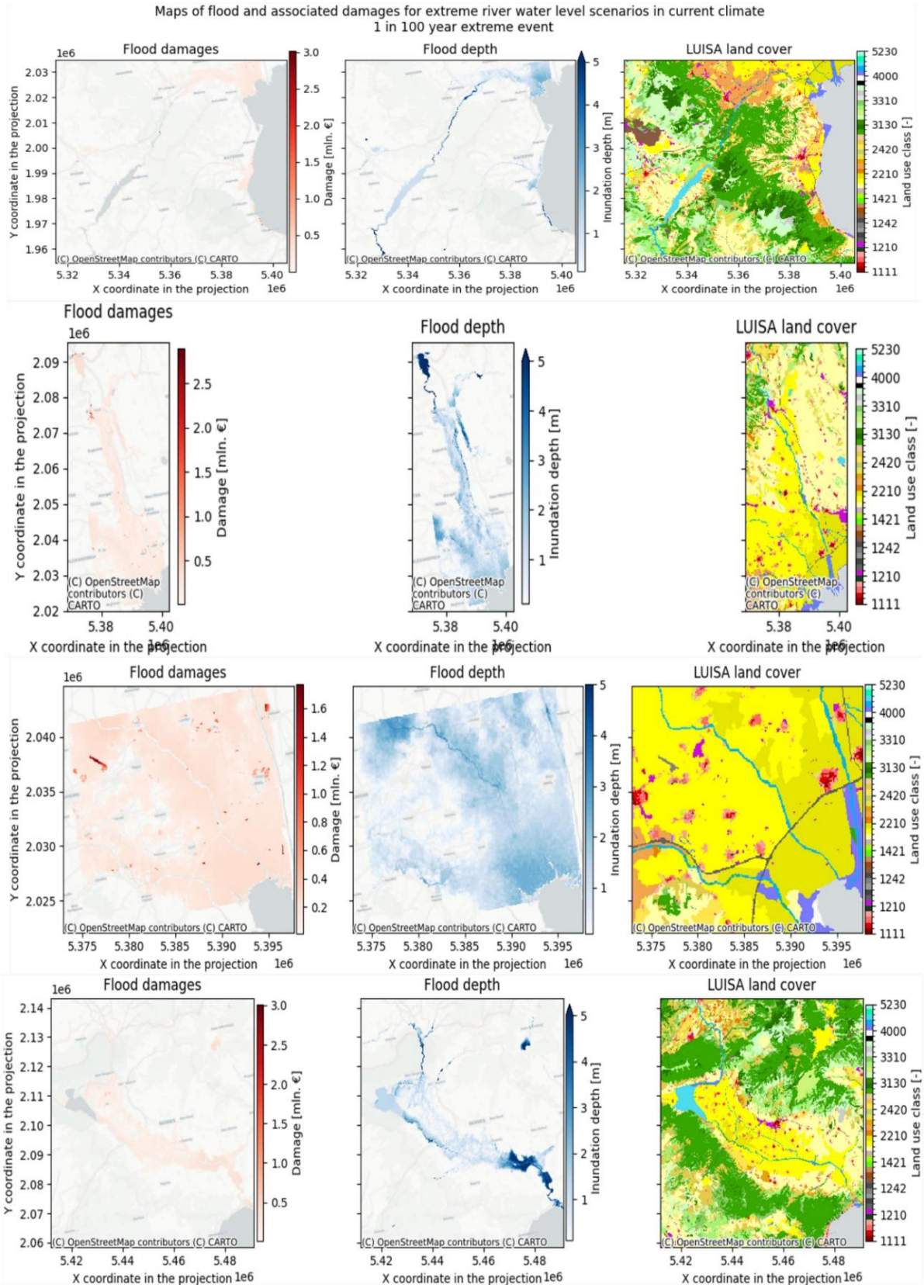

Figure 24: Overview maps showing modeled flood extent, inundation depth (up to 5 meters), and estimated economic damage for a “1-in-100-year” flood event under current climate conditions. These outputs are presented for the RCM, enabling spatial prioritization of adaptation measures.

The concluding step of this workflow links the flood hazard maps, land use data, and vulnerability estimates to evaluate the potential economic damages associated with a "1-in-100-year" river flood event under current climate conditions. As illustrated in Figure 24, this integrated visualization combines flood extent, inundation depth, and land use to provide a comprehensive spatial overview of risk exposure in the RCM. The final visual outputs include:

- A flood damage map indicating the estimated financial losses for the selected return period.
- A map showing maximum flood depths across the region.
- A corresponding land use map, colored by LUISA classification, helping to contextualize the source of damages.

This tri-panel approach allows for a sounder understanding of spatial disparities in risk. For instance, areas showing moderate flood depths may still produce substantial economic losses if they overlap with high-value land use types, such as irrigated farmland or industrial zones. Conversely, some zones with greater inundation depth may exhibit comparatively lower damages if the exposed land uses are of lower economic value or ecological rather than productive in nature. Across all four (4) river basins examined, the analysis consistently identifies irrigated croplands and rice cultivation areas as the most affected categories in terms of monetary loss. This reflects both the location of these agricultural areas in low-lying flood-prone regions and their relatively high replacement costs. Industrial and commercial land uses are also highly exposed, particularly in proximity to urban centers such as Thessaloniki and Serres. The results offer useful insight into how land use and flood hazards interact to shape risk. They also highlight the importance of aligning high-resolution land cover data with flood modeling outputs to produce actionable risk metrics. While the European-scale flood maps provide a valuable baseline, their precision at the regional scale may be constrained by local factors such as drainage infrastructure, topography, or unmodeled hydraulic dynamics. This underscores the need to critically assess:

- The spatial accuracy of flood predictions for the specific physiographic and infrastructural conditions of RCM.
- The completeness of exposure data, especially for critical infrastructure and vulnerable communities.
- The validity of applying general danage curves to specific regional contexts.

Despite these limitations, the workflow demonstrates a coherent method to estimate flood-related damages by combining hazard, exposure, and vulnerability components. This approach provides a sound foundation for future planning decisions and can be refined further with locally verified datasets.

2.2.2.1.2 Coastal floods

The coastal workflow relied on the subsections of the CLIMAAX workflow for coastal floods, and specifically the hazard assessment for water levels and floods maps and the risk assessment for the coastal floods. The template combined sea level rise projections (SLR), Digital Elevation Models (DEMs), and exposure and vulnerability datasets to assess the risk of sea-induced flooding. The methodology evaluated the spatial extent and economic impact of coastal inundation under current and future scenarios.

Hazard assessment - Water level (extreme sea levels and SLR)

The initial component of the coastal flood hazard workflow assesses extreme sea level events and future sea level rise to determine coastal flood thresholds. The expected data sources that the expert team that was appointed included the GTSMv3.0 (Global Tide and Surge Model for current sea level extremes), and the NASA Sea Level Projection Tool (Global Sea level rise projections) based on IPCC (Intergovernmental Panel on Climate Change) pathways). For three (3) scenarios, those of short- (2030, low emissions or historical baseline), mid-(2050, SSP2-4.5), and long-term (2100, SSP5-8.5), time series data of sea level and tidal components for the RCM coastline extracted to derive the return levels events via statistical models. Then, the projected SLR increments (e.g., +0.44 m under SSP2-4.5 by 2100) were added to derive future thresholds. The result is a set of sea surface height thresholds (in meters) for application in flood extent modeling.

Hazard assessment – Coastal Flood Maps: the sea level thresholds and coastal flood extremes based on elevation data and surface modeling were calculated by using data sources such as (i) EU-DEM v1.1, and (ii) Global Flood Maps (JRC). The methodology initiated using static inundation to delineate flooded areas where pixels below sea level threshold connected to the cost pixels classified as inundated. Map flood extends, and depth rasters for each scenario (baseline and future) were created, resulting in output rasters for flood extent and flood depth.

Exposure assessment: the exposure estimation identifies which land uses, populations, and assets will fall within the flooded and potentially damaged areas under each case selected scenario. Data sources such as the LUISA Land Use dataset and others such as population grids, and OSM infrastructure were used when needed. The methodology was initiated by a raster overlay between flood depth and land use grids, where each flooded cell was assigned a land use class and corresponding exposure value. Then, categorical and spatial analysis quantified the total surface, the population, and/or the economic sector exposure for each case-selected scenario. This step created tables and maps of exposed land use types (e.g., residential, commercial, agricultural) within each inundation zone.

Vulnerability assessment: this component translated physical exposure into economic damages based on the sensitivity of the land use to flood depth. JRC coastal depth-damage functions and land cover specific to a GDP-based calibration file were considered. The methodology was initiated by matching each flooded land use cell to a depth-damage curve. Then, the economic loss was calculated as the product of the asset value multiplied by the damage ratio. If possible, a region-specific calibration would improve and result in a more realistic outcome.

Risk calculation: risk was calculated in terms of monetary losses by integrating hazard (depth), exposure (land use), and vulnerability (damage ratio). Hazard and land use rasters were loaded, and aligned to the expected resolutions and coordinate systems. Each cell with its vulnerability function was matched and the damage was computed at pixel level, aggregated to regional scale if necessary. The expected outcome was summarized in raster maps where the economic losses in terms of €/ha or €/cell were presented, and summaries by land use, region, and scenario will be concluded in dedicated tables. The total outcomes from the coastal flood subsection included: (i) flood hazard maps (extent and depth under baseline and future sea levels), (ii) exposure maps, (iii) maps representing spatial distribution of economic loss, (iv) risk tables (including total and per land use), and (v) time-series projections of coastal damage under SSPs. These outputs provide the basis to potentially support climate adaptation, zoning, insurance planning, and critical infrastructure

protection. In the RCM coastal flooding risks were concentrated along the wide areas of coastline including the Thermaic Gulf coastal municipalities, particularly low-elevation zones west and south of the city of Thessaloniki, industrial zones and wetlands adjacent to the Axios River Delta, and tourism areas and vulnerable residential developments in peri-urban coastal settlements especially in the regions of Chalkidiki (a high NUTS3 index value area) and Pieria. The exposed groups and assets include permanent and seasonal populations in low-lying housing zones, coastal road networks, wetlands and protected ecological habitats, tourism infrastructure, and small business facilities dependent on their income on the coastline activities. This comprehensive workflow enables regional authorities to assess, visualize, and mitigate coastal flood risks under climate change, integrating the outputs into regional spatial plans, investment prioritization, and long-term resilience strategies.

Hazard assessment

Coastal water levels and coastal flood maps

The first step of this hazard assessment sub-workflow focuses on the extreme water levels and sea lever rise, allowing for any potential detection of changes in the water level in the coastal locations and for exploring scenarios of sea level rise by comparing the output of the selected scenarios. Two (2) main datasets initiate the procedure: (1) the water time series based on reanalysis climate data (representing the typical range of water level), and (2) the statistical indicators as derived from the water level timeseries (representing statistics for extreme water levels). The region of interest will have the following coordinates as specified in WFS84 coordinates:

```
bbox = [21.6495,39.904,24.4137,41.5807]; areaname = 'RCM'
```

All datasets have been sources from the Copernicus Climate Change databases. In accordance with the methodology outlined in the CLIMAAX Handbook, the time series of water levels for all months of the year *2015* have been downloaded using information from approximately 43.119 stations globally. The following figure presents the daily maximum water levels for the year 2015, referenced to the mean sea level over the period 1986–2005, and accounting for sea level rise.

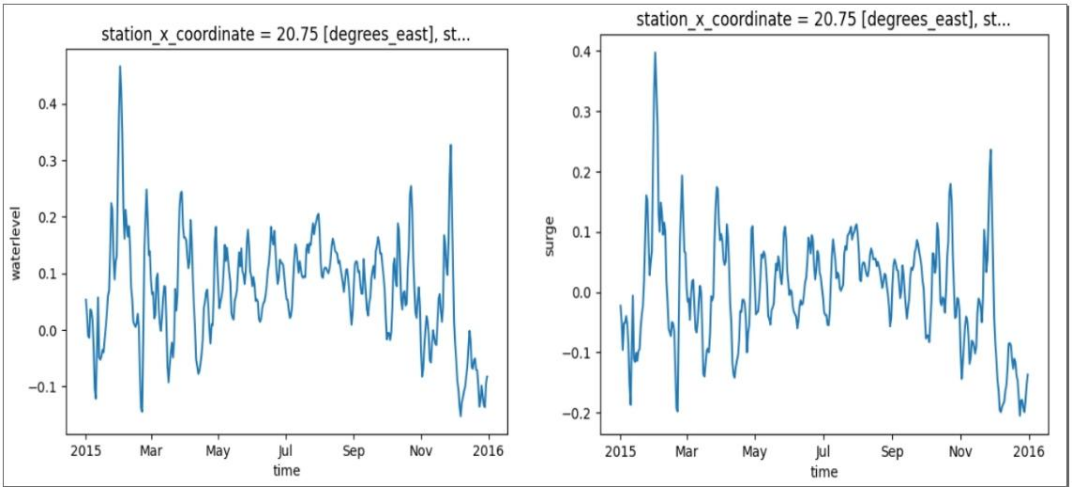

Figure 25: Daily maximum water levels (left) and corresponding surge levels (right) for the year 2015 at the selected location, relative to the mean sea level over 1986–2005. Both datasets incorporate the effects of sea level rise.

Figure 3 illustrates the variability of daily maximum water levels (left-side) and surge levels (right-side) throughout 2015 at the RCM. The water levels are primarily influenced by tidal fluctuations, while the surge component reflects variations are linked to storm events. Water level statistics derived from ERA5 covering the period 1979–2018 were used to estimate extreme sea levels for the region of interest. After selecting the relevant observation station from a dataset comprising approximately 43.000 locations, the following estimates were obtained: for a 5-year return period/100-year return period, the extreme water level was approximately 0.4 meters/0.5 meters above mean sea level. These estimates were referenced to the mean sea level around the year 2000 and do not yet include the contribution of future sea level rise, which should be added separately to project future extreme conditions.

The second step of the hazard assessment sub-workflow focuses on using global flood maps[9] for two (2) scenarios: (1) Present-day climate (ca. 2018), and (2) Climate in 2050 under RCP8.5 climate scenario. The search was restricted to the MERIT-DEM (Multi-Error-Removed Improved-Terrain DEM) at 90 m resolution. The dataset was converted to a geospatial array, unnecessary coordinates were removed, and the data were reprojected to the European projected coordinate system for accurate mapping in meters. Figure 4 (left) depicts a representative example of a floodmap retrieved for the RCM. A “zoomed-in”/cropped version of the same representative example is shown in Figure 4 (right), focusing on the coastal area surrounding the metropolitan region of the Thessaloniki regional unit, including a limited section of the coastal borders shared with adjacent regional units.

[9] Global flood maps are accessible via API from the Microsoft Plenary Computer: https://planetarycomputer.microsoft.com/dataset/deltares-floods.

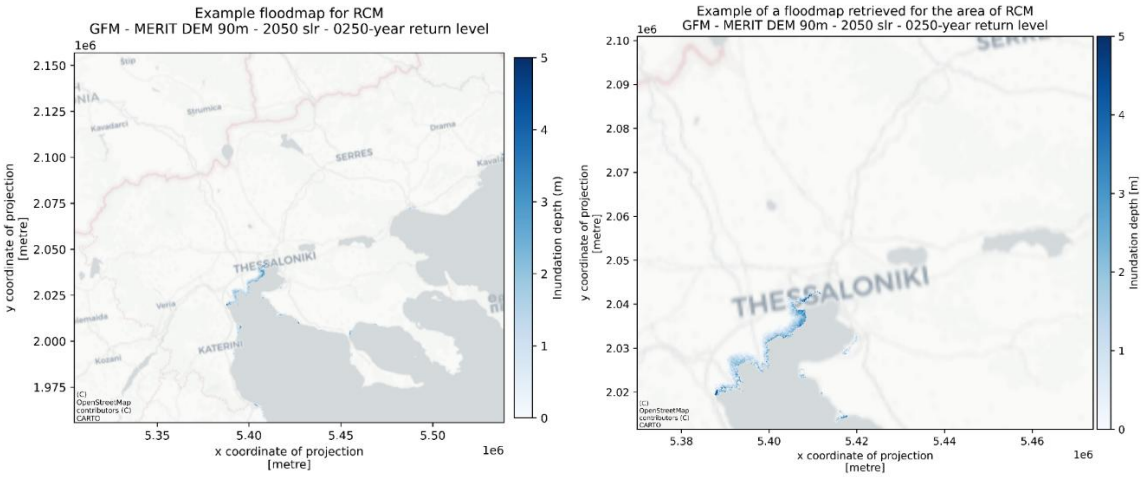

Figure 26: (left) Example flood map for the RCM (left). Example of a floodmap retrieved for the area of RCM, focused on the Thessaloniki regional unit's coastline.

In the final part of the hazard assessment for the coastal flooding, maps were retrieved and processed for the RCM under different scenarios and return periods. Datasets were obtained for both the present-day scenario (2018) and a future scenario (2050) reflecting sea level rise projections under a high-emission pathway (RCP8.5). Selected return periods included 2, 10, and 100 years, capturing a range of extreme event probabilities.

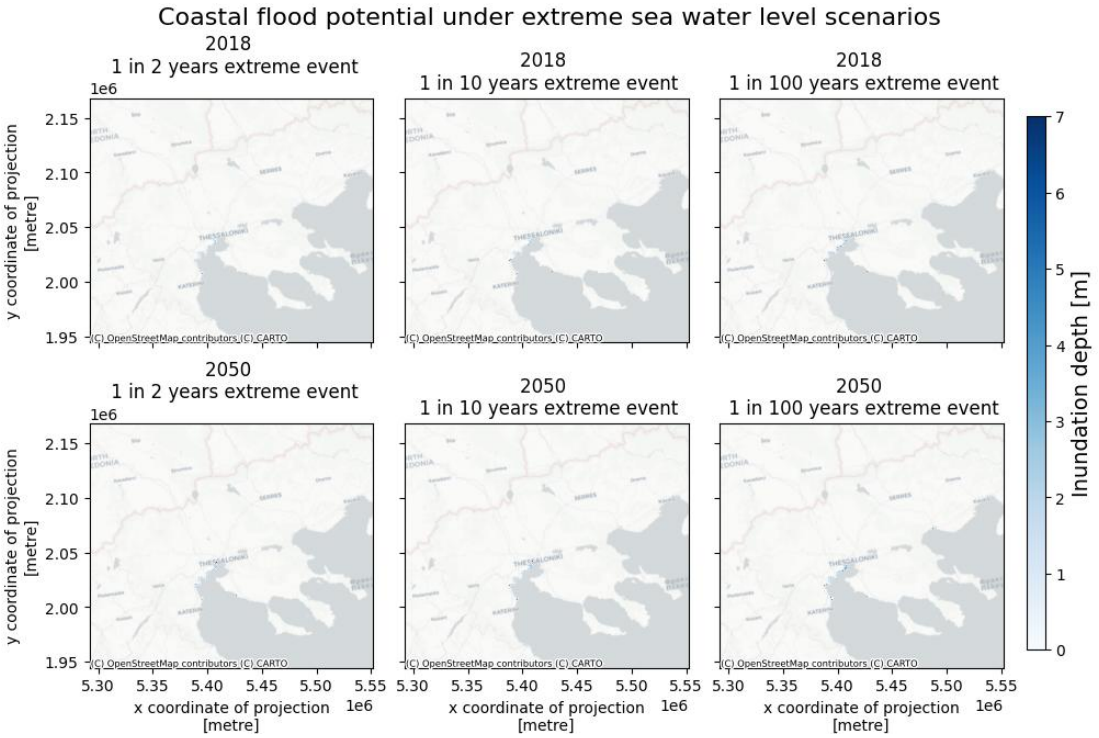

Figure 27: Comparison of coastal flood potential for an extreme event from 2018 and up to 2050[10].

[10] It is clear that a dedicated subfigure focusing on a targeted area would provide a more informative output map when compared to the original figure produced while following the template.

The comparison for the flood extents including a storm extreme event within 1 to 5 and within 1 to 100 years can be seen in Figure 7, and the extreme water level scenarios for 2018 and 2050 in Figure 8 respectively.

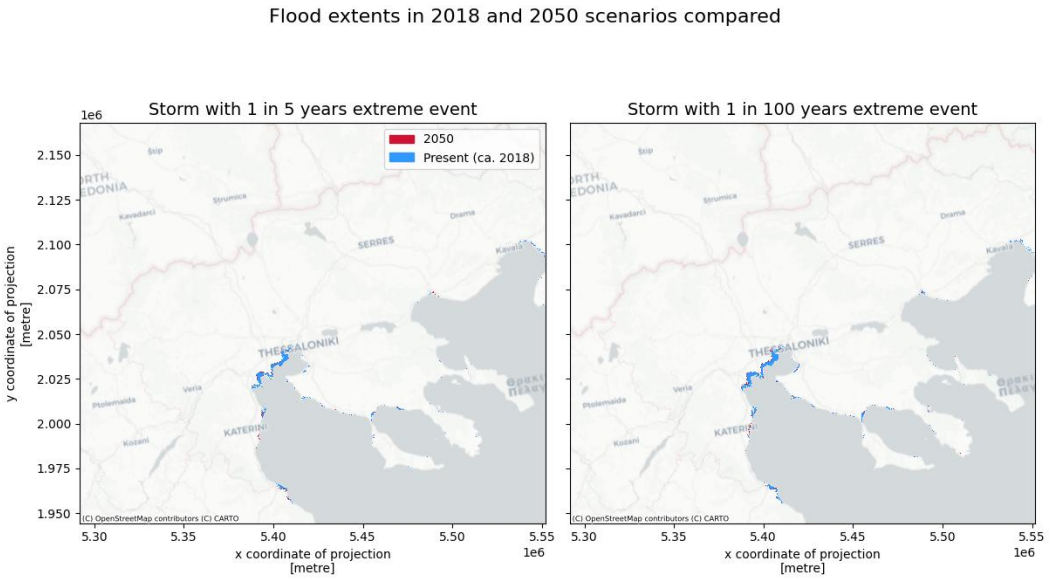

Figure 28: Flood extents for extreme storm events for “1 in 5 years” and for “1 in 100 years” events.

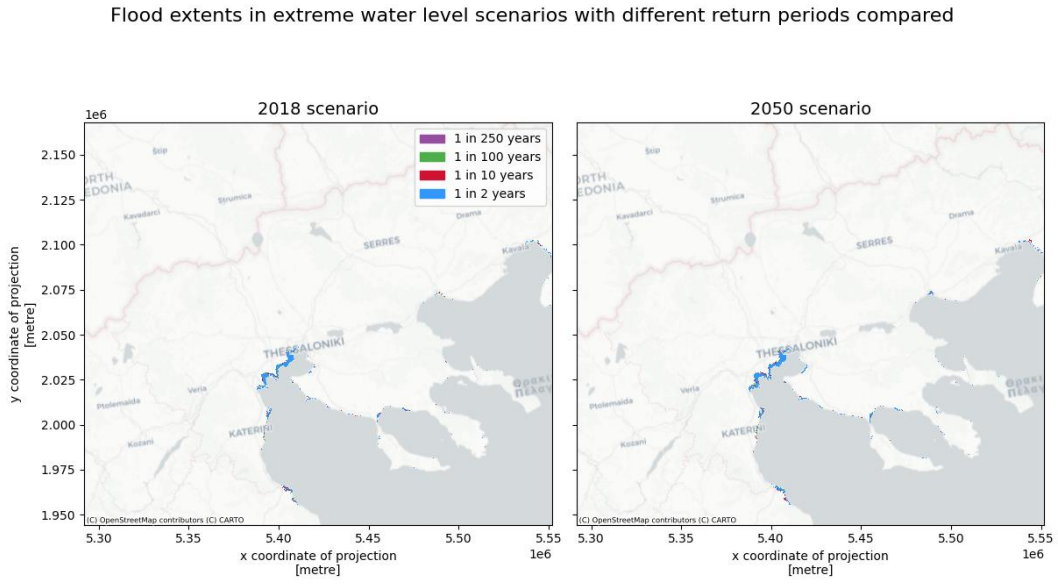

Figure 29: Comparison of extreme water levels scenarios (2018 (left), and 2050(right) respectively) for four (4) storm events (“1 in 2”, “1 in 12”, “1 in 100” and “1 in 250” years period).

The datasets were downloaded, clipped to the ROI, and merged into a single structure, facilitating straightforward comparison across scenarios and return periods. Visualizations were produced to highlight the differences in flood extent both between present and future climate conditions and across different return periods. In particular, the additional inundation extent expected by 2050 due to sea level rise was illustrated, although its contribution to extreme flood levels remains relatively

modest compared to the influence of return period and a focus on dedicated marked ROIs within the region could produce more updated maps. Through this process, the following objectives were achieved:

- Retrieval of coastal flood hazard maps for RCM.
- Assessment of the applicability of global-scale coastal flood.
- Comparative analysis of flood extents across scenarios and return periods.

The resulting coastal flood hazard datasets, stored locally, will serve as critical inputs for the subsequent coastal flood risk assessment workflow.

Risk assessment

Coastal flood risks for infrastructure are quantified by combining pre-processed flood maps with land use data (LUISA Land Cover) and economic vulnerability information (JRC depth damage curves). The methodology estimates damages in economic terms using simplified global datasets. An example of an extreme event can be seen in Figure 30.

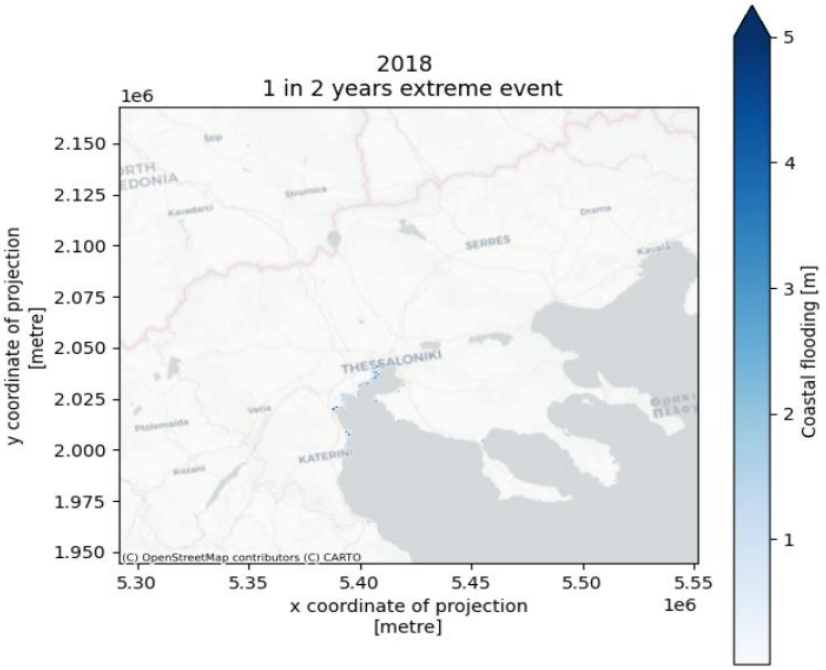

Figure 30: Example hazard map of an extreme event (“1 in 2” years).

The land use dataset (Europe in 2018) was sourced from the JRC data portal using maps of 100 by 100m resolution. The dataset provides a variety of land types including but not limited to urban areas, natural land, agricultural fields, infostructure, and waterbodies. The dataset was modified to secure the purposes of the RCM resulting in a LUISA Land cover map as shown in Figure 31.

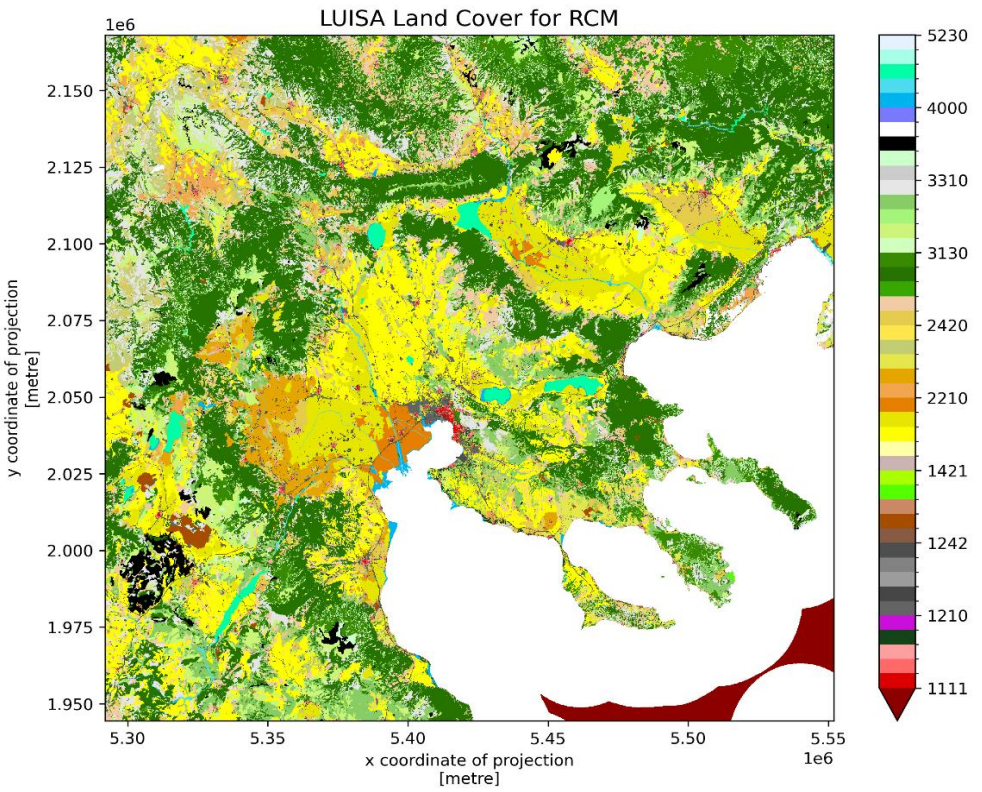

Figure 31: The LUISA Land Cover map for the RCM.

The colors on the right side of Figure 31 represent the CLC codes from the LUISA Land cover datasets. For further assignment of the economic damages, the CLC codes should exist and correspond to the land use categories that assignment of a monetary values is the goal.

The second step of the risk assessment sub-workflow for the coastal flooding focuses on estimating the exposure of infrastructure and economic assets to coastal floods via the preparation of the dataset's resolution, the vulnerability maps and the calculation of the damage. The flood and land use datasets utilized in this analysis differ in spatial resolution. Specifically, the flood extent maps have a resolution ranging between 30 and 75 meters, depending on latitude, while the land use data are provided at a constant resolution of either 100 meters or 50 meters. To enable direct comparison and integrated analysis, it was necessary to bring both datasets to the same resolution. Thus, the flood maps were interpolated onto the grid of the land use dataset, rather than vice versa, as land use classifications represent discrete categories and are defined on a regular, convenient grid. Therefore, the flood maps were resampled to match the resolution, extent, and projection of the land use dataset. The resulting resampled flood maps were subsequently saved locally in GeoTIFF format to be used as inputs in the economic damage assessment. For the estimation of flood-related economic damages, each land use type must be assigned an associated monetary value, expressed as a potential loss in euros per square meter (€/m²). These values were derived using the template provided in the accompanying file *LUISA_damage_info_curves.xlsx*, which links land use categories to corresponding economic vulnerability parameters. The GDP per capita value was chosen for Greece (that of "*26.861*") and introduced in the modified xlsx file. Further, the structural €/m², content €/m², and agricultural €/m² were adjusted to a scaling factor (see below, *0.8346*). The original value ("*32.169*") represents the GDP per capita (in EUR) that was used to

originally calibrate the damage values in the template. The damage values (€/m²) in the template are originally proportional to the GDP of that reference year. Thus, for the adaptation to another country (e.g., Greece) or to another year, all values should be scaled proportionally: modified value = original value * (Country's GDP per capita / template value) which results to the "*0.8346*" scaling factor for Greece. The modified damage curves can be seen in Figure 11.

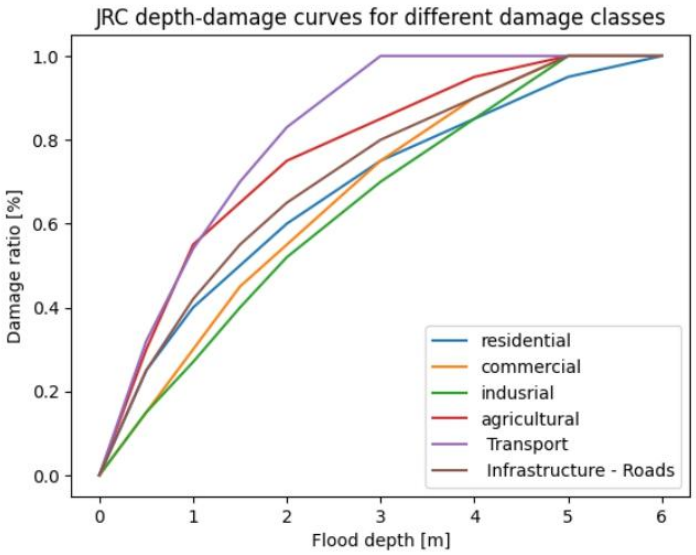

Figure 32: Modified damage curves for Greece.

Extracting the 'total €/m²' column to get the maximum damage for reconstruction it results to the table below:

Table 10: Total damage values for example CLC codes.

Land use code	total €/m²
1111	435.471384
1121	301.449853
1122	177.769315
1123	50.409522
1130	0.000000
1210	288.913514
1221	28.666369
1222	401.329170
1230	171.998216
1241	401.329170

The vulnerability curves for a specific number of CLC codes can be seen below in Figure *33*:

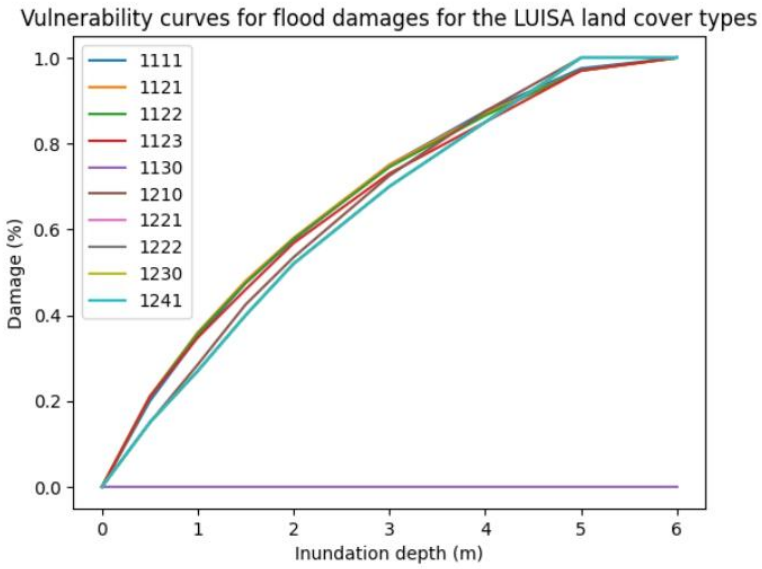

Figure 33: Vulnerability curves for the first ten (10) land cover types.

Calculate potential economic damage to infrastructure

Having prepared all necessary input data, the risk calculation can now be performed. The DamageScanner Python library was again used to facilitate the estimation of potential damages and the following datasets were used as input:

- The clipped and resampled flood maps,
- The clipped land use maps,
- The vulnerability curves assigned to each land use category,
- A table of maximum potential damages (expressed in €/m²) per land use category

Damage calculations were carried out for all defined scenarios and return periods and outputs were stored in a DataFrame, which wes then further processed to enhance interpretability. The post-processing steps included:

- Merging the damage results with the LUISA land use legend to obtain descriptive labels,
- Converting the calculated damages into units of million euros (€M),
- Sorting the results based on total damage magnitude, prioritizing the land use categories with the highest losses,
- Displaying a summary of the top 10 categories with the largest economic damages.

The first ten (10) categories with the largest economic damages are reported in Table 11.

Table 11: Codes with the largest economic damages.

Code	Type	2018_rp0002	2018_rp0005	2018_rp0010	2018_rp0050	2018_rp0100	2018_rp0250	2050_rp0002	2050_rp0005	2050_rp0010	2050_rp0050	2050_rp0100	2050_rp0250

40000	Wetlands	561.8	598.1	626.5	691.9	724.8	758.0	650.6	691.8	724.6	783.0	808.0	842.2
21300	Rice fields	464.2	494.6	516.0	573.2	597.3	628.5	537.5	572.1	596.2	653.2	678.9	713.7
12100	Industrial or commercial units	205.2	216.7	226.9	263.2	275.7	293.3	239.2	263.3	276.3	303.1	317.0	337.1
12411	Airport areas	41.0	46.4	50.7	81.9	88.0	96.3	72.8	81.1	87.7	102.5	109.0	116.9
11123	Isolated or very low density urban fabric	35.9	45.0	49.8	58.6	62.4	68.4	53.8	58.8	62.3	72.3	76.9	83.3
21100	Non irrigated arable land	16.4	24.9	28.5	38.5	42.1	48.4	31.6	38.9	42.4	53.8	60.8	67.8
24200	Complex cultivation patterns	14.0	16.2	23.3	31.3	34.0	41.3	26.5	30.8	33.6	45.1	49.0	53.4
22300	Olive groves	16.8	18.6	20.0	23.0	25.5	27.4	21.7	24.5	25.8	29.7	31.0	33.5
21200	Permanently irrigated land	6.1	7.0	7.9	11.8	19.3	22.8	8.6	11.7	19.1	24.9	27.2	31.2
12300	Port areas	13.5	14.5	15.8	18.7	19.3	20.5	16.5	18.7	19.3	22.1	23.0	24.2

To assess the economic damages from coastal flooding, flood hazard maps for different scenarios and return periods were retrieved and prepared. Selected return periods (2, 10, and 100 years) were used to load and merge the damage maps into one dataset. The damages were then spatially visualized to identify the most economically affected areas. A combined view of flood depth, land use, and estimated damages was created for a specific return period (2050, 100-year event), offering insight into the spatial distribution of potential impacts. Contextual information such as land use and inundation depth were integrated to better interpret the damages. The reliability of the results was critically examined by revisiting the assumptions used in the vulnerability curves and land use values. Finally, the outputs were interpreted by reflecting on the accuracy, limitations, and learning potential of the produced maps in the context of local flood risk assessments.

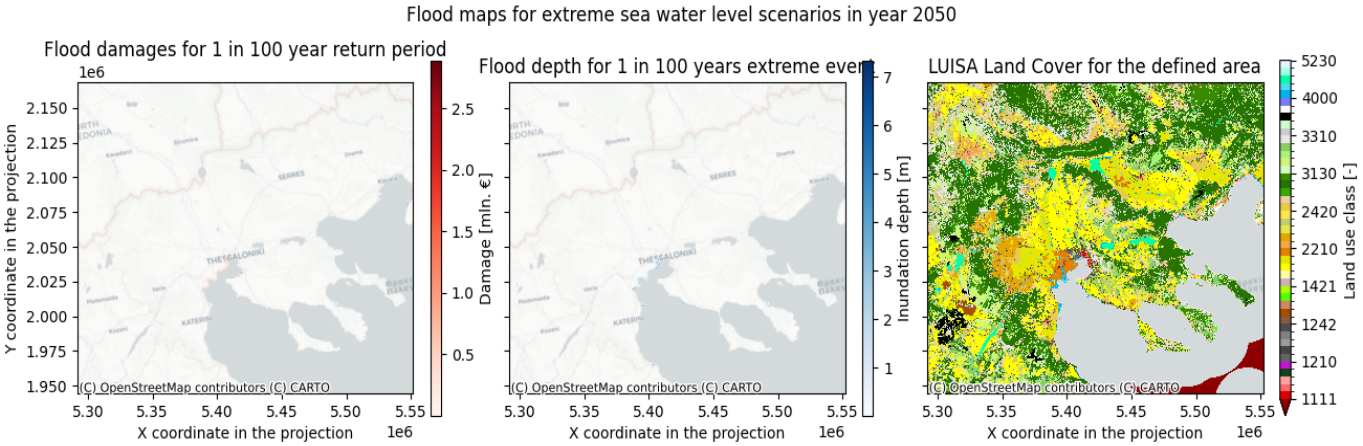

Figure 34: The left sub-figure shows flood damages; the Middle sub-figure shows inundation depth; the Left sub-figure shows land use with custom colors.

In this sub-workflow, flood hazard, land use exposure, and vulnerability information were combined to calculate and map potential economic damages from coastal flooding. Spatial plots of damages, flood depth, and land use were created to understand risk drivers. The workflow concludes with critical reflection on the accuracy and applicability of results, emphasizing the importance of local data for improving flood risk assessments.

2.2.2.1.3 Flooding building damage and population exposed

In this section, we present the methodology and results concerning the assessment of flood-related building damages and the population exposed to flooding hazards. Hazards affect assets such as buildings, impact critical infrastructure (e.g., hospitals), and affect the population. Based on the European flood maps linked to river flooding, a two-fold risk analysis was conducted:

- Quantification of the potential economic damages to buildings, and
- Estimation of the exposed and displaced population to support comprehensive risk assessment.

The adopted approach followed a two-step procedure, consistent with previous assessments undertaken for both riverine and coastal flood hazards. Initially, flood maps for different return periods were utilized, and then, for a given flood event (flood map), the total damage was estimated. The main datasets used included the flood maps from the Copernicus Emergency Management Service, the GHS-POP R2022A (Global Human Settlement (GHS Population Grid European

Commission GHS-POP-R2023A)) dataset from the JRC for population mapping and projections, and the building characteristics provided by OSM.

Hazard assessment

Retrieving flood maps for risk assessment of buildings and population exposure

Initially, the geographical bounds of the area of interest, either by defining polygons (in shapefile or geopackage (". *gpkg"; Geopackage open format*) format) or by manually inserting coordinate values were defined. Return periods for hazard calculation, projections for the population data, and the plotting conventions were also specified. The proper setting of input parameters ensured the consistency and reproducibility of the workflow across all subsequent stages of the analysis. Using the bounding box specified, the flood datasets were cropped to match the area of interest. The geographical coordinates were converted from latitude/longitude to the projection system of the flood map raster, and the bounding area was exported as a shapefile. This ensured spatial consistency between different datasets and allowed subsequent operations to focus exclusively on the defined study area. River flood maps cropped to the area of interest for 10-, 50-, 100-, and 500-year return periods can be seen in Figure 35 below.

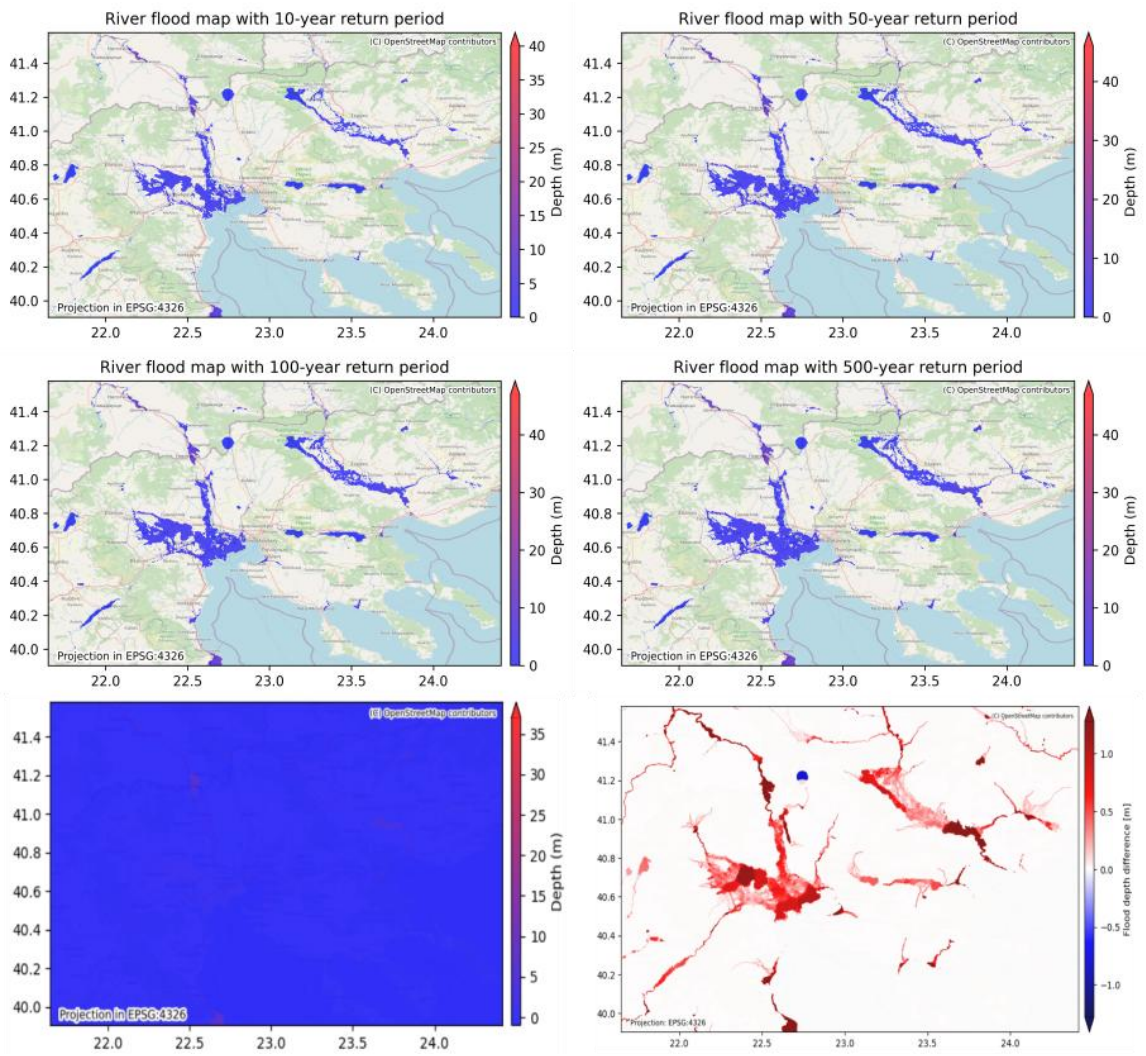

Figure 35: First and second row: Flood water depths for 10-, 50-, 100-, and 500-year return periods for the RCM. Third row: Example of difference flood depth between 10-, and 500-year periods.

The spatial clipping and format conversion steps produced a harmonized subset of the global flood datasets, centered on the RCM. Flood maps for all selected return periods were plotted together to provide a comparative overview. The initial example provided by the CLIMAAX handbook comparing 10- and 500-year return periods was included. Subsequently, the difference maps were created to illustrate variations in flood depths between two (2) selected return periods, highlighting how hazard magnitude changes with event probability. Finally, visual comparisons across return periods enhance understanding of hazard variability and help interpret the risk associated with different flood scenarios.

Risk assessment for flooding

Building damage and population exposure

Damage caused to buildings can be determined in relation to flood depth that the buildings are subjected to and is based on the JRC depth-damage curves. Damage classes include but are not limited to residential, commercial, industrial, and agriculture classes. "*In the default code, Agriculture,*

Cultural, and Transportation as well as unclassified buildings are set to Universal". The damage-depth functions for the four (4) mentioned classes. The integration of flood hazard maps with building footprint data enables a preliminary estimation of the total economic damage to assets such as buildings, infrastructure, and population exposure. Flood-related risks to infrastructure were assessed by calculating the total damage per flood event, based on parameters including flood depth, building characteristics and footprint, reconstruction or repair costs, and relevant datasets containing all required information. These values were then integrated across all return periods to estimate the Expected Annual Damage (EAD). Building attribute data were sourced from OSM, while the applied damage functions were based on methodologies developed by the JRC. Critical infrastructure exposure was also mapped against flood hazard data. The resulting maps of building damage per return period, together with critical infrastructure exposure maps, illustrated the spatial distribution of flood-related economic losses and identified potentially vulnerable infrastructure. Similarly, population exposure and displacement due to flooding was estimated using flood maps in combination with population distribution datasets. (Exposure refers to individuals located within flooded zones, whereas displacement accounts for those affected by water depths exceeding a defined threshold). Results across return periods are used to derive the Expected Annual Population Exposure (EAPE) and the Expected Annual Population Displacement (EAPD). Population exposure and displacement maps, along with corresponding exposure/displacement curves for selected return periods, offered a quantitative foundation for evaluating population-level vulnerability to river flooding under varying severity levels. In Figure 36 below the depth-damage curves for RCM are depicted.

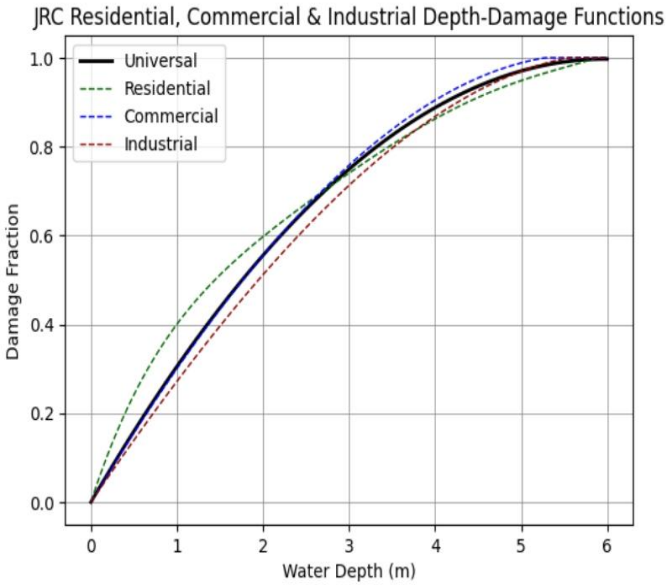

Figure 36: Depth-damage functions scale for the RCM.

The damage curve calculations for RCM were produced by adjusting the maximum damage values (in €/m²) using the GDP per capita scaling factor (Greece: €26,861 vs EU baseline: €32,169), resulting in a scaling factor of 0.8348. This factor was applied to the original 2010 EU damage values for:

- Residential: €480 (structure) and €240 (content) → scaled by 0.8348.
- Commercial: €502 and €502 → scaled by 0.8348.
- Industrial: €328 and €492 → scaled by 0.8348.

The depth-damage curves themselves were not changed. These remain the standard JRC curves were fitted as 5th-order polynomials as provided in the CLIMAAX Handbook. Each damage class (residential, commercial, industrial, and universal) uses its corresponding coefficient set from the JRC report. Only the maximum damage (€/m²) was adjusted. The results based on the OSM for the flood maps per return period for the example cases of 10- and 500-year return period (up), and for the population (down) can be seen in Figure 37 and the population raster in Figure 38 below, for the example case of the Metropolitan area of Thessaloniki.

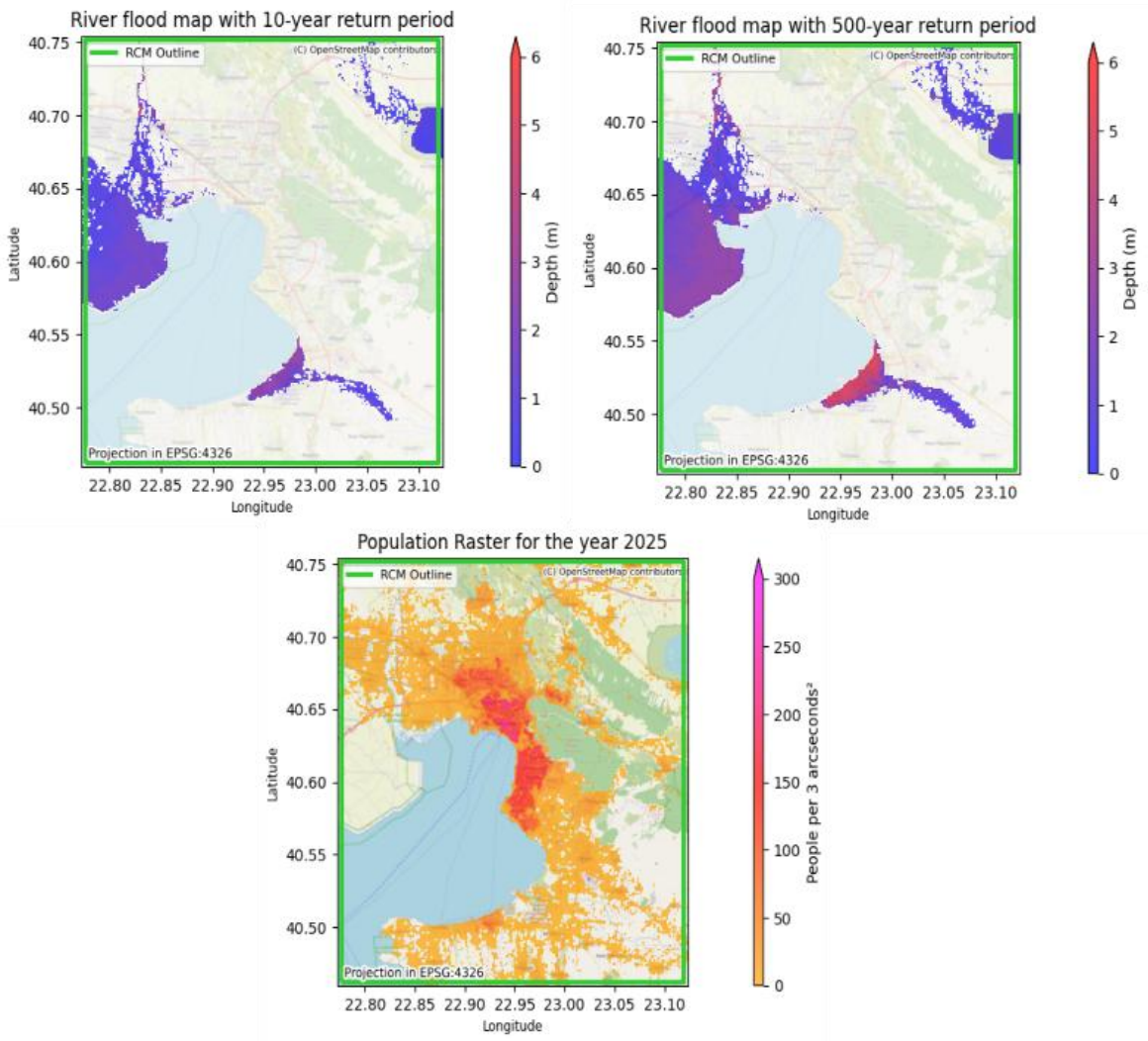

Figure 37: (up) River flood maps for selected return periods for the selected bounding box shapefile. (down) Population map for the selected bounding box area.

The selected area of Thessaloniki illustrates the strengths of the CLIMAAX Handbook, as the differences between the flood maps for the 10- and 500-year return periods are clearly observable. The tool enables artificial zooming into local areas, even in the absence of local or regional datasets. Taking into account the sparsity of the available outputs, it offers a preliminary yet qualitative indication of the extent and magnitude of the flooding in affected areas. While certain regions of the map would benefit from further zooming in order to examine more closely the extent of the flood phenomenon, for the purposes of the current deliverable, the focus remains on capturing the overall figure and general trends. In the figure depicting the exposed population, although the image appears crowded, it is still possible to discern the spatial distribution and extent of potentially

affected individual areas. A comparison of the two (2) figures reveals a discrepancy, as a more homogeneous or one-to-one correspondence between the flooded areas and the exposed population would be expected. This divergence highlights certain limitations of the tool or suggests the need for additional tailored approaches to maximize its effectiveness, as well as the potential necessity of incorporating more specific local or regional datasets. To explore further the suitability of the current example, the OSM data were loaded for the selected area, where the unclassified building use is depicted as seen in Figure 38 below.

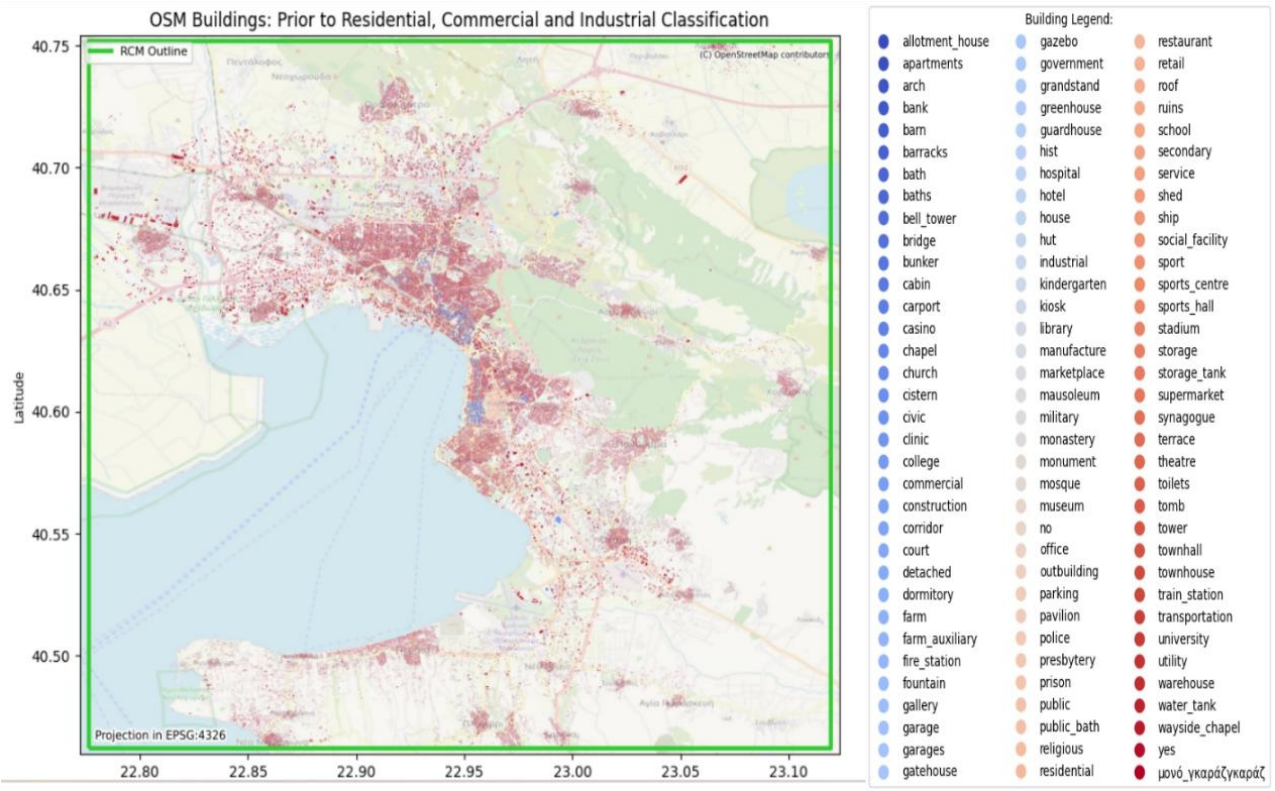

Figure 38: Unclassified buildings for the selected area of Thessaloniki based on the OSM data[11].

Further, assuming separate building classifications for distinct categories such as residential, commercial, industrial, cultural, agricultural, transport, and agriculture, with particular attention to “Critical Infrastructure”, for the same area of interest selected in the previous step, the transformation of the building classes into a dataset result in a map that illustrates the number of buildings to which a specific type has been assigned, as presented in Figure 39 below.

[11] The Greek letters on the third column of the legend were generated automatically. The phrase “μικρό_γκαράζ" translates as: "small garage". The expression repeats mistakenly the word “γκαράζ" was given automatically from the dataset.

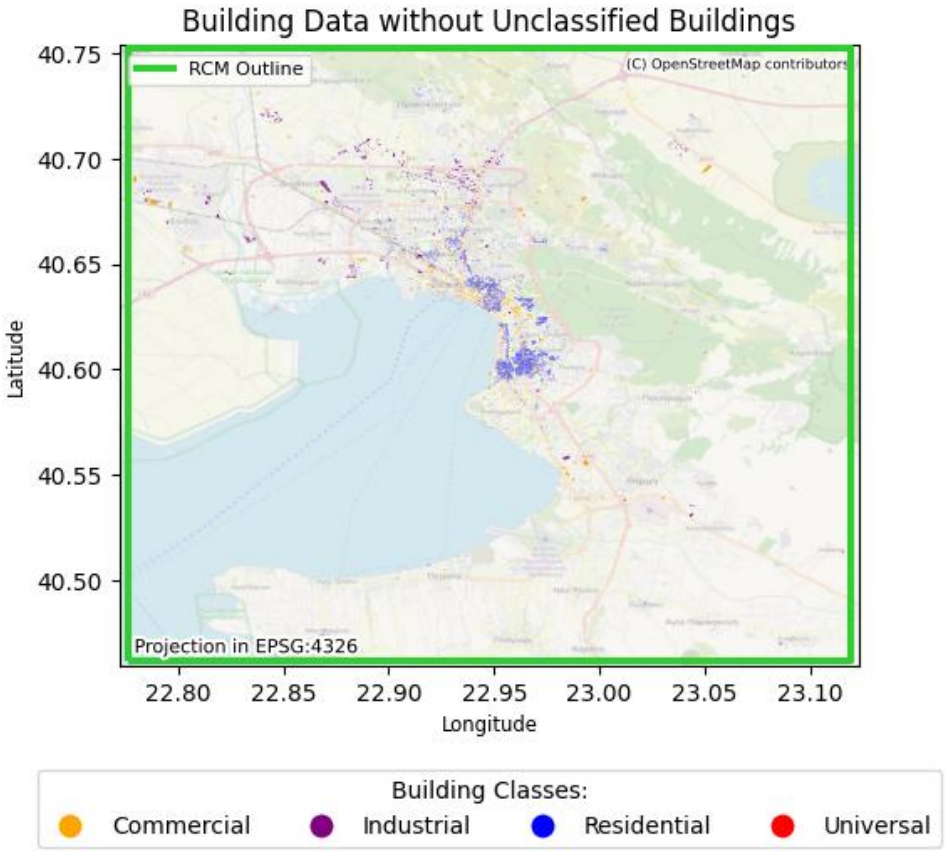

Figure 39: The selected example area of Thessaloniki is depicted where all buildings that a type was assigned to them can be seen.

The difference between the two (2) figures (Figure 37 (with the classification type assigned to the buildings) and Figure 38 (without the classification type assigned to the buildings)), is far from marginal, and is depicted in Figure 39.

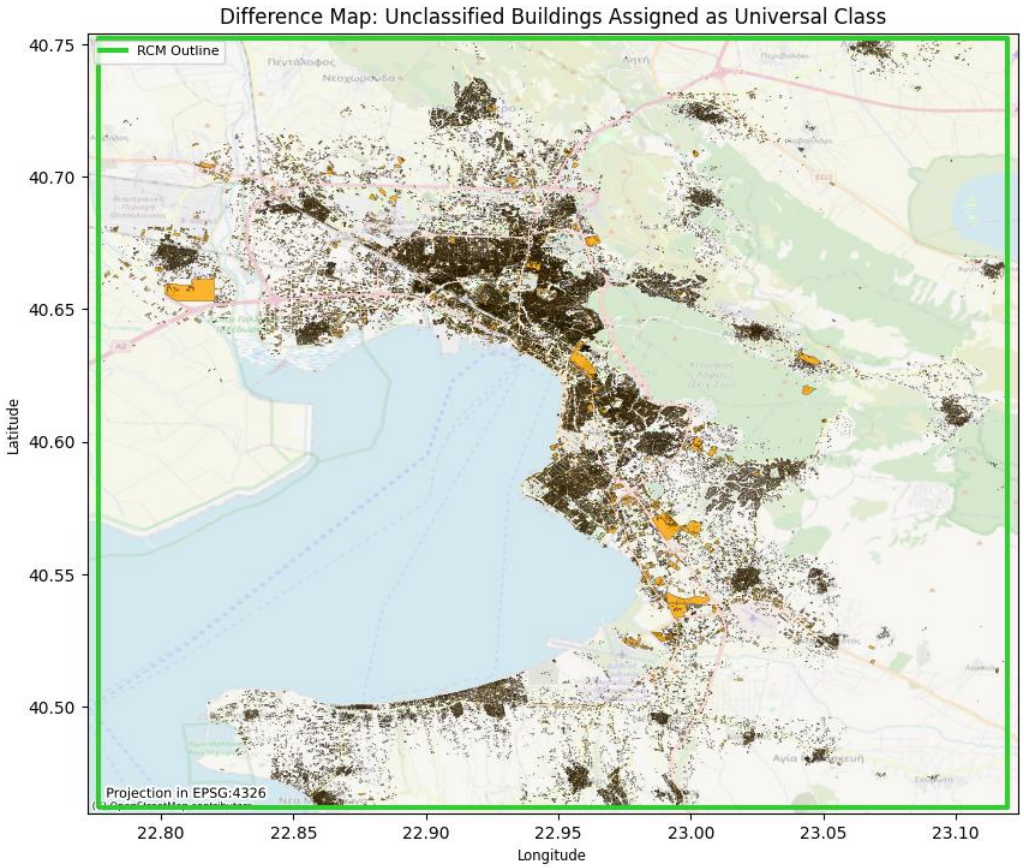

Figure 40: Difference map for the example case of Thessaloniki, between the classified and unclassified building. The dark brown color depicts the vast majority of the buildings lacking a specific type.

It demonstrates that the vast majority of existing buildings have not yet been assigned to any available or newly defined classification type. This considerably complicates the procedure of assigning the total economic damage to the buildings and critical infrastructure, resulting in outcomes that are not as representative as they ought to be. It is likely that, if local or regional datasets were available, the difference between the two (2) figures would be reduced.

In the following step, flood depth values at the building level were derived from raster flood maps corresponding to each return period. The process begined by retaining only the relevant attributes: building classification, geometry, and identifier. Building footprints were then used to compute areas in square meters, and zonal statistics were applied directly on the raster data to extract flood depths per building using a selected metric such as mean, maximum, or minimum. The data frame was updated accordingly, and a map wass produced showing the mean flood depth at building locations based on the flood map for the selected return period. Building and river maps, and mean flood depth can be seen in for different return periods in Figure 41.

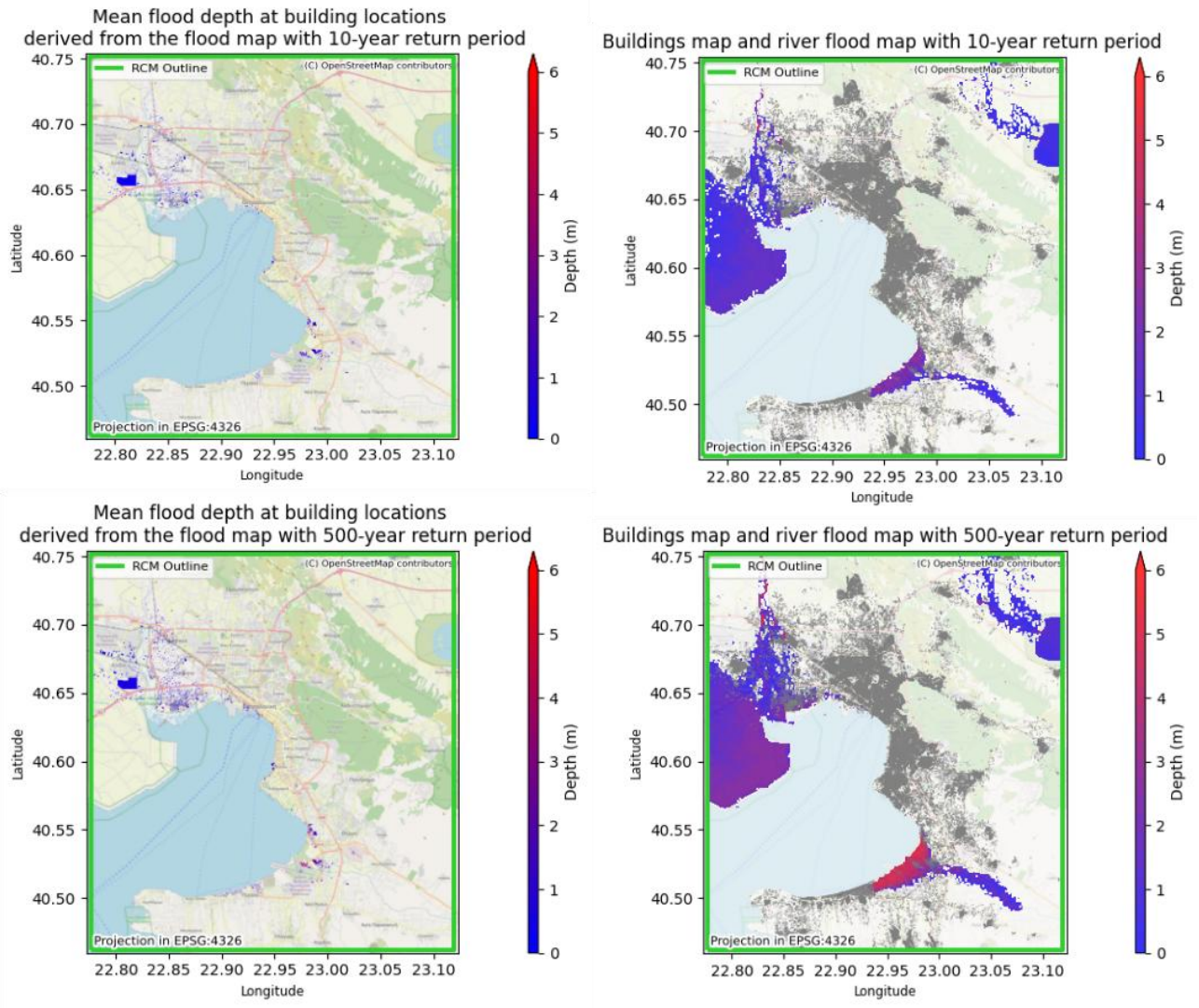

Figure 41: Left column depicts the mean flood depth maps for the 10- and 500-year return periods for the example case of Thessaloniki. The right column depicts the buildings and river maps for the 10- and 50-year return period for the example case of Thessaloniki.

Calculating economic damage to buildings, and total damage to buildings

Reconstruction costs were determined by extracting the fractional damage for each building using the provided JRC damage functions for each classification type. "*Then the fractional damage is multiplied with the maximum damage value per square meter and the building footprint area in meters and written to a shapefile*" as provided in the CLIMAAX Handbook plotting the building damages in relation to the return periods of the flooding maps will allow us to estimate the predicted regional damage on average for a given year.

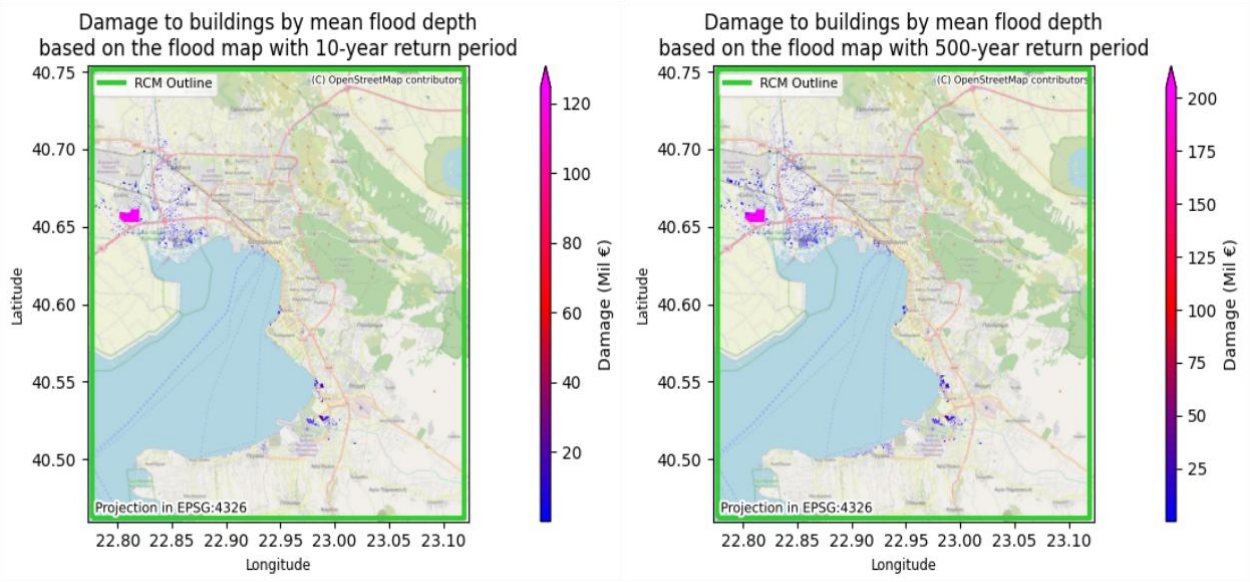

Figure 42 Mean flood depth damage to buildings based on the flood maps with 10- and 500-year return periods for the example case of Thessaloniki.

In Figure 42 a depiction of the economic damage for the area of Thessaloniki is given based on the flood map. The next step was the estimation of the EAD in millions in Euros as a plot of the buildings in relation to the return periods of the flood maps as shown in Figure 43, where the EAD is estimated at 90.05 Mil. €

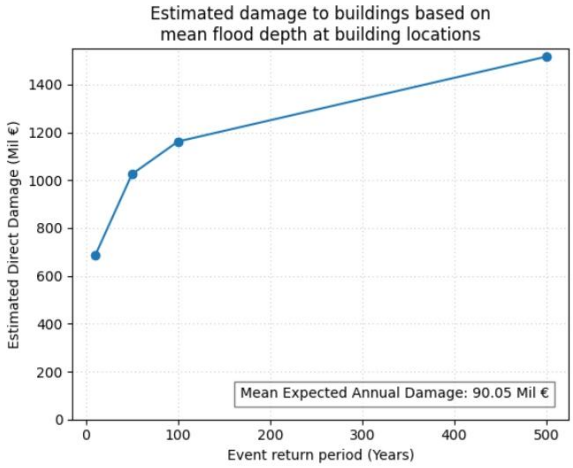

Figure 43: Estimated damage to buildings for the RCM.

Further, it was key to quantify the exposure of critical infrastructure assets to flooding based on categorized overlaying types on flood maps, producing critical infrastructure exposure maps for different return periods where all potential disruptions to services are highlighted as shown in Figure 44.

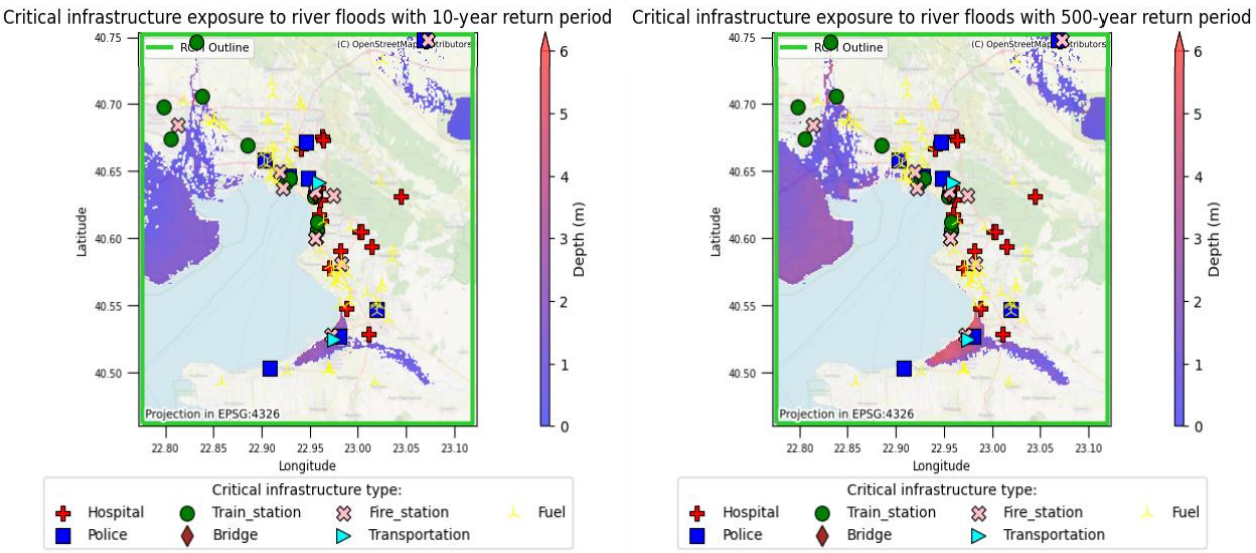

Figure 44: Critical infrastructure for the example case of Thessaloniki with 10- and 500-year return period is depicted.

Additionally, population exposure and displacement were estimated by overlaying flood depth maps with population distribution grids and identifying individuals affected by inundation. Exposure was calculated by aggregating all individuals located in flooded areas, while displacement was determined by applying a minimum flood depth threshold to define the subset of the exposed population likely to be displaced. These calculations were performed for each return period, and integrated to estimate the Expected Annual Exposed Population (EAEP) and Expected Annual Displaced Population (EADP), respectively. The resulting exposure and displacement maps, along with their corresponding curves, provide insights into societal vulnerability and inform emergency planning by highlighting areas with heightened risk of humanitarian impact. In Figure 45 the estimated and displaced population diagram is depicted and the river flood event for the 10- and 500-years return period for the example case of Thessaloniki.

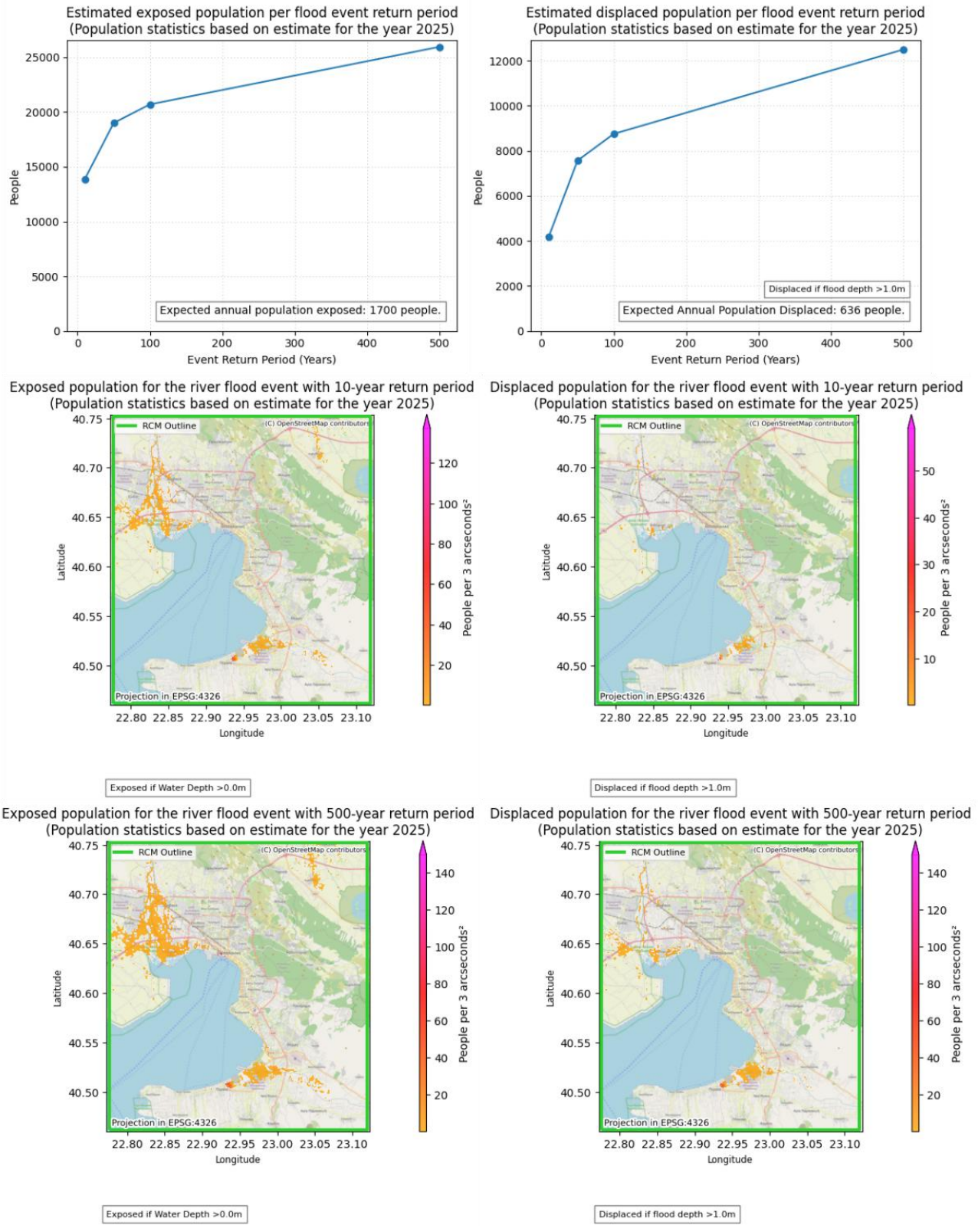

Figure 45: First row: diagrams of the exposed and displaced population for the example case of Thessaloniki area. Second and third row: left column shows the exposed and right column the displaced population in the areas respectively.

The flooding damage assessment workflow provides a structured methodology for quantifying potential economic losses to buildings arising from river flood events of varying return periods. By

integrating hazard data, building footprints, classification schemes, and standardized depth-damage functions, the workflow produces spatially resolved estimates of direct damage and calculates the EAD for the selected region. These outputs contribute to the understanding of spatial risk distribution and support evidence-based planning for resilience and adaptation strategies.

2.2.2.2 Workflow #2: Fire

Wildfire risk arises from a complex interaction of various factors, including climate, vegetation, and human influences, and it has significant impacts on ecosystems and society. There is one key approach used for hazard assessment in fire workflow, the FWI, which calculates fire danger based on daily weather variables and predicts future trends under climate change scenarios.

2.2.2.2.1 Wildfire (FWI)

The present methodology outlines the procedure to evaluate wildfire development risk by integrating seasonal FWI data with vulnerability-related parameters. The objective was twofold: to determine which areas within the RCM present the most favorable conditions for wildfire development based on climatic and vegetative factors, and to identify zones with the highest sensitivity from a human, economic, and environmental standpoint. Wildfire risk was defined as the combination of wildfire danger and vulnerability; danger was assessed through the interaction of the presence of burnable vegetation, with the former represented by the FWI and its contributing variables such as temperature, humidity, wind speed, and precipitation. These variables were derived from ERA5-Land reanalysis data and processed to compute daily and seasonal FWI. Outputs include maximum FWI, the number of days above specific danger thresholds, and fire season length. Burnable vegetation datasets were included, and both components were normalized and equally weighted to produce the fire indicator. The methodology excludes past burnt areas to reduce historical bias and improve applicability across all European regions. Vulnerability was defined through five (5) parameters: population in the WUI, protected area coverage, ecosystem irreplaceability, population density, and ecosystem restoration cost. Exposure was determined by overlaying FWI hazard maps with spatial datasets on land use, vegetation, and population, including land use and cover datasets, WorldPop data, and OSM data for infrastructure. Zones intersecting high-FWI areas during the fire season, such as WUIs and Natura 2000 sites, were classified as exposed. The integration of hazard, exposure, and vulnerability layers was carried out to generate semi-quantitative risk maps. This approach allows users to select relevant vulnerability parameters, facilitating tailored risk assessments. The final outputs of the methodology include hazard maps, critical fire danger day counts, exposure and vulnerability layers, composite risk maps, and tabular summaries of affected land use categories and municipalities.

Hazard assessment

Changes in seasonal FWI intensity

The FWI hazard workflow allows for spatial and temporal FWI trends visualization and for detecting any changes in the fire weather season duration and onset. Changes in seasonal FWI values reflect

evolving climatic conditions that may increase the likelihood of wildfire development. Understanding the lengthening of the fire season is essential for adaptation planning and the strategic allocation of wildfire response resources. The workflow started by defining the study area. Boundaries of the selected region were downloaded in GeoJSON (Geographic JavaScript Object Notation) format and the geometry was saved as a shp format for plotting. The bounding box coordinates were reprojected to match the climate data projection and a scale parameter was applied to expand the bounding box to ensure full coverage of the region. Seasonal FWI data were sourced from the CDS (Copernicus Climate Data Store), using the EURO-CORDEX (Coordinated Downscaling Experiment - European Domain) projections and parameters including time period (e.g., 2046–2050, 2051–2055), emission scenario (e.g., RCP2.6), model (multi-model ensemble), and projection severity ('best', 'worst', or 'mean') were specified on purpose. These datasets represented the mean FWI during the European fire season (June–September), calculated by averaging daily FWI values over this period. FWI datasets were concatenated, and an auxiliary function sliced the data to the bounding box of the selected region. The FWI variable was extracted from the dataset for further processing. Finally, the seasonal FWI intensity was plotted both as an average over the selected period and year-by-year.

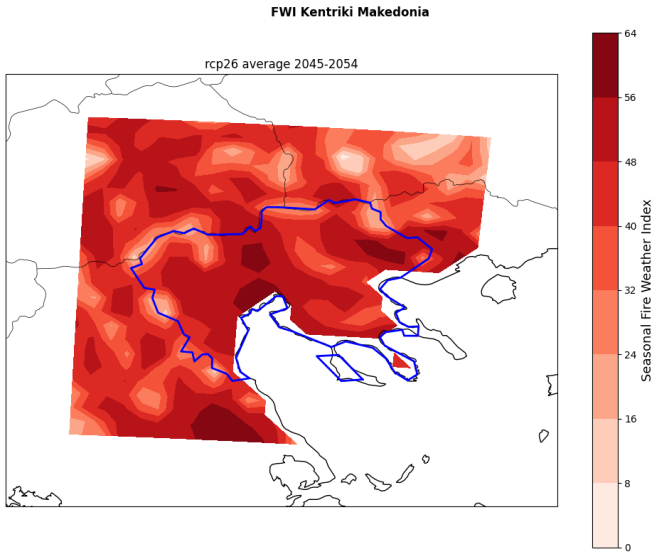

Figure 46: Seasonal weather index map for the RCM under the RCP2.6 scenario for the period of 2045-2054.

A depiction of the seasonal weather index maps under the RCP2.6 scenario for the period 2045-2054 for each year separately can be seen in Figure 47 below.

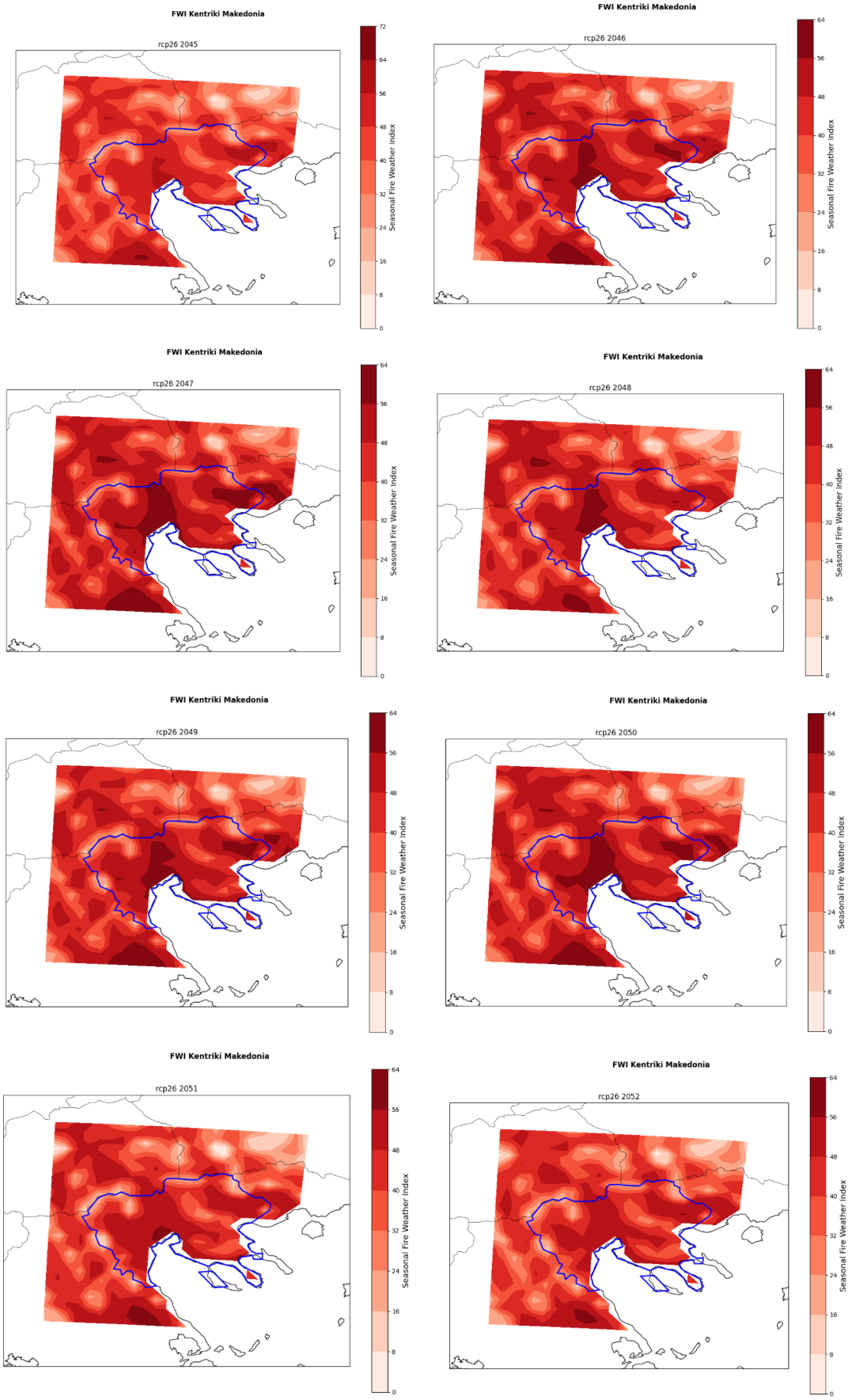
FWI Kentriki Makedonia
rcp26 2045
FWI Kentriki Makedonia
rcp26 2046
FWI Kentriki Makedonia
rcp26 2047
FWI Kentriki Makedonia
rcp26 2048
FWI Kentriki Makedonia
rcp26 2049
FWI Kentriki Makedonia
rcp26 2050
FWI Kentriki Makedonia
rcp26 2051
FWI Kentriki Makedonia
rcp26 2052
Seasonal Fire Weather Index

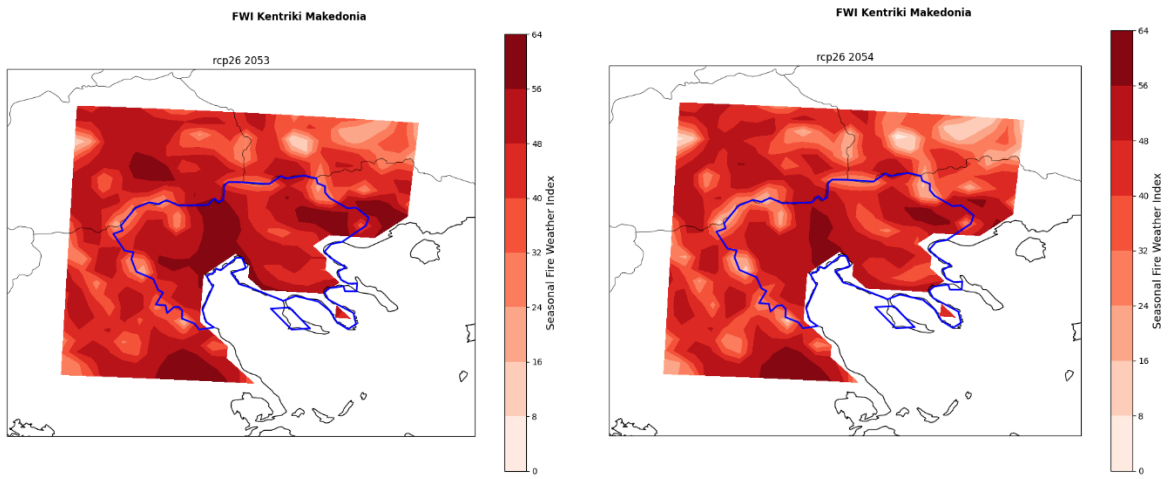

Figure 47: Seasonal FWI intensity over the selected periods ranging from 2045 and up to 2054 under the RCP8.5 scenario.

In the resulting Figure 47, the applied index proposes a fire danger categorization that is predominantly characterized by the "Very High" (FWI value between 38.0 and 50.0) and "Very Extreme" (FWI value above 70.0) classes. This representation clearly illustrates that, although areas subject to extreme fire conditions are fewer and more spatially limited, they are not negligible. Moreover, the entire region, including certain zones in the northwest and northeast that appear to fall within lower fire danger classes, displays a general tendency toward elevated wildfire probability. It is noted that in the area of Chalkidiki, no specific fire index appears to have been applied. This likely represents an artifact of the handbook tool, as there are zones within Chalkidiki that are susceptible to wildfire events, though these are not reflected in the plot. Figure 47 depicts the temporal evolution of fire danger starting in the year 2045. The initial conditions display a classification ranging from low to mild fire danger. A gradual and consistent increase is then observed across the entire period, with each subsequent year showing a progressive elevation in the fire danger class. This upward trend continues uniformly, and each part of the region transitions to a higher fire danger level. In the central part of the region, the distribution of areas classified under extremely high or high fire danger remains largely stable up to the year 2050. However, in 2050, there is a notable decline in danger levels, producing a spatial configuration more closely resembling that of 2045. This year, the previously dominant extremely high-danger conditions in the central part of the region are significantly reduced. Following this, the upward trend resumes and continues into 2051, which exhibits a similar distribution to 2050 but with a slightly greater intensity. In contrast, the years 2045 and 2053 show a leapfrogging pattern of increase and decrease in fire danger levels. This results in an irregular alternation between high and low fire danger conditions, interrupting the otherwise steady progression and indicating variability in the projected climatic and vegetative influences on fire risk.

Fire season length

This methodology focuses on assessing the projected evolution of fire weather season length based on daily FWI data. The datasets were sourced from the CDS and included projections from multiple global climate models under historical, RCP2.6, RCP4.5, and RCP8.5 scenarios, choosing to study the example of RCP2.6 as illustrated in the CLIMAAX handbook. Data from the historical period were used as a baseline against which future changes were evaluated. To ensure regional specificity, a

predefined extraction function was applied immediately after download to clip the data to the extent of the selected region, while discarding the original Europe-wide files. The analysis involved calculating the annual fire weather season length, defined as the number of days exceeding a designated FWI threshold, as set to 30 in this case. The fire weather season was assessed for both historical and future periods, allowing for the quantification of projected changes. Maps of season length were generated for each case scenario, mean, best, and worst-case condition, by accounting for inter-model and inter-annual variability. These scenarios provided a range that captures a high percentage of the possible distribution. The methodological framework enables users to understand the potential variability in future fire weather conditions and to use these projections to support the design of robust adaptation strategies.

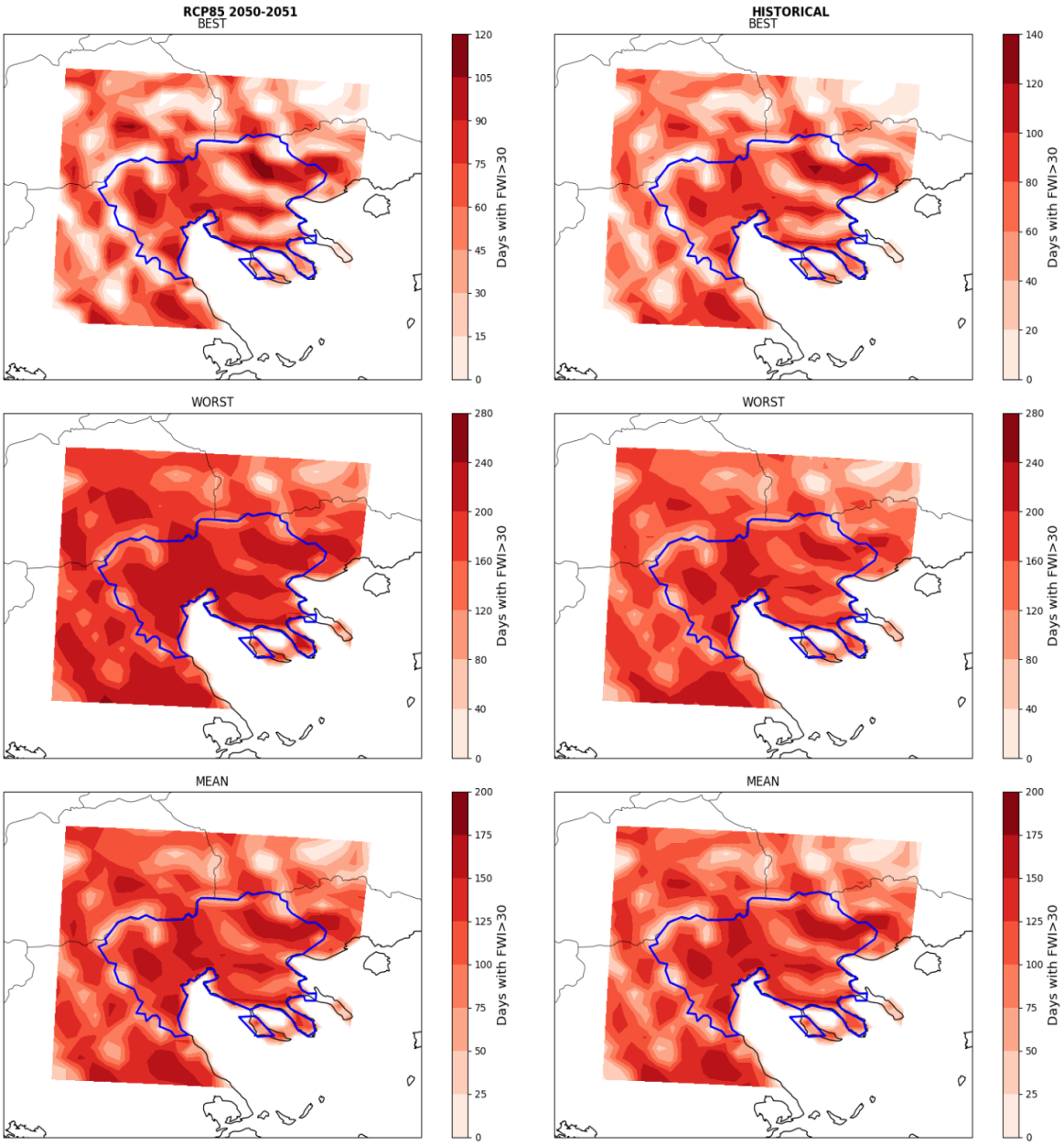

Figure 48: Comparison of future and historical fire index for three (3) case conditions ("best", "worst", and "mean"), under the RCP8.5 scenario for the period 2050-2051.

Figure 48 presents two (2) columns of subplots comparing future and historical fire weather season length conditions. The left column displays the projected results under the RCP8.5 scenario for the period 2050–2051, while the right column corresponds to the historical datasets. Each row of the figure represents a different case condition ("best", "worst", and "mean") allowing a comparative interpretation between scenarios. The best-case condition reveals that the quantitative distribution between the RCP8.5 and the historical data is similar. However, while the historical scenario shows lower fire danger classes in the north-eastern part of the region, the RCP8.5 projection indicates an increase in fire danger. A similar pattern is observed in the mid-western area. In the second and third rows of the figure, additional contrasts become apparent between the historical and RCP8.5 projections. In the worst-case scenario, the historical dataset shows predominantly lower fire danger classes with isolated occurrences of higher danger zones. In contrast, the RCP8.5 projection significantly over-represents extreme fire danger classes across the majority of the region. The mean-case scenario depicts a spatial pattern with recurring zones of susceptibility, showing consistency between both historical and RCP8.5 data in terms of the location and relative intensity of fire danger areas.

Risk assessment

This workflow provides an assessment of wildfire development risk by combining the seasonal FWI with vulnerability indicators, defining areas with favorable conditions for wildfire ignition based on climate and fuel availability. Risk was defined as the combination of fire danger, calculated from normalized FWI values and burnable vegetation, and vulnerability, which includes selected indicators for exposure and sensitivity (e.g., people living in the WUI area, protected land area, irreplaceable index, population density, and restoration costs). An economic analysis was carried out to highlight areas with the highest overall risk. Historical burnt areas from the fire danger calculation were excluded aiming to avoid underestimating risk in regions with limited wildfire history data, thereby ensuring applicability to areas facing climate-driven wildfire threats.

Defining fire danger

Fire danger was defined as the combined effect of climatic conditions and fuel availability. Climatic conditions regulated the potential rate of fire spread through their influence on fuel moisture, while the presence of burnable vegetation is a prerequisite for ignition and propagation. Their complementarity was reflected in the risk assessment framework, where both parameters were extracted, normalized, and integrated to form a synthetic danger indicator. Climatic suitability for wildfire development was assessed through the seasonal FWI which integrates daily meteorological variables (e.g., temperature, humidity, wind speed, and rainfall) into a synthetic index that reflects both the effects of weather and fuel moisture on fire potential. As the first step in the risk assessment process, a user-defined threshold was selected to constitute the fire danger. For reference, a value of 30 is often used in pan-European contexts, though regional variations may apply, especially in higher latitude areas that may experience lower FWI values while remaining susceptible to wildfire. The FWI data used in this assessment were sourced from the CDS and derived from EURO-CORDEX model outputs. The scenario of interest was specified within the code (e.g., RCP = "rcp26"). As the FWI represents only climatic conditions, further filtering was necessary to exclude land categories without combustible material, such as lakes or barren ground. This is

accomplished by masking the FWI using classifications from the ESA-CCI Land Cover dataset. A mask was generated to remove non-flammable land cover types, and the filtered dataset was incorporated into the risk dataset where all fire danger and vulnerability parameters are compiled. Fuel availability was estimated through a separate indicator representing the proportion of land covered by burnable vegetation. After retrieval, the data were reprojected and interpolated to match the resolution and coordinate system of the FWI. Once both the climatic and fuel-based danger components had been processed, they were normalized, averaged, and assigned equal weights to each, producing a unified wildfire danger index. This index was stored in the shared risk dataset and used in subsequent phases of the analysis. In Figure 49 the output maps can be seen.

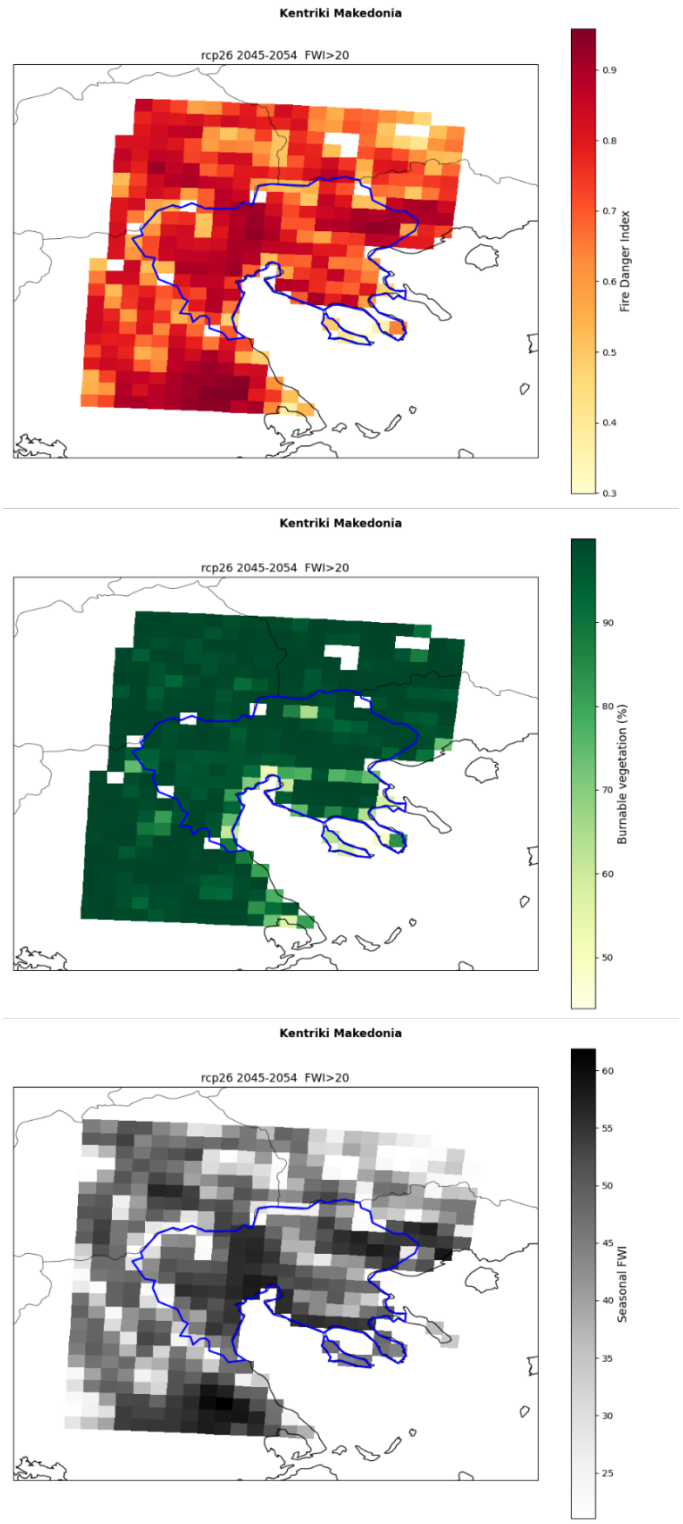

Figure 49: From top to down maps of the fire danger index (variations of red and yellow colors), burnable vegetation (variations of green and yellow colors) and seasonal FWI (variations of black and white colors) are given for the RCM area.

Three (3) thematic maps were generated as outputs (see Figure 49) of this procedure: a wildfire danger index map, a seasonal FWI intensity map, and a burnable vegetation map. The wildfire danger index map displays a heterogeneous pattern, with spatial variability ranging from low to very extreme fire danger classes. In contrast, the burnable vegetation map shows a more homogeneous

distribution, with the majority of areas falling into the highest danger class, and only limited zones corresponding to lower values. The seasonal FWI map indicates elevated fire danger particularly in and around the Thessaloniki metropolitan area, with a gradual decline in fire danger classification observed as distance from this urban center increases. Across all three (3) maps, certain zones appear in white, indicating either an absence of fire susceptibility or a lack of reliable data. In such areas, the scarcity or coarse resolution of input data limits the applicability of the framework.

Vulnerability

The methodology applied for the extraction and reprojection of vulnerability indicators is identical to that used for the burnable vegetation dataset. Each processed layer was compiled into a common risk dataset for integrated analysis. The selected vulnerability indicators were as follows: the population living in the WUI, representing the proportion of inhabitants in peri-urban areas adjacent to vegetated land; the distribution of protected areas, indicating the share of each map pixel covered by designated natural protection zones; the ecosystem irreplaceability index, quantifying the uniqueness and inherent ecological value of the respective ecosystem; the population density; and the restoration cost index, denoting the relative cost of land restoration in the event of wildfire loss. For each vulnerability indicator the same preprocessing function used for burnable area data was applied. Each dataset was subsequently processed using an extraction function, and the output was assigned to the shared risk dataset. For each of the four (4) main indicators (WUI population, protected area fraction, ecosystem irreplaceability, and restoration cost) a corresponding visualization was generated as shown in Figure 29.

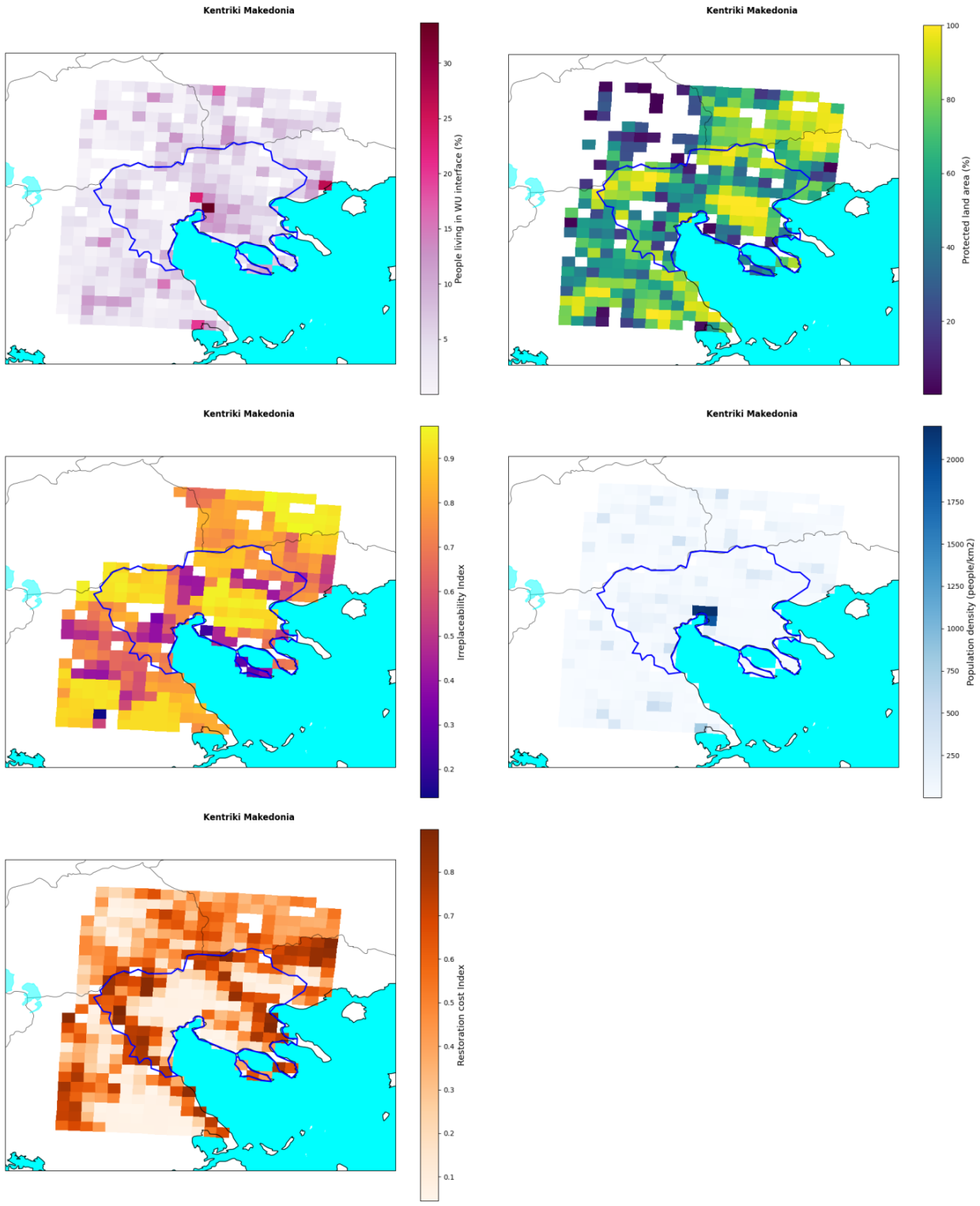

Figure 50: WUI population, protected area fraction, ecosystem irreplaceability, and restoration cost indicator are plotted for the RCM.

Upon completion of the vulnerability data processing, the risk index was constructed through a Pareto analysis, which combines the vulnerability layers with the previously derived fire danger index. This step determines which regions exhibit the highest or lowest composite wildfire risk. The analysis represents the set of pixels displaying the highest risk profile assuming that all considered indicators contribute equally to the overall wildfire risk. The selection of indicators included in the

analysis allows for adjustment by the user to reflect specific priorities. For example, if the goal is to assess ecological wildfire risk, the user may include only the protected area coverage and irreplaceable index. The danger component, represented by the FWI, must always be retained as it constitutes the foundational condition upon which wildfire risk develops. The structure of the analysis allows for the integration of additional vulnerability indicators. The algorithm was then applied to identify the maximum values of the selected variables, thereby determining the set of pixels with the highest risk. Conversely, to compute the lowest risk, the algorithm searches for the minimum values. A wildfire risk map was generated after (see Figure 51), combining the identified high-risk locations with the underlying fire danger index.

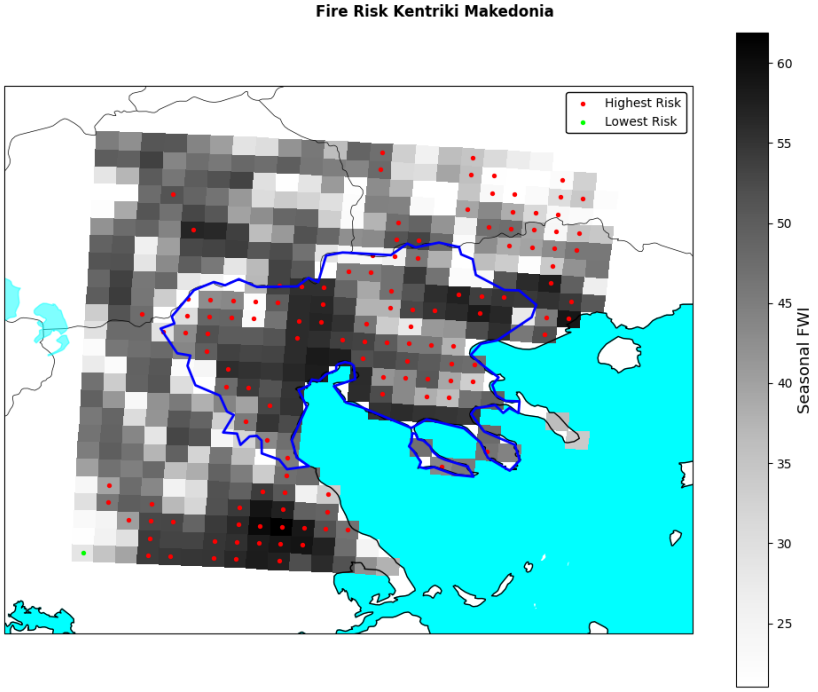

Figure 51: Wildfire risk plot indicating region's areas with the highest risk and how ti compares to with the cliamte danger estiamted by the FWI.

The visualization provides spatial insight into the distribution of wildfire risk across the region. The map resolution corresponds to the *11 × 11 km* resolution of the FWI dataset. Red markers indicate the centroids of grid cells identified as having the highest risk, and their size adjusts upon zoom to maintain clarity. These markers were not intended to reflect the exact coordinates of the highest risk but represent the spatial units where risk is concentrated.

The resulting plot highlights the areas of the region where the combined indicators identify the highest wildfire risk. Each red-marked pixel denotes an equally high-risk location, based on the selected vulnerability components. Generally, high risk coincides with areas of high climatic danger, as indicated by FWI values (grey tones in the background). However, this is not always consistent; for example, in certain parts of the city of Thessaloniki, areas with high FWI scores are not classified among the highest-risk zones due to lower values in the accompanying vulnerability indicators. This underlines the multifactorial nature of wildfire risk, which acts as a function not only of climatic conditions but also of their interaction with human, ecological, and economic vulnerability. The map provides information for regional authorities, supporting evidence-based planning and prioritization

of adaptation measures. By modifying the selected vulnerability inputs, different perspectives on risk (e.g., human, ecological, or economic) can be derived and compared. As the datasets are at a continental scale, the outputs are expected to diverge compared to local realities. Users are encouraged to validate the results through local and/or regional expertise and, where possible, to substitute these datasets with higher-resolution local equivalents.

2.2.3 Choose Scenario

For RCM, scenario assumptions related to climate change indicate a significant intensification of fire risk due to rising average and maximum temperatures, increased heatwave frequency, and extended drought conditions. These trends are particularly relevant during the critical fire season (April–October), where the FWI is expected to show more frequent and prolonged exceedances of high-risk thresholds. In the short term (0–5 years), existing hazard conditions might already justify immediate implementation of fire prevention measures, land use regulation in wildland-urban interface zones, and investment in monitoring systems. Medium-term scenarios (20–30 years), aligned with SSP2-4.5, might suggest not only a higher number of extreme fire danger days but also an earlier onset and delayed end of the fire season. Vegetation stress, soil moisture deficits, and the accumulation of unmanaged biomass due to land abandonment may further amplify hazard conditions. Long-term scenarios (50–100 years), especially under high-emissions pathways such as SSP5-8.5, might indicate the geographic expansion of fire-prone zones into higher altitudes and ecologically sensitive areas that were not historically exposed. In parallel, intensifying land-use pressures (e.g., peri-urban sprawl, and abandonment of traditional land management) contribute to the proliferation of unmanaged vegetation that can serve as fuel.

The CLIMAAX wildfire workflow will accommodate these conditions by enabling the generation of bias-adjusted FWI indicators based on EURO-CORDEX and CMIP6 datasets, and will ensure consistency with European climate policy frameworks. FWI-based projections will help identify shifts in fire seasonality, magnitude, and frequency, and will support scenario-informed spatial planning. When results from the expert team conclude, for RCM, these projections will have the potential to be directly applied to test the effectiveness of fire mitigation strategies over different planning horizons. Moreover, the workflow has the potential to support comparative evaluation of scenarios, to help stakeholders prioritize investments in ecosystem management, infrastructure resilience, and emergency response. These scenario-based descriptions are grounded in the methodology and tools provided by the CLIMAAX framework.

2.3 Risk Analysis

This section presents the implementation of the CLIMAAX risk analysis methodology applied to the RCM for the two (2) main hazard categories: floods and wildfires. The risk assessment follows the integration of hazard, exposure, and vulnerability datasets described in the previous sections, and provides spatially explicit outputs (e.g., maps, tables) that quantify expected impacts under current and projected scenarios.

2.3.1 Workflow #1: Floods

Table 12: Data overview Workflow #1

Hazard Data	Vulnerability Data	Exposure Data	Risk Output
JRC flood hazard maps for return periods of 10, 50, 100, and 500 years	Global flood depth-damage curves (per land use category), economic unit values by land cover	CORINE land cover, LUISA land use, OSM building data	Flood extent and depth rasters, damage maps in €/ha, summary statistics by municipality and scenario

2.3.1.1 Hazard assessment

Flood hazard layers were sourced from the JRC and cover four return periods: 10, 50, 100, and 500 years. These layers include both flood extent and depth rasters and were clipped to the boundaries of the RCM. Where applicable, local topographic data and hydrological insights were also incorporated. The resulting hazard datasets form the core input for exposure overlay and risk estimation.

2.3.1.2 Risk assessment

Flood risk was computed by overlaying hazard maps with exposure layers such as land use and building footprints. Vulnerability was captured using depth-damage curves corresponding to different land use types. The result is a set of risk maps showing expected damages in €/ha and tables summarizing economic losses per municipality and return period. These outputs support local adaptation planning and prioritization of protective measures.

2.3.2 Workflow #2: Wildfires

Table 13: Data overview Workflow #2

Hazard Data	Vulnerability Data	Exposure Data	Risk Output
Seasonal FWI from EURO-CORDEX climate scenarios	EFFIS: Wildland-Urban Interface population, Protected Area coverage, Ecosystem Irreplaceability, Restoration Cost Index	CORINE Land Cover, LUISA 2020, GHSL population grids, OSM infrastructure, Natura 2000 zones	Wildfire danger maps, raster layers for high-risk pixels, municipality-level risk summaries

2.3.2.1 Hazard assessment

Wildfire hazard was assessed using the FWI, calculated from EURO-CORDEX downscaled projections for RCP2.6 and RCP4.5 scenarios over the period 2045–2055. Daily temperature, humidity, wind speed, and precipitation were used to calculate seasonal FWI values. Vegetation

masks were applied to exclude non-burnable areas, resulting in layers identifying regions with high susceptibility to wildfires.

2.3.2.2 Risk assessment

Risk was evaluated by integrating the FWI with vulnerability layers from EFFIS, which include the population living in the wildland-urban interface, ecosystem restoration cost, and ecological irreplaceability. A specified methodology was used to identify pixels with the highest combined hazard and vulnerability scores. Exposure data included land use categories, population density, and critical infrastructure. The analysis generated risk maps and accompanying tables indicating spatial clusters of high wildfire risk, informing future resilience strategies and land use planning.

2.4 Preliminary Key Risk Assessment Findings

Following the implementation of the technical workflows outlined in the CLIMAAX Handbook, the RCM has produced a comprehensive set of spatial climate risk assessments covering river flooding, coastal exposure, wildfire susceptibility, and infrastructure vulnerability. The risk findings below reflect both quantitative outputs (e.g., damage estimates, exposure maps) and qualitative considerations related to severity, urgency, and adaptive capacity.

2.4.1 Severity

The analysis identified river flooding and wildfire susceptibility as the two most severe and recurring climate-related hazards for the RCM.

- River flooding: quantitative flood maps for four major rivers were generated for return periods ranging from “1-in-10” to “1-in-500-years”. Damage estimates revealed that
    - Permanently irrigated land and rice fields seems to contribute the largest share of total economic damages.
    - In Strymonas and Axios, modeled damages exceed 5 to 7 billion € (for future scenarios), confirming the economic exposure of agricultural zones and floodplain settlements.
    - Industrial areas and urban fabrics also show consistent damage patterns, with critical infrastructure affected in all return periods.
- Coastal exposure: sea-level rise projections and flood extent maps suggest moderate but increasing risk along the Thermaic Gulf coastline, particularly in low-elevation municipalities and industrial corridors near river estuaries (e.g., Axios Delta).
- Infrastructure risk: overlay analysis of building stock, topology, and hazard datasets shows that dispersed peri-urban development faces compounded exposure to both fluvial and coastal hazards, especially under higher return periods.
- Wildfire susceptibility: key findings include:
    - Persistent hotspots along the southern and western forested zones of the region.
    - High risk concentration in mixed agro-forestry areas, confirming the susceptibility of transitional landscapes under warming trends and land abandonment pressures.

Overall, the severity of climate risk in RCM seems to be high, particularly for economic losses in agriculture and physical infrastructure, with clear spatial patterns emerging from the workflows.

2.4.2 Urgency

- River flooding is characterized by a “rapid-onset” hazard, with potential for severe impacts in short timeframes. Given that high-damage events were modeled under different scenarios, action is required in the near term, especially for maintenance of existing flood resilience infrastructure and zoning enforcement in flood-prone areas.
- Coastal risks are progressive, with high urgency for planning even if physical impacts (e.g., inundation) manifest over longer time horizons. Strategic retreat and land-use restrictions in low-lying areas must be planned to prevent lock-in.
- Wildfire susceptibility represents a seasonal and escalating hazard. Although onset is rapid once ignition occurs, the underlying risk is slow-onset driven by climate trends, land-use change, and forest degradation. Preventive actions, management and early detection should be prioritized immediately, as the risk is showing indications to intensify in the next 5–10 years.

Therefore, the combination of rapid-onset (river flood, wildfire ignition) and slow-onset (climate shifts, sea-level rise) hazards calls for both short-term preparedness and long-term adaptation planning.

2.4.4 Capacity

RCM has taken first steps toward developing institutional and technical capacity for climate risk management:

- Social resources: while local government staff have participated actively in this first phase, technical expertise for model implementation and geospatial analysis currently relies on external support. This highlights the need for capacity building and training to ensure continuity and ownership.
- Existing physical resilience infrastructure and protected areas (e.g., wetlands near Axios Delta) offer partial mitigation benefits. However, infrastructure in vulnerable zones seems to remain exposed, and ecosystem services (e.g., natural buffers) seems that are not yet fully integrated into the region's resilience planning.

Opportunities could include: (i) using the generated datasets to inform regional planning and land-use zoning; (ii) enhancing interdepartmental coordination, especially between civil protection, agriculture, and environmental departments; (iii) applying the new evidence base to secure additional funding for climate adaptation (Phase 3 of the CLIMAAX Project).

In sum, while RCM’s current capacity is based on concrete previous planning, the implementation of the CLIMAAX workflows marks a significant improvement in both situational awareness and readiness to act.

2.5 Preliminary monitor and evaluation

The first deliverable of the climate risk assessment in the RCM highlighted the capabilities of implementing the CLIMAAX framework using exclusively EU-level datasets. The process offered valuable insight into the hazard typologies and their spatial patterns, but also revealed challenges linked to data granularity and applicability at the regional scale, for which additional data is expected to be seen in the second deliverable. In the case of flood hazards, the available datasets primarily sourced from the JRC and Aqueduct Floods enabled the production of preliminary flood hazard maps for riverine and coastal events. Certain urban or industrial areas appeared to be under- or overestimated in terms of flood extent, due to the coarse resolution of the input data.

Regarding wildfire risk, the use of the FWI index combined with land cover and population datasets allowed the identification of general patterns of climatic danger and vulnerability. Nonetheless, in areas such as Chalkidiki and parts of eastern Thessaloniki, the FWI maps showed high danger classes despite the lack of any historical fire data raising interpretative challenges in the absence of validated local wildfire records or vegetation moisture indices. As expected, initial informal exchanges suggested interest in adapting the risk outputs to local administrative units and including indicators more familiar to civil protection stakeholders. These insights will inform the next steps, particularly in terms of stakeholder engagement design

At present, no regional datasets were integrated into the climate assessment framework, and all risk assessments were conducted exclusively using the default EU-level data made available within the CLIMAAX framework. This constraint guided both the spatial resolution and the perceived credibility of certain outputs. Going forward, the availability of national or regional datasets, such as recent floodplain delineations, local land use inventories, or wildfire occurrence records would significantly enhance the robustness of the assessment. Additional resources and cooperation with national authorities will be required to support this. Moreover, some competencies particularly in geospatial data processing and post-processing of hazard layers were found to be necessary at the regional level to customize outputs more effectively.

3 Conclusions Phase 1- Climate risk assessment

The first phase of the selected climate risk assessment workflows outlined in the CLIMAAX Handbook has now been completed for the RCM. This marks a key transition from the preparatory phase focused on organizational readiness and methodological familiarization to the delivery of spatially explicit results grounded in technical implementation. The workflows have been applied to assess river flood risk, coastal flood exposure, wildfire susceptibility, and building-scale hazard mapping. Their execution was based on the transferable structure of the CLIMAAX framework and adapted to the specific data availability, geographic characteristics, and priorities and needs of the RCM. All analyses were developed closely with regional authorities (when needed) to ensure contextual relevance and institutional alignment. As a result, a comprehensive set of high-resolution outputs has been produced, including:

- Spatially detailed flood risk maps for the Aliakmonas, Axios, Loudias, and Strymonas rivers, accompanied by economic damage estimates across return periods up to the “1-in-500-year” event, based on land use exposure and vulnerability profiles.
- An assessment of coastal flood exposure derived from sea-level rise projections and topographic data, supporting the identification of vulnerable areas within coastal municipalities.
- A wildfire susceptibility index based on historical fire data, vegetation cover, and climate variables, allowing the identification of priority zones for fire risk mitigation.
- Building-level overlay analyses combining land use, elevation, and infrastructure datasets, providing a first-level screening of exposure to multiple hazards.

The results have supported the refinement of regional risk knowledge, laid the groundwork for strengthening cross-sectoral coordination, and informed early discussions on investment prioritization and resilience planning. Through the execution of the CLIMAAX workflows, local technical capacity has been strengthened, practical familiarity with the CLIMAAX platform has been increased, and a shared knowledge base across departments has been established. As a next step, the results are considered to be communicated to local stakeholders through targeted engagement activities. This will support the co-development of adaptation strategies informed by the workflow outputs and integrated within existing policy frameworks and planning instruments. Additionally, it will help with an adaptation to selecting and collecting the data for the regional dataset workflows. With the technical implementation now concluded, the RCM has gained the necessary knowledge and experience to proceed to the next phase of the climate risk management process namely, translating analysis into actionable planning and operational decision-making.

4 Progress evaluation and contribution to future phases

The current phase focused on the full implementation of the CLIMAAX methodology in the RCM, resulting in the successful execution of both flood and wildfire risk workflows. All hazard, exposure, and vulnerability datasets were processed, and the relevant outputs, including spatial risk maps and quantitative damage assessments were delivered following the aimed plan. The tables below summarize the achieved Key Performance Indicators (KPIs) and milestones for this reporting period. These results provide a robust basis for the upcoming phases, where they will support adaptation planning, prioritization of measures, and regional engagement. The work completed so far ensures technical readiness for further integration of climate risk outputs into operational and strategic frameworks at the regional level.

Table 14: KPIs overview.

KPIs	Progress
T1.1 Inventory of relevant risks and EU dataset collection – Identification and classification of European/regional data categories	Completed
T1.1 Inventory of relevant risks and EU dataset collection – Use all the provided datasets for at least two (2) different types of climate risks	Completed
T1.1 Inventory of relevant risks and EU dataset collection – Three (3) stakeholders involved in the task activities	Completed
T1.2 Application of the framework for selected hazards – At least two (2) workflows successfully applied on Deliverable 1	Completed
T1.2 Application of the framework for selected hazards – Implementation in at least two (2) different cliamate change impact phenomena during Phase 1	Completed
T1.2 Application of the framework for selected hazards – Three (3) stakeholders involved in the task activities	Completed

Table 15: Overview of the milestones.

Milestones	Progress
Initial Discussions and first results	Achieved
Initial framework application and data collection	Achieved

5 Supporting documentation

Technical data, analytical results, or visual materials produced at this deliverable have been included and described following the step-by-step process as given in the CLIMAAX framework. Accordingly, no additional, sharable, and transferable datasets or outputs have been generated to date that would qualify for publication on Zenodo or other open-access repositories. If any additional relevant outputs are produced by the technical implementation, these will be documented, properly curated, and shared in the Zenodo repository in line with the project's open science and data management requirements. The only output available at this stage is the current main report, which documents the status and results of the work in Phase 1. If needed, all future materials, including visual outputs, communication pieces, and structured datasets, will be prepared and shared accordingly as the project advances into its next stages. Outputs produced during this stage:

- Main report: climate risk assessment – Phase 1, pdf version.
- Visual outputs: both for floods and fire hazards.
- Communication outputs: none produced at this stage.
- Datasets: no specific reproducible and transferable datasets were produced.

All produced materials are available, and when needed can be uploaded and classified in the Zenodo repository, following the required format and standards for open-access dissemination. RCM and the external collaborator (CDXi) remain dedicated to the FAIR data initiative supporting the open sharing of "Findable, Accessible, Interoperable, and Reusable" data.

6 References

CLIMAAX: Deliverable 1.4 – Climate risk assessment framework. WP1 – Framework for local and regional climate risk assessment. [CLIMAAX – Horizon Europe, Grant Agreement No. 101093864]. Available at: https://files.cmcc.it/climaax/Deliverables/CLIMAAX_D1.4_Climate%20Risk%20Assessment%20Framework_revised.pdf.=, 2023.

CLIMAAX: Deliverable 2.1 – Report on the specifications for toolbox methods. WP2 – Co-design of the supporting toolbox. [CLIMAAX – Horizon Europe, Grant Agreement No. 101093864]. Available at: https://www.climaax.eu/wp-content/uploads/2023/07/CLIMAAX_D2.1_v3_corrected.pdf, 2023.

CLIMAAX: Deliverable D2.2 – Report on hazard tools of relevance to the CRA Toolbox. WP2 – Co-design of the supporting toolbox [CLIMAAX – Horizon Europe, Grant Agreement No. 101093864]. Available at: https://www.climaax.eu/wp-content/uploads/2024/07/CLIMAAX_D2.2.pdf, 2024.

CLIMAAX: Deliverable D2.3 - Report on pan European vulnerability and exposure projections. WP2 – Co-design of the supporting toolbox. [CLIMAAX – Horizon Europe, Grant Agreement No. 101093864]. Available at: https://www.climaax.eu/wp-content/uploads/2024/07/CLIMAAX_D2.3.pdf, 2024.

CLIMAAX: Deliverable D2.4 – Report on integrated risk assessment tools of relevance to the CRA Toolbox. WP2 – Co-design of the supporting toolbox. [CLIMAAX – Horizon Europe, Grant Agreement No. 101093864]. Available at: https://files.cmcc.it/climaax/CLIMAAX_D2.4.pdf, 2024.

Muis S, Irazoqui Apecechea M, Dullaart J, de Lima Rego J, Madsen KS, Su J, Yan K and Verlaan M, A High-Resolution Global Dataset of Extreme Sea Levels, Tides, and Storm Surges, Including Future Projections. Front. Mar. Sci. 7:263, https://doi.org/10.3389/fmars.2020.00263, 2020.

Dottori, F., Alfieri, L., Bianchi, A., Skoien, J., and Salamon, P.: A new dataset of river flood hazard maps for Europe and the Mediterranean Basin, Earth Syst. Sci. Data, 14, 1549–1569, https://doi.org/10.5194/essd-14-1549-2022, 2022.

Trucchia Andrea, Meschi Giorgio, Fiorucci Paolo, Provenzale Antonello, Tonini Marj, Pernice Umberto, Wildfire hazard mapping in the eastern Mediterranean landscape. International Journal of Wildland Fire 32, 417-434, https://doi.org/10.1071/WF22138, 2023.

El Garroussi, S., Di Giuseppe, F., Barnard, C., & Wetterhall, F., Europe faces up to tenfold increase in extreme fires in a warming climate. Npj Climate and Atmospheric Science, 7(1). https://doi.org/10.1038/s41612-024-00575-8, 2024.

Jacome Felix Oom, D., De Rigo, D., Pfeiffer, H., Branco, A., Ferrari, D., Grecchi, R., Artes Vivancos, T., Durrant, T., Boca, R., Maianti, P., Liberta`, G. and San-Miguel-Ayanz, J., Pan-European wildfire risk assessment, EUR 31160 EN, Publications Office of the European Union, Luxembourg, 2022, ISBN 978-92-76-55137-9, doi:10.2760/9429, JRC130136.

Aerts, J.C.J.H., Bates, P.D., Botzen, W.J.W. et al. Exploring the limits and gaps of flood adaptation. Nat Water 2, 719–728, https://doi.org/10.1038/s44221-024-00274-x, 2024.

Bachmann, M., Mechler, R., Higuera Roa, O., Pirani, A., Pal, J., Reimann, L., Mazzoleni, M., Buskop, T., and Mysiak, J.: An adaptive and flexible Climate Risk Assessment Framework for regions, EGU General Assembly 2024, Vienna, Austria, 14–19 Apr 2024, EGU24-16910, https://doi.org/10.5194/egusphere-egu24-16910, 2024.